UNDERSTANDING THE ROLE OF LIPOCALIN 2 AS AN IMPORTANT REGULATOR OF ENERGY METABOLISM

A DISSERTATION
SUBMITTED TO THE FACULTY OF THE GRADUATE SCHOOL
OF THE UNIVERSITY OF MINNESOTA
BY

YUANYUAN ZHANG

IN PARTIAL FULFILLMENT OF THE REQUIREMENTS
FOR THE DEGREE OF
DOCTOR OF PHILOSOPHY

Name of Advisor: XIAOLI CHEN

MARCH, 2013

ACKNOWLEDGEMENTS

I'd like to thank my advisor Dr. Xiaoli Chen for her guidance and support over all these years. She is always patient and encouraging, willing to work closely with her students and provide them with help in every possible way. I would also like to express my gratitude to my committee members: Dr. David Bernlohr, Dr. Douglas Mashek, and Dr. Daniel Gallaher. They have been conscientious and helpful in making suggestions on my research projects. I also want to thank my colleagues, especially Dr. Hong Guo and Dr. Daozhong Jin, for their inspirations and assistance. Finally, I'm grateful for having loving parents and lovely friends, who have made my life in Minnesota enjoyable despite the lengthy winter. I wouldn't have completed the projects without all their support.

ABSTRACT

Lipocalin 2 (Lcn2) is a recently identified adipose tissue-derived cytokine which functions in innate immunity, inflammation, and insulin resistance. Nonetheless, the metabolic regulation and function of adipose Lcn2 is not completely understood. Herein, we investigated how adipose Lcn2 expression is regulated by metabolic challenges and nutrient signals, as well as how Lcn2 deficiency affects whole-body energy metabolism and lipid homeostasis. We found that *Lcn2* mRNA expression was significantly upregulated during fasting and cold exposure in mice. Insulin stimulated Lcn2 expression and secretion in 3T3-L1 adipocytes in a dose-dependent manner, which was enhanced by glucose and attenuated by aspirin treatment. Multiple fatty acids also induced Lcn2 expression and secretion in adipocytes. The regulation of adipose Lcn2 by metabolic challenges and nutrient signals indicated a potential role of Lcn2 in energy metabolism. Next, we explored the metabolic consequences of Lcn2 deficiency in mice under high fat diet (HFD) conditions. We found that Lcn2 deficiency potentiated diet-induced obesity, dyslipidemia, fatty liver disease, and insulin resistance in mice. Moreover, *Lcn2* knockout (KO) mice exhibited impaired adaptive thermogenesis and cold intolerance. Further studies showed that Lcn2 deficiency reduced the efficiency of cold-induced mitochondrial oxidation of lipids and blunted cold-induced UCP1 activation and expression of thermogenic (PGC-1α and PRDM16) and angiogenic (VEGF-A) genes, leading to lipid accumulation and thermogenic dysfunction of brown adipocytes. Interestingly, the administration of PPARγ agonist effectively improved HFD-induced

insulin resistance in *Lcn2* KO mice without increasing body weight, subcutaneous fat mass, or lipid accumulation in liver. PPARγ agonist administration also fully prevented cold-intolerant phenotype in *Lcn2* KO mice. Our results indicate that Lcn2 plays a critical role in the regulation of lipid homeostasis and thermogenic activation via a possible mechanism of modulating PPARγ activation.

TABLE OF CONTENTS

LIST OF TABLES ..... **vii**

LIST OF FIGURES ..... **viii**

CHAPTER 1

LITERATURE REVIEW **1**

1. Metabolic diseases 2

1.1 Prevalence of metabolic diseases 2

1.2 Molecular mechanisms 3

2. White adipose tissue (WAT) 3

2.1 Features of WAT 3

2.2 Functions of WAT 5

2.2.1 Lipid Storage 5

2.2.2 Adipokine secretion 5

3. Brown adipose tissue (BAT) 6

3.1 Features of BAT 6

3.2 Origins of BAT 7

3.3 Cold-induced metabolic changes in BAT 9

3.3.1 Adaptive thermogenesis 9

3.3.2 Substrate mobilization and utilization 10

3.3.3 Mitochondrial biogenesis 11

3.3.4 Increased angiogenesis 13

3.3.5 Remodeling of white adipose tissue 14

3.4 Regulation of thermogenesis 14

3.4.1 Sympathetic nerve system 14

3.4.2 Other hormones 16

3.4.3 Transcriptional regulators 17

4. Lipocalin-2 19

4.1 Discovery and distribution of LCN2 19

4.2 Regulation of LCN2 expression …… 20
4.3 Function of LCN2 …… 21
4.3.1 Immune response to bacterial infection …… 21
4.3.2 Inflammation …… 22
4.3.3 Cancer …… 23
4.3.4 Obesity and insulin resistance …… 23
CHAPTER 2
REGULATION OF ADIPOSE LCN2 EXPRESSION IN RESPONSE TO METABOLIC CHALLENGES AND NUTRIENT SIGNALS …….. **25**
SUMMARY …… 26
INTRODUCTION …… 26
RESULTS …… 28
Adipose Lcn2 expression is upregulated during metabolic challenging …… 29
Glucose and insulin regulation of Lcn2 expression in 3T3-L1 adipocytes …….. 30
Blocking NFκB signaling pathway reduces insulin-stimulated Lcn2 secretion ….. 31
Fatty acids regulated Lcn2 expression in 3T3-L1 adipocytes …….. 32
DISCUSSION …….. 33
CHAPTER 3
THE ROLE OF LCN2 IN DIET-INDUCED OBESITY AND INSULIN RESISTANCE…… **53**
SUMMARY …… 54
INTRODUCTION …… 54
RESULTS …… 56
Lcn2 KO mice are more susceptible to diet-induced obesity …….. 56
Lcn2 deficiency aggravates diet-induced dyslipidemia and insulin resistance …… 57
TZD rescues diet-induced dyslipidemia and insulin resistance in *Lcn2* KO mice …….. 57
Lcn2 deficiency diminishes the effects of Rosi on weight gain and lipid accumulation …… 58

DISCUSSION …….. 59
CHAPTER 4
THE ROLE OF LCN2 IN ADAPTIVE REMODELING AND THERMOGENIC ACTIVATION OF BROWN ADIPOSE TISSUE …… 82
SUMMARY …….. 83
INTRODUCTION …… 83
RESULTS ……. 86
Lcn2 deficiency impairs BAT thermogenic activation by cold stimulation ……. 86
Lcn2 KO mice exhibit normal sympathetic nervous system activation during cold exposure …… 87
Isolated mitochondria and brown adipocytes from *Lcn2* KO mice have no evident oxidative dysfunction ……. 88
Lcn2 deficiency leads to inefficient mitochondrial oxidation in vivo and the development of hypertrophic brown adipocytes during cold exposure ……. 89
Lcn2 deficiency reduces UCP1 protein and thermogenic gene expression in BAT during cold exposure ……... 90
Lcn2 deficiency eliminates cold-induced VEGF-A and HIF-1α expression in BAT …….. 90
PPARγ agonist reverses adaptive thermo-dysregulation in *Lcn2* KO mice …… 91
DISCUSSION …….. 92
SUMMARY ……...……...….. 129
MATERIALS AND METHODS ……... 133
BIBLIOGRAPHY …….. 147

LIST OF TABLES

Table 1 Serum metabolic parameters in WT and *Lcn2* KO mice ……... 80
Table 2 Plasma lipid profile in WT and *Lcn2* KO mice ……. 81
Table 3 List of real-time PCR primer sequence …….. 146

LIST OF FIGURES

Figure 1A The expression of Lcn2 in adipose tissues of C57/BL6 mice ……..... 38

Figure 1B Lcn2 gene expression in response to cold stimulation ……...…… 39

Figure 1C Lcn2 gene expression in response to starvation……..…… 40

Figure 1D Lcn2 protein levels in response to cold stimulation…… 41

Figure 1E Norepinephrine increased Lcn2 expression in 3T3-L1 adipocytes…..… 42

Figure 1F Lcn2 protein expression in response to starvation……..…… 43

Figure 2A Lcn2 expression and secretion was upregulated by insulin in a dose-dependent manner in 3T3-L1 adipocytes……..… 44

Figure 2B Lcn2 expression and secretion was upregulated by insulin……... 45

Figure 2C 3-O-methyl-d-glucose abolished insulin-stimulated Lcn2 expression and secretion in 3T3-L1 adipocytes (different doses of insulin)…….……..… 46

Figure 2D 3-O-methyl-d-glucose abolished insulin-stimulated Lcn2 expression and secretion in 3T3-L1 adipocytes……..… 47

Figure 2E TNFα stimulated Lcn2 expression and secretion in 3T3-L1 adipocytes…… 48

Figure 2F Aspirin attenuated insulin-stimulated Lcn2 secretion in 3T3-L1 adipocytes…… 49

Figure 3A The effect of 12-hour treatment of fatty acids on Lcn2 expression…… 50

Figure 3B The effect of 24-hour treatment of fatty acids on Lcn2 expression…… 51

Figure 3C The effect of phytanic acid on Lcn2 expression……..… 52

Figure 4A Growth curve of WT and *Lcn2* KO mice on RCD……..…… 62

Figure 4B Growth curve of WT and *Lcn2* KO mice on HFD…….. 63

Figure 4C Tissue weight of WT and *Lcn2* KO mice on RCD……. 64

Figure 4D Tissue weight of WT and *Lcn2* KO mice on HFD……...…….. 65

Figure 4E Liver triacyglyceride content in WT and *Lcn2* KO mice on RCD…….. 66

Figure 4F Oil-red O staining of liver section of WT and *Lcn2* KO mice on RCD and HFD……... 67

Figure 5A Assessment of glucose tolerance in WT and *Lcn2* KO mice on RCD… 68
Figure 5B Assessment of glucose tolerance in WT and *Lcn2* KO mice on HFD… 69
Figure 5C Assessment of systemic insulin sensitivity in WT and *Lcn2* KO mice on RCD…… 70
Figure 5D Assessment of systemic insulin sensitivity in WT and *Lcn2* KO mice on HFD…… 71
Figure 6A Glucose tolerance tests in the HFD-fed WT mice treated with H_2O or Rosi…….. 72
Figure 6B Glucose tolerance tests in the HFD-fed *Lcn2* KO mice treated with H_2O or Rosi…….. 73
Figure 6C Insulin tolerance tests in the HFD-fed WT mice treated with H_2O or Rosi……... 74
Figure 6D Insulin tolerance tests in the HFD-fed *Lcn2* KO mice treated with H_2O or Rosi……... 75
Figure 7A Body weight gain in the HFD-fed WT and *Lcn2* KO mice treated with H_2O or Rosi…… 76
Figure 7B Tissue weight in the HFD-fed WT and *Lcn2* KO mice treated with H_2O or Rosi…… 77
Figure 7C Triglyceride content in liver of the HFD-fed WT and *Lcn2* KO mice treated with H_2O or Rosi……... 78
Figure 7D De novo lipogenesis in HFD-fed WT and *Lcn2* KO mice…….. 79
Figure 8A Body temperature in WT and *Lcn2* KO mice during acute cold exposure……... 96
Figure 8B Serum glucose levels in WT and *Lcn2* KO mice at 22^0C or after exposed to 4^0C for 4 hours……... 97
Figure 8C Serum lactate levels in WT and *Lcn2* KO mice after exposed to 4^0C for 4 hours…… 98
Figure 8D Serum fatty acid levels in WT and *Lcn2* KO mice at 22^0C or after exposed to 4^0C for 4 hours……... 99

Figure 8E Liver glycogen content in WT and *Lcn2* KO mice at 22^{0}C or after exposed to 4^{0}C for 4 hours..... 100
Figure 8F mRNA expression levels of gluconeogenic genes in liver..... 101
Figure 9A Serum catecholamine levels in WT and *Lcn2* KO mice after exposed to 4^{0}C for 4 hours..... 102
Figure 9B mRNA expression levels of thyroid hormone receptor α/β in BAT of mice..... 103
Figure 9C HSL phosphorylation at Ser563 in BAT and WATs of WT and Lcn2 KO mice..... 104
Figure 9D Glycerol and fatty acid release from BAT explants in response to norepinephrine..... 105
Figure 9E Glycerol release from WAT explants in response to isoproterenol..... 106
Figure 9F Glycerol and fatty acid release from SV-differentiated brown adipocytes..... 107
Figure 9G Triglyceride hydrolase activity in BAT..... 108
Figure 9H The protein levels of ATGL in BAT of WT and *Lcn2* KO mice at 22^{0}C or after exposed to 4^{0}C for 4 hours..... 109
Figure 10A Oxygen consumption of mitochondria isolated from BAT and liver of mice under 22ºC and after exposed to 4ºC for 3 hours 110
Figure 10B Oxidation of 14C-labled oleate in SV-differentiated brown adipocytes during pulse and chase phase..... 111
Figure 10C Brown adipose tissue from WT and *Lcn2* KO mice exposed to 4°C for 4 hours..... 112
Figure 10D Triglyceride content of BAT in WT and *Lcn2* KO mice after cold exposure..... 113
Figure 10E Quantitative analysis of perimeter of brown adipocytes from mice exposed to 4°C for 4 hours..... 114
Figure 10F Quantitative analysis of mitochondria number per cell area from mice exposed to 4°C for 4 hours..... 115

Figure 10G The mRNA expression of mitochondrial genes in BAT of mice…..... 116
Figure 11A Cold-induced UCP1 protein expression in BAT of WT and Lcn2 KO mice…….. 117
Figure 11B Cold-induced mRNA expression of PGC-1α……... 118
Figure 11C Cold-induced mRNA expression of PRDM16…….. 119
Figure 11D mRNA expression of VEFG-A in BAT of mice……..... 120
Figure 11E mRNA expression of HIF-1α in BAT of mice……..... 121
Figure 12A Body temperature of WT and *Lcn2* KO mice with or without Rosi treatment……... 122
Figure 12B Liver glycogen content in mice with and without Rosi treatment…..... 123
Figure 12C Serum glucose levels in mice with and without Rosi treatment……... 124
Figure 12D Serum lactate levels in mice with and without Rosi treatment……. 125
Figure 12ESerum fatty acid levels in mice with and without Rosi treatment…….. 126
Figure 12F mRNA expression of PGC-1α and PRDM16 in BAT…… 127
Figure 12G mRNA expression of Cox4 and Nrf1 in BAT…….....….... 128
Figure 13A The model of the regulation of Lcn2 expression and secretion in 3T3-L1 adipocytes……...……..…… 131
Figure 13B The model of Lcn2-mediated PPARγ activation……... 132

CHAPTER 1

LITERATURE REVIEW

Yuanyuan Zhang wrote this chapter.

1. Metabolic diseases

1.1 Prevalence of metabolic diseases

The prevalence rate of obesity is dramatically increasing and becoming a global epidemic. Obesity is a major risk factor for cardiovascular diseases, type II diabetes, obstructive sleep apnea, and certain types of cancers, such as gallbladder cancer, esophagus cancer, pancreas cancer, colon and rectum cancer, etc.(National Cancer Institute Fact Sheet, 2012). According to the data from National Center for Health Statistics, 78 million U.S. adults, as well as 12.5 million U.S. children and adolescents, were obese in 2009–2010, which were 35.7% and 16.9% of total population respectively (Ogden et al., 2012).

It is well known that obesity is the result of energy imbalance; hence dietary intake and sedentary lifestyle play a significant role in the development of obesity. However, the etiology of obesity is rather complicated and hereditary factors cannot be ignored. Studies have shown that 80% of the offspring of two obese parents are obese, in contrast to the number of less than 10% in the offspring of two parents who are normal weight (Kolata, 2007). As of Oct. 2005, 127 candidate genes have been reported to be positively associated with human obesity phenotypes; 244 genes could affect body weight and adiposity when mutated or expressed as transgenes in mice (Snyder et al., 2004). The scientific findings indicate that the number of genes associated with obesity is still growing.

1.2 Molecular mechanisms

From the molecular and physiologic insight, obesity is regulated at multiple levels. First, central nervous system (CNS) integrates afferent signals that influence energy balance. The melanocortin pathway in hypothalamus is one of the best defined pathways: the melanocortin 4 receptor (MC4R) receives both agonist ligands like α-melanocyte stimulating hormone (α-MSH) and antagonistic ligands like agouti-related peptide (AGRP) to regulate appetite, energy expenditure and body weight (Fan et al., 1997; Huszar et al., 1997; Ollmann et al., 1997). Secondly, endocrine signals from the gut are also known to affect appetite, such as peptide Y (PYY), glucagon-like peptide-1 (GLP-1), cholecystokinin (CCK), and ghrelin. Most of the gut hormones inhibit feeding, while ghrelin stimulates feeding (Flier, 2004). Thirdly, adipose tissue-secreted cytokines have been recognized to play an important role in regulating the systemic energy balance. The discovery of leptin (Zhang et al., 1994) and leptin receptor (Tartaglia et al., 1995) refreshed the understanding of the function of white adipose tissue as an endocrine organ. Last but not least, the thermogenic function of brown adipose tissue has been recently addressed as an organ for energy expenditure. In this review, I will focus on the white and brown adipose tissue and their functions in regulating whole-body energy metabolism.

2. White adipose tissue (WAT)

2.1 Features of WAT

WAT is composed of adipocytes and stromal-vascular fraction, which includes macrophages, fibroblasts, endothelial cells, and preadipocytes. According to the regional depots, WAT can be mainly divided into visceral fat, subcutaneous fat, and intramuscular fat. For mice, there are four major adipose depots within the abdominal cavity: gonadal (epididymal fat in males), retroperitoneal, mesenteric, and omental depots and two superficial depots: inguinal and subscapular depots.

Visceral fat and subcutaneous fat are significantly different in metabolic activities. Studies have shown that visceral adipose tissue is more lipolytically active than subcutaneous adipose tissue, therefore contributing more to the plasma free fatty acid levels (Hajer et al., 2008; Hoffstedt et al., 1997; Wajchenberg, 2000). Other studies showed that visceral fat is more sensitive to insulin (Virtanen et al., 2002) and more endocrinologically active than subcutaneous fat (Bergman et al., 2001; Fried et al., 1998; Wajchenberg, 2000); epididymal adipocytes in rats contained more mitochondria than inguinal adipocytes (Deveaud et al., 2004). These metabolic differences may explain the fact that visceral fat correlates more closely with the development of cardiovascular diseases, insulin resistance, type II diabetes, inflammation diseases, and other obesity-related pathologies than subcutaneous adipose tissue (Dhaliwal and Welborn, 2009; Marette, 2003; Montague and O'Rahilly, 2000; Porter et al., 2009; Wajchenberg, 2000; Weyer et al., 2000).

In addition to the depot difference, fat cell size and sex are also factors for predicting significant clinical consequences. Larger adipocytes are associated with hyperglycemia and predict type II diabetes independent of insulin resistance or percent

body fat (Weyer et al., 2000). It has been suggested that increased fat cell size may represent a failure of adipocyte proliferation (Heilbronn et al., 2004) and fat mass expansion, leaving the cells susceptible to hypertrophy under nutrient oversupply (Heilbronn et al., 2004). As far as sex is concerned, adipocytes from females are reported to be more sensitive to insulin and lipogenesis than those from males, which may account for the lower level of insulin resistance and diabetes risk in females than in males despite similar or higher fat content (Macotela et al., 2009).

2.2 Functions of WAT

2.2.1 Lipid Storage

The main function of WAT is to store energy, meanwhile cushioning and insulating the body. In the fed state, free fatty acids are liberated from lipoprotein by lipoprotein lipase and enter the adipocytes, and then they are re-esterified to form triglyceride for storage in adipose tissue. In the fast state, triglyceride is hydrolyzed into glycerol and fatty acids for energy source.

The storage of lipids in WAT attenuates the deleterious effects of circulating FFAs and prevents ectopic lipid accumulation in non-adipose tissues such as muscle, liver, heart and pancreas. Elevation in plasma fatty acid levels and ectopic lipid accumulation are both implicated as the culprit of insulin resistance and type II diabetes (Boden, 1997; Kelley et al., 1993; Yki-Jarvinen, 2005).

2.2.2 Adipokine secretion

Besides serving as fat storage reservoir and buffering system, WAT also functions as an endocrine organ. To date, more than 100 products have been identified to be secreted by adipose tissue, covering a broad range of protein families, fatty acids, and prostaglandins (Hauner, 2005). Especially, adipose-derived cytokines are widely involved in whole body metabolism, such as glucose metabolism (e.g. adiponectin, resistin), lipid metabolism (e.g. cholesteryl ester transfer protein/CETP), inflammation (e.g. tumor necrosis factor α/TNFα, interleukin 6), coagulation (e.g. plasminogen activator inhibitor-1/PAI-1), blood pressure regulation (e.g. angiotensinogen), and feeding behavior (e.g. leptin) (Hajer et al., 2008). In obese state, dysfunctional adipose tissue leads to altered endocrine function and increased macrophage infiltration of WAT, contributing to insulin resistance and metabolic disturbance (Weisberg et al., 2003; Xu et al., 2003).

3. Brown adipose tissue (BAT)

3.1 Features of BAT

Different from white adipose tissue which stores energy, BAT dissipates energy through non-shivering thermogenesis. BAT is abundant in newborns and hibernating mammals (Gesta et al., 2007), for example, in the interscapular region of rodents and in axillary, cervical, perirenal, and periadrenal regions of human newborns (Cannon and Nedergaard, 2004). BAT was traditionally considered insignificant in human adults; nonetheless, recent studies have detected metabolically active BAT in the axillary,

cervical, supraclavicular, and paravertebral regions of human adults using [18F]-2-fluoro-D-2-deoxy-D- glucose (FDG) positron emission tomography (PET) (Nedergaard et al., 2007). Since then, the role of BAT in energy metabolism has been revisited and emphasized.

Brown adipocytes contain multilocular lipid droplets, abundant mitochondria, rich vascularization, and a high level of uncoupling protein 1 (UCP1). UCP1 is a 32kDa protein expressed in the inner membrane of mitochondria. During oxidative phosphorylation, electrons from electron donors such as NADH are transferred to electron acceptors such as oxygen through electron transport chain, at the same time pumping protons into the intermembrane space of mitochondria. This electrochemical proton gradient is used to generate ATP through ATP synthase; whereas UCP1 mediates a proton influx into the mitochondrial matrix, which bypasses the ATP synthase and leads to heat production.

Besides UCP1, some other genes are also preferentially expressed in brown adipocytes compared with white adipocytes, such as cell death-inducing DFF45-like effector A (Cidea), iodothyronine deiodinase, type II (DIO2), elongation of very long chain fatty acids (Elovl3 or Cig30), peroxisome proliferator-activated receptor α (PPARα), peroxisome proliferator-activated receptor gamma coactivator 1 (PGC1α), and factors involved in mitochondrial biogenesis and function (Gesta et al., 2007).

3.2 Origins of BAT

Both BAT and WAT appear to originate from mesodermal / mesenchymal stem cells, but multiple studies have demonstrated that the origin of brown adipocytes is closer to myocytes than white adipocytes. First, the genetic fate mapping showed that engrailed-1 (En1)-expressing cells of the central dermomyotome gave rise to not only dermis and muscle but also BAT (Atit et al., 2006). Secondly, microarray analysis demonstrated that brown preadipocytes exhibited a myogenic transcriptional signature (Timmons et al., 2007). Thirdly, the quantitative mass spectrometry showed that the mitochondrial proteomics of brown adipose tissue were more similar to that of muscle than white adipose tissue at transcript and proteome levels (Forner et al., 2009). The examination of microRNA in murine primary cell cultures also demonstrated that miRNAs were differentially expressed in white and brown adipocytes: three classical "myogenic" miRNAs miR-1, miR-133a and miR-206 were expressed in brown adipocytes, but not white adipocytes (Walden et al., 2009). Fourthly, a serious of studies unveiled that brown adipocytes are differentiated from myogenic factor 5 (Myf5)-expressing myoblastic precursors. Seale et al. reported that PR domain containing 16 (PRDM16) played a key role in triggering brown adipocyte differentiation, mitochondrial biogenesis and UCP1 expression (Seale et al., 2007; Seale et al., 2008). Later, mechanistic investigations showed that PRDM16 formed a transcriptional complex with the active form of CCAAT/enhancer-binding protein β (C/EBPβ), controlling the cell fate switch from myoblastic precursors to brown adipocytes (Kajimura et al., 2009). Moreover, Tseng et al. demonstrated that bone morphogenetic protein 7 (BMP7) promoted the differentiation of brown preadipocyte and induced the expression of early regulators of brown adipocyte

differentiation such as PRDM16 and PGC1α (Tseng et al., 2008). Overall, current studies provide the evidence supporting that brown adipocytes share the same origin with muscle cells.

3.3 Cold-induced metabolic changes in BAT

3.3.1 Adaptive thermogenesis

Cold exposure induces a serious of metabolic response in animal species, among which adaptive thermogenesis is an important component. Cold-induced adaptive thermogenesis can be categorized into shivering thermogenesis and non-shivering thermogenesis. Shivering thermogenesis refers to energy production due to muscle contraction, which converts chemical energy of ATP into kinetic energy and some of the energy shows up as heat. Non-shivering thermogenesis occurs mainly in BAT through the proton leak mediated by UCP1, as previously mentioned. With the extension of cold adaptation, shivering thermogenesis disappears and non-shivering thermogenesis becomes prominent in heat production for maintaining body temperature.

The thermogenic capacity of BAT is enormous in rodents. As reported, the oxygen consumption during cold exposure increased by 100% compared with the basal metabolic rate in rats (Foster and Frydman, 1979). Several reports also demonstrated that BAT was enlarged in experimental animals under cold condition. This enlargement was due to the proliferation and differentiation of brown adipocyte precursor cells (Bukowiecki et al., 1982; Bukowiecki et al., 1986).

It is estimated that UCP1-mediated heat production contributes between 20% and 70% to non-shivering thermogenesis (G. Heldmaier et al., 1989). Recent studies also showed the existence of other mechanism for non-shivering thermogenesis besides UCP1, such as calcium cycling, substrate cycling and protein turnover (Wijers et al., 2009). Interestingly, UCP1-deficient mice were not only cold-intolerant (Enerback et al., 1997), but also exhibited increased susceptibility to age- and diet-induced obesity (Feldmann et al., 2009; Kontani et al., 2005), suggesting that the metabolic function of BAT at room temperature was not inconsiderable, either. In a different study, targeted ablation of BAT gave rise to diet-induced obesity, diabetes, and hyperlipidemia in mice (Lowell et al., 1993).

3.3.2 Substrate mobilization and utilization

During cold-induced adaptive thermogenesis, substrate mobilization and utilization is markedly activated in BAT. The oxygen consumption in BAT is increased by two to four folds in rodents after cold exposure (Lowell and Spiegelman, 2000); the glucose uptake rate in BAT is 10-15-fold higher in cold than in normal room temperature (Virtanen and Nuutila, 2011). Meanwhile, lipid metabolism is also significantly stimulated by cold exposure. It has been reported that both fatty acid synthesis and oxidation are increased in BAT, constituting a cycle for thermogenesis during cold adaptation (Trayhurn, 1981). As judged from respiratory quotients, UCP1-knockout mice showed a delayed transition toward lipid oxidation during acute cold challenge compared

with wild type mice, indicating that BAT took charge of a rapid switch toward lipid-fuelled thermogenesis in response to cold (Meyer et al., 2010).

Therefore, mice with defects in fatty acid metabolism in BAT could be anticipated to experience cold-intolerance. For example, mice lacking long chain acyl-CoA dehydrogenase (LCAD) or long chain acyl-CoA synthetase-1 (ACSL1) are reported to be cold intolerant (Ellis et al., 2010; Guerra et al., 1998a). LCAD is the enzyme involved in fatty acid oxidation, while ACSL1 is the first enzyme activating acyl-CoA for metabolism. Interestingly, β3-adrenergic agonist could not increase oxygen consumption in ACSL1 knockout mice, although the adrenergic signaling was normal in BAT, suggesting that ACSL1 deficiency impaired thermogenesis due to the failure in activating fatty acid for oxidation (Ellis et al., 2010). Similarly, mice lacking fatty acid binding protein 3 (FABP3), a protein involved in transporting fatty acids throughout the cytoplasm, exhibited extreme cold sensitivity as a result of defects in oxidizing fatty acids in BAT despite normal lipolysis and the expression of uncoupling and oxidative genes (Vergnes et al., 2011).

3.3.3 Mitochondrial biogenesis

Mitochondrial function is directly related to the efficiency of fuel utilization and energy production, thus playing an indispensable role during cold adaptation. It has been reported that the number of mitochondria in brown adipocytes is significantly increased in animals exposed to cold environment (Butow and Bahassi, 1999; Rial and Nicholls, 1984). Transcriptional factors that regulate mitochondria biogenesis, such as PGC1α,

nuclear respiratory factor 1 (NRF1), mitochondrial transcription factor A (mtTFA), and estrogen receptor-related receptor α (ERRα), are upregulated during cold stimulation (Wu et al., 1999). PGC1α is known to stimulate mitochondrial biogenesis and respiration through regulating the NRFs. PGC1α induces Nrf1 and Nrf2 gene expression and coactivates the transcriptional function of Nrf1 on the promoter of mtTFA, which directly regulates mitochondrial DNA replication and transcription. Animals with impaired mitochondrial biogenesis had defects in oxidative capacity in BAT and exhibited cold-intolerance in spite of normal transcriptional induction of UCP1, as shown in ERRα knockout mice (Villena et al., 2007). Interestingly, cold acclimation alters the lipid composition of mitochondrial membranes in BAT (Ocloo et al., 2007); this alternation is not UCP1-dependent. But the detailed mechanism is still unclear.

Besides mitochondria, other organelles are also actively involved in lipid metabolism and thermogenesis. For example, peroxisome is the organelle that catabolizes very long chain fatty acids (VLCFA) and branched-chain fatty acid through fatty acid β-oxidation. It has been reported that peroxisome proliferation and peroxisomal β-oxidation are induced by thyroid hormone and cold exposure (Kramar, 1986). The activity of peroxisomal acyl-CoA oxidase (ACOX1), the first and rate-limiting enzyme in fatty acid β-oxidation (Fournier et al., 1994), is increased by 10 fold in rats after exposed to 5^0C for 4 weeks, indicating the involvement of peroxisome in thermogenesis (Nedergaard et al., 1980). The association between peroxisome function and thermogenesis remains to be further explored.

3.3.4 Increased angiogenesis

During cold exposure, BAT requires highly effective energy metabolism for thermogenesis, which consumes a lot of oxygen and induces hypoxia. Correspondingly, genes related to angiogenesis, such as vascular endothelial growth factor (VEGF) and hypoxia-inducible factor 1α (HIF1α) are significantly upregulated in BAT. As reported, the VEGF mRNA level in BAT was increased by 2-3 folds in 4 hours when rats were exposed to 4^0C, but returned to the basal level within 24 hours; while the VEGF expression in other tissues such as heart, kidney and lung was not changed after cold exposure (Asano et al., 1997). Similarly, the gene expression of Hif1α was also increased by 2.5 folds in BAT of mice within 4 hours of cold exposure (Nikami et al., 2005). Interestingly, cold-induced expression of VEGF and Hif1α mRNA also exists in BAT of UCP1-ablated mice, although hypoxia was not induced in these animals (Fredriksson et al., 2005; Nikami et al., 2005). It was concluded that the activation of VEGF and Hif1α was independent of thermogenic oxygen consumption, but directly regulated by adrenergic signaling. Moreover, VEGF receptors seem to play a role in the regulation of thermogenesis. VEGFR2 blockage abolished the cold-induced angiogenesis and significantly impaired nonshivering thermogenic capacity. Unexpectedly, VEGFR1 blockage resulted in the opposite effects, leading to increased adipose vascularity and nonshivering thermogenesis (Xue et al., 2009). The detailed regulation of angiogenesis in response to cold exposure and its effect on thermogenesis remain to be further investigated.

3.3.5 Remodeling of white adipose tissue

Recently, increasing attention has been given to the remodeling of white adipose tissue in response to cold stimulation. Brown fat-like adipocytes derived from non-myf5-lineage can be induced by β3-adrenergic receptor stimulation within WAT (Guerra et al., 1998b; Seale et al., 2008). These cells, named as "brite" or "beige" cells, have a gene expression pattern distinct from either white or brown adipocytes (Wu et al., 2012). Interestingly, the administration of β3-adrenoceptor agonist CL316243 was able to induce the brite cells, while the administration of β1-adrenoceptor agonist xamoterol increased only the number of preadipocytes. This study indicated that preadipocyte recruitment is mediated by β1-adrenoceptor, whereas trans-differentiation of white adipocytes requires β3-adrenoceptor activation (Barbatelli et al., 2010).

3.4 Regulation of thermogenesis

3.4.1 Sympathetic nerve system

Cold-induced thermogenesis in animals is mediated mainly by sympathetic nervous system. Studies have shown that animals treated with blockers of the sympathetic nervous system, or mice lacking noradrenaline or adrenaline by knocking out dopamine β-hydroxylase, or mice with combined targeted disruption of β1, β2, and β3-adrenergic receptors, are cold sensitive (Jimenez *et al*. 2002).

One proposed mechanism of sympathetic regulation is that norepinephrine (NE) released by sympathetic nerve fibers binds to adrenergic receptors (AR), especially β-AR. The activation of β-AR stimulates lipolysis at least in two ways: first, β-ARs in

adipocytes couple to heterotrimeric Gs to increase cyclic AMP (cAMP) level and activate protein kinase A (PKA). PKA is able to phosphorylate various targets like lipase and perilipin to stimulate lipolysis; PKA also activates the p38 MAP kinase pathway to stimulate the transcription of *Ucp1* and *pgc1α* genes for adaptive thermogenesis, mitochondrial biogenesis and fatty acid oxidation. Secondly, β3-ARs in adipocytes could also activate the ERK MAP kinase pathway which in turn activates lipolysis independent of PKA (Collins et al., 2010).

Although β3-adrenergic receptor has higher affinity for norepinephrine, the relative contribution of each β-AR isoform to thermogenesis is still controversial. On the one side, mice treated with agonist of β3-adrenergic receptor have increased oxygen consumption and energy expenditure, indicating an enhanced capability for thermogenesis (Susulic et al., 1995). Affinity studies in isolated brown adipocytes also showed that β3-AR played the leading role in norepinephrine-induced thermogenesis (Zhao J, Cannon, Nergaard 2011). On the other side, the targeted inactivation of β1-AR resulted in hypothermia and limited cold-induced acceleration of energy expenditure, demonstrating that β1-AR plays a role in mediating sympathetic-stimulated thermogenesis in BAT (Ueta et al., 2012). Moreover, studies in β3-AR knockout mice showed that β1-AR signaling activation could fully compensate for β3-AR deficiency in adrenergic activation of glucose uptake in BAT, supporting the role of β1-AR in thermogenesis (Chernogubova et al., 2005). In recent studies, the activation of either β1-AR or β3-AR was able to increase UCP1 mRNA and protein levels in human brown adipocytes differentiated from multipotent adipose-derived stem cells (Chernogubova et

al., 2005; Mattsson et al., 2011). It is speculated that both ARs participate in the regulation of cold-induced thermogenesis in BAT through different mechanisms: it is possible that the stimulation of β1-AR is associated with the proliferation of brown adipocyte precursor cells (Bronnikov et al., 1992); while β3-AR stimulation controls the differentiation and maturation of brown adipocytes and the induction of the expression of BAT-specific genes (Watanabe et al., 2008).

Sympathetic nerve system not only regulates the activation of UCP1-mediated thermogenesis, but also controls angiogenic signaling pathway through regulating VEGF levels in brown adipose tissue. Studies in rats have shown that cold-induced VEGF expression in BAT was abolished by surgical sympathetic denervation, but mimicked by the administration of NE or CL316243, a β3-AR agonist (Asano et al., 1997). Studies in cultured primary mouse brown adipocytes also showed that NE induced VEGF expression by 3-fold in a dose- and time-dependent manner, which was through cAMP / PKA signaling pathway (Fredriksson et al., 2000). Similarly, studies in endothelial cells (Iaccarino et al., 2005), pancreatic cancer cells (Hu et al., 2010), and human umbilical vein endothelial cells (Lamy et al., 2010) demonstrated that β-AR stimulation upregulates VEGF expression and angiogenesis.

3.4.2 Other hormones

In addition to NE, many other hormones participate in the regulation of cold-induced thermogenesis, such as thyroid hormone, leptin, and glucocorticoids (Silva, 2006). Mammals treated with thyroid hormone have increased heat production (Cannon

and Nedergaard, 2010), while mice with targeted disruption of deiodinase 2 (DIO2) exhibited impaired BAT thermogenesis. Specifically, cold-induced upregulation of UCP1 requires a high concentration of local T3, which depends on the activation of deiodinase in BAT, but not closely related to the serum T3 levels (Bianco and Silva, 1987). DIO2 knockout mice exhibited dramatically impaired thermogenesis in BAT, leading to hypothermia during cold exposure and a greater susceptibility to diet-induced obesity (Hall et al., 2010). Moreover, mice with mutated thyroid-stimulating hormone receptor (TSHR) exhibited cold intolerance when exposed to 4 ℃, which can be reversed by exogenous thyroid hormone supplementation, indicating that not only thyroid hormone but also thyroid-stimulating hormone is involved in BAT thermogenesis (Endo and Kobayashi, 2008).

3.4.3 Transcriptional regulators

Cold-induced changes in gene expression are directly regulated by various transcription regulators in BAT. PGC1α is a master regulator of mitochondrial biogenesis, oxidative metabolism and thermogenic function in BAT. Genetic ablation of PGC1α resulted in reduced capacity for cold-induced thermogenesis in mice and a blunted response to cAMP signaling activation in cultured brown adipocytes; while ectopic expression of PGC1α in white adipocytes induced the expression of mitochondrial and thermogenic genes (Puigserver et al., 1998).

PRDM16 is another important transcription regulator that plays a dominant role in regulating BAT development, as well as increasing transcriptional activities of many

other transcription factors, such as PPARα, PPARγ, p53, and several members of the C/EBP family (Kajimura et al., 2009; Seale et al., 2008). PRDM16 also directly binds to PGC1α in addition to inducing PGC1α gene expression (Seale et al., 2007).

Peroxisome proliferator-activated receptors (PPARs) contribute to the regulation of cold-induced thermogenesis through activating UCP1 expression and angiogenesis. The 5'-flanking region of rodent UCP1 gene has putative peroxisome proliferator (PPRE) response elements (Larose et al., 1996; Sears et al., 1996; Silva and Rabelo, 1997). Studies have shown that PPARα activator increased UCP1 mRNA levels in rodent BAT (Barbera et al., 2001; Nedergaard et al., 2005); PPARγ agonist thiazolidinediones also elevated UCP-1 mRNA in rodent BAT (Kelly et al., 1998) and in the cultured human preadipocytes (Digby et al., 1998). Consistently, transgenic mice expressing dominant-negative PPARγ displayed reduced thermogenic function in BAT (Gray et al., 2006). The effects of PPARγ on VEGF expression and angiogenesis vary depending on the cell types. Systemic PPARγ stimulation increased angiogenesis in adipose tissue through the combined production of VEGF and angiopoietin-related protein 4 (ANGPTL4) (Gealekman et al., 2008). Similarly, PPARγ ligand troglitazone increased VEGF expression in human vascular smooth muscle cells (Yamakawa et al., 2000), cultured cardiac myofibroblasts (Chintalgattu et al., 2007), and osteoblasts (Yasuda et al., 2005); whereas PPARγ inhibitor, GW9662, suppressed ox-LDL-induced VEGF expression in cultured bovine articular chondrocytes (Kanata et al., 2006). On the other hand, two previous reports showed that PPARγ ligand inhibited VEGF-mediated angiogenesis in

human retinal pigment epithelial cells and bovine choroidal endothelial cells (Murata et al., 2000) and in chick chorioallantoic membrane model (Aljada et al., 2008).

The rodent UCP1 gene also contains retinoic acid response elements (RARE) in addition to PPRE (Larose et al., 1996). Indeed, both all-trans-RA and 9-cis-RA markedly increased UCP mRNA levels in isolated rat brown adipocytes; while non-BAT cells were less responsive (Larose et al., 1996; Rabelo et al., 1996).

The effect of RA on VEGF and angiogenesis is controversial. Several studies supported that all-trans RA induced the transcription of VEGF promoter in human umbilical vein endothelial cells (Saito et al., 2007), human bronchioloalveolar carcinoma cells (Maeno et al., 2002) and retinoblastoma Y79 cells (Akiyama et al., 2002). Whereas many other studies showed that all-trans RA inhibited VEGF production / secretion and angiogenesis in acute promyelocytic leukemia (Kini et al., 2001), rhabdomyosarcoma cell lines (Gee et al., 2005), human skin keratinocytes (Kim et al., 2006; Lachgar et al., 1999), thyroid cancer cell lines and endothelial cells (Hoffmann et al., 2007). One study pointed out that vascular remodeling and endothelial cell proliferation were regulated by independent signaling hierarchy downstream of RA, indicating that the effect of RA on angiogenesis may be regulated by more than one mechanism (Bohnsack et al., 2004).

4. Lipocalin-2 (LCN2)

4.1 Discovery and distribution of LCN2

Lipocalin 2, also named as neutrophil gelatinase-associated lipocalin (NGAL), was first discovered in human neutrophils (Kjeldsen et al., 1993; Kjeldsen et al., 1994). As a member of lipocalin family, LCN2 has a lipid binding domain constituted by eight stranded antiparallel β-barrel, indicating that LCN2 is able to bind small hydrophobic molecules, such as retinoid, steroid, and fatty acids (LaLonde et al., 1994). The structure of LCN2 is similar to fatty acid binding proteins (FABPs) and retinol binding proteins (RBPs), whereas the cavity in LCN2 is unusually large with more polar and positively charged amino acids compared with other proteins in lipocalin family (Kjeldsen et al., 2000), suggesting that LCN2 may have unique function in lipid binding and transport (Kjeldsen et al., 1993).

LCN2 is highly expressed in uterus, bone marrow, and granulocytes immune cells (Aigner et al., 2007; Huang et al., 1999). Mice at 3 weeks of age also expressed LCN2 in liver, spleen, testis and lungs; however, the expression declined progressively with age, particularly in the liver, kidney and spleen with complete disappearance by the age of 11 weeks in adult mice (Garay-Rojas et al., 1996). In most of the early studies, LCN2 expression was examined in non-adipose tissues. In 2005, LCN2 was first reported to be secreted from adipocytes, since then the role of LCN2 as a new adipokine in metabolism has been widely discussed (Chen et al., 2005; Yan et al., 2007).

4.2 Regulation of LCN2 expression

LCN2 expression is regulated by environmental stress such as hypoxia and infection, as well as metabolic conditions like hyperlipidemia and obesity (Li and Chan,

2011). The promoter region of LCN2 contains the binding sites of transcription factors nuclear factor-κB (NFκB), CCAAT/enhancer-binding protein (C/EBP) (Shen et al., 2006) and glucocorticoid response element (Garay-Rojas et al., 1996), indicating that the expression of LCN2 may be controlled by inflammation and metabolic conditions. Lipopolysaccharide (LPS), interleukin-1β, TNFα, and interleukin-17 are all the inducers of LCN2 gene expression in 3T3-L1 cells (mouse embryo fibroblast cell line), ST2 cells (mouse bone marrow-derived stroma cell line), and A549 cells (adenocarcinomic human alveolar basal epithelial cells) respectively (Karlsen et al., 2010; Shen et al., 2006; Sommer et al., 2009). Dexamethasone and retinoic acid were also reported to increase LCN2 expression in mouse L cells (sarcoma cell line isolated from mouse fibroblasts) through an autocrine mechanism (Garay-Rojas et al., 1996). Additionally, Lcn2 expression is upregulated by administration of X-rays or H_2O_2 in HepG2 cells (Roudkenar et al., 2007) and by thermal stresses in liver, heart and kidney of mice (Roudkenar et al., 2009). Recent studies demonstrated that LCN2 gene expression in adipose tissue was upregulated in genetic and dietary-induced obese rodents (Wang et al., 2007; Zhang et al., 2008), as well as in obese humans (Lee et al., 2010; Panidis et al., 2010; Wang et al., 2007); thiazolidinedione administration reduces LCN2 gene expression in adipose tissue of obese animals (Zhang et al., 2008).

4.3 Function of LCN2

4.3.1 Immune response to bacterial infection

LCN2 is able to bind bacterial ferric siderophores and deprive the bacteria of iron, thus playing a pivotal role in acute immune response to bacterial infection (Flo et al., 2004; Goetz et al., 2002). LCN2-deficient mice exhibited an increased susceptibility to bacterial infection (Berger et al., 2006; Flo et al., 2004; Wu et al., 2010). LCN2 has been used as a biomarker for early detection of bacterial infection in human studies (Behairy et al., 2011).

4.3.2 Inflammation

Although LCN2 is strongly upregulated by pro-inflammatory stimuli (Andre et al., 2006), its role in inflammation is still unclear. Some reports have showed that LCN2 functions as a chemoattractant for neutrophils and plays a pro-inflammatory role in transplanted heart (Aigner et al., 2007; Huang et al., 1999), respiratory mucosa (Bachman et al., 2009), and central nervous system (Lee et al., 2011). Moreover, the intraperitoneal injection of Lcn2 led to the stimulation of neutrophils mobilization in C57/BL6 mice; while neutrophil chemotactic activity was significantly reduced in *Lcn2* KO mice, suggesting that LCN2 is not only a chemoattractant, but also functions in neutrophils adhesion during inflammation (Schroll et al., 2012). Other reports, however, demonstrated that LCN2 had anti-inflammatory effect in 3T3-L1 adipocytes by activating PPARγ and its target genes, as well as attenuating TNFα and LPS-induced cytokine production (Zhang et al., 2008). Therefore, the role of LCN2 in regulating inflammation under different stimuli requires further investigation.

4.3.3 Cancer

LCN2 is over-expressed in many types of non-microbially-associated cancers, including breast, pancreatic, and ovarian carcinomas (Yang and Moses, 2009). Studies have shown that LCN2 facilitates tumorigenesis by promoting tumor cell survival, proliferation, and metastatic potential; blocking LCN2 expression delays or even abrogates tumorigenesis in several types of cancer (Berger et al., 2010; Iannetti et al., 2008; Yang et al., 2009).

4.3.4 Obesity and insulin resistance

As previously mentioned, LCN2 gene expression is increased in the adipose tissue of genetic and diet-induced obese mice, while thiazolidinedione administration significantly reduces LCN2 expression in the adipose tissue of obese animals (Wang et al., 2007; Zhang et al., 2008). In our previous studies, mice lacking LCN2 exhibit increased body fat mass, dyslipidemia, fatty liver and insulin resistance induced by HFD, suggesting that LCN2 plays a protective role against HFD and age-induced insulin resistance (Guo et al., 2010). However, studies from others showed a different role of LCN2 in mediating obesity and insulin resistance. One study concluded that male *Lcn2* KO mice on HFD displayed an improvement in glucose tolerance, but not in insulin sensitivity (Jun et al., 2011). Two studies claimed that reduced LCN2 expression in mice or 3T3-L1 adipocytes improved insulin action (Law et al., 2010; Yan et al., 2007).

Human studies on the association between plasma LCN2 levels and metabolic parameters are also controversial. Wang et al. showed that circulating LCN2

concentration was positively correlated with adiposity, hypertriglyceridaemia, and insulin resistance, but negatively correlated with HDL cholesterol (Wang et al., 2007). One study in patients with type II diabetes confirmed the association between serum LCN2 and fasting triglycerides (Moreno-Navarrete et al., 2010). However, another study in nondiabetic severely obese women showed that circulating LCN2 was associated with obesity but not insulin resistance (Auguet et al., 2011); studies in healthy young men (Liu et al., 2011) and two groups of obese children (Akelma et al., 2012; Kanaka-Gantenbein et al., 2008) also concluded that plasma LCN2 was not related to metabolic parameters. Interestingly, one study pointed out although no differences in plasma LCN2 concentrations were observed, obese individuals showed an increased level and higher activity of circulating LCN2/MMP-9 complex (Catalan et al., 2009), suggesting that using serum LCN2 as an independent marker for obesity and insulin resistance may be more complicated.

To summarize, LCN2 potentially serves as a transporter for hydrophobic molecules, and functions in innate immune system, inflammation, and lipid metabolism. However, it is not clear how LCN2 is regulated by nutrient status, or how LCN2 deficiency affects whole-body metabolism or lipid homeostasis. Since the regulation of LCN2 in adipose tissue has not been investigated, looking into adipose LCN2 regulation and function may give a hint of the function of LCN2 and its association with metabolic diseases such as obesity and insulin resistance.

CHAPTER 2

REGULATION OF ADIPOSE LCN2 EXPRESSION IN RESPONSE TO METABOLIC CHALLENGES AND NUTRIENT SIGNALS

The manuscript authored by Yuanyuan Zhang and Xiaoli Chen is to be submitted.

Yuanyuan Zhang performed all the experiments and wrote this chapter.

SUMMARY

Lipocalin 2 (Lcn2) has been recently characterized as a new adipokine having a role in innate immunity and whole body metabolism. Nonetheless, the metabolic regulation of adipose Lcn2 expression has not been comprehensively studied. To better understand the Lcn2 biology, we investigated the regulation of adipose Lcn2 expression in response to metabolic challenges in mice and nutrient signals in 3T3-L1 adipocytes. Our results showed that the mRNA expression of *Lcn2* gene was significantly upregulated in white and brown adipose tissues as well as liver during 48 h fasting and 5 h acute cold exposure in mice, while changes in Lcn2 protein levels were depot-dependent. In 3T3-L1 adipocytes, the treatment of norepinephrine for 24 h significantly increased the expression, but not secretion of Lcn2 protein. Interestingly, 24 h treatment of insulin stimulated both the expression and secretion of Lcn2 protein in a dose-dependent manner; the magnitude of insulin action was significantly enhanced in the presence of high concentration of glucose, while attenuated when glucose was replaced by 3-O-methyl-d-glucose or by aspirin treatment. Additionally, different types of fatty acids including saturated, mono- and poly-unsaturated fatty acids consistently induced Lcn2 expression and secretion. Our results demonstrated that the expression of adipose Lcn2 is highly responsive to metabolic challenges and nutrient signals, suggesting a potential role of Lcn2 in energy metabolism.

INTRODUCTION

Lcn2 was initially identified as a secreted protein from human neutraphils (Kjeldsen et al., 1993; Kjeldsen et al., 1994). Belonging to the same lipocalin superfamily members of fatty acid binding proteins and retinol binding proteins, Lcn2 also possesses a lipid binding domain, capable of binding small hydrophobic molecules (LaLonde et al., 1994). Lcn2 is highly expressed in uterus, bone marrow, and granulocytes immune cells (Aigner et al., 2007; Huang et al., 1999). Other studies also showed that Lcn2 is expressed in liver, spleen, and kidney of young mice, but the expression level declined with age (Garay-Rojas et al., 1996). Recently, our group and others have discovered that Lcn2 is abundantly expressed and secreted by adipocytes, since then the role of Lcn2 as a new adipokine in metabolism has been explored (Yan et al., 2007; Zhang et al., 2008).

The promoter region of Lcn2 contains the binding sites of nuclear factor-κB (NFκB) and CCAAT enhancer binding protein (C/EBP) (Shen et al., 2006) as well as several response elements including glucocorticoid response element (Garay-Rojas et al., 1996) and estrogen response element (Seth et al., 2002), indicating that the expression of Lcn2 may be controlled by inflammation and metabolic conditions. Indeed, many factors have been reported to induce *Lcn2* gene expression in different types of cells, such as lipopolysaccharide (LPS) and tumor necrosis factor α (TNFα) in human neutrophils (Kjeldsen et al., 1994), dexamethasone and retinoid acid in L cells (sarcoma cell line isolated from mouse fibroblasts) (Garay-Rojas et al., 1996), interleukin-1β in 3T3-L1 cells (mouse embryo fibroblast cell line) (Sommer et al., 2009), interleukin-17 in ST2 cells (mouse bone marrow-derived stroma cell line) and A549 cells (adenocarcinomic

human alveolar basal epithelial cells) (Karlsen et al., 2010; Shen et al., 2006), and X-rays or H_2O_2 in HepG2 cells (Roudkenar et al., 2007). Additionally, Lcn2 expression was found to be increased in response to thermal stresses in liver, heart and kidney of mice (Roudkenar et al., 2009).

However, most of previous studies focused on the regulation of Lcn2 in non-adipose tissues; the metabolic regulation of Lcn2 expression in adipose tissue has not been well studied. Our group and others have reported that adipose Lcn2 is upregulated in genetic and dietary-induced obese rodents, but reduced by thiazolidinedione administration (Wang et al., 2007; Zhang et al., 2008). In this chapter, we used C57BL6 mice and 3T3-L1 adipocytes as *in vivo* and *in vitro* models, respectively to further investigate the expression of adipose Lcn2 in response to metabolic challenges and nutrient signals. We found that *Lcn2* gene expression was significantly upregulated by fasting and acute cold exposure in mice. Insulin treatment stimulated the expression and secretion of Lcn2 protein in 3T3-L1 adipocytes; the magnitude was significantly enhanced by high concentration of glucose, while attenuated by aspirin treatment. Fatty acids also induced Lcn2 expression and secretion in 3T3-L1 adipocytes. The changes in adipose Lcn2 expression in response to metabolic challenges and nutrient signals indicated that Lcn2 may play a role in energy metabolism.

RESULTS

Adipose *Lcn2* gene expression is upregulated during metabolic challenging

It has been reported that Lcn2 is expressed in multiple murine tissues, such as liver, spleen, lung, testis (Garay-Rojas et al., 1996; Yan et al., 2007). Nonetheless, there has been no attempt to compare Lcn2 expression in different depots of adipose tissue. Herein we examined Lcn2 protein expression levels in inguinal adipose tissue (Ing, subcutaneous fat), epididymal adipose tissue (Epi, visceral fat) and brown adipose tissue (BAT) of C57/BL6 male mice at the age of 12 weeks. As shown in Fig 1A, Lcn2 protein abundance was higher in Ing than in Epi adipose tissue or BAT.

We next investigated how adipose Lcn2 expression is regulated in response to metabolic challenges. Male mice at the age of 12 weeks were exposed to 22 ℃ or 4 ℃ for 5 hours; *Lcn2* gene expression in adipose tissue was determined by real-time qPCR. We found that *Lcn2* gene expression was significantly upregulated in all adipose tissue depots examined and liver (Fig 1B). Unlike Lcn2 gene transcription, Lcn2 protein expression levels were regulated differently by cold stimulation. Cold stimulation led to an increase in Lcn2 protein expression in BAT (Fig 1C), while Lcn2 protein levels were decreased in white adipose tissue depots, so were serum Lcn2 levels during cold exposure. To further determine if cold-induced Lcn2 expression in adipose tissue is mediated by adrenergic stimulations, we treated 3T3-L1 adipocytes with 1 μM norepinephrine (NE), an agonist of β3-adrenergic receptor, to examine the direct effect of the adrenergic stimulation on Lcn2 expression in adipocytes. As shown in Fig 1D, NE treatment for 24 hours led to a marked increase in intracellular levels of Lcn2 protein and a slight increase in Lcn2 secretion.

We then determined how Lcn2 expression is altered in response to fasting. The effect of starvation on adipose Lcn2 expression was examined. Compared with mice at

the fed state, the mRNA expression levels of Lcn2 gene had a trend towards an increase in white adipose tissue and liver of male mice with 48 hour fasting (Fig 1E), but Lcn2 protein levels had a trend toward a decrease in white adipose tissues (Fig 1F). Therefore, our result demonstrated that *Lcn2* gene expression was upregulated by cold stimulation and starvation in adipose tissue, whereas Lcn2 protein levels were regulated differently depending on depots.

Glucose and insulin regulation of Lcn2 expression in 3T3-L1 adipocytes

Since the flux of nutrients is changed during cold exposure and fasting, it is of interest to know if Lcn2 expression is regulated by nutrient signals. Glucose and insulin are the important nutrient and hormone that regulate metabolic homeostasis. In this experiment, 3T3-L1 adipocytes were used as a model system to investigate how glucose and insulin directly regulate Lcn2 expression and secretion in adipocytes. Fully-differentiated 3T3-L1 adipocytes were treated with or without 100nM insulin in DMEM containing either high glucose (4.5g/L glucose) or low glucose (1g/L glucose) for 24 hours. In the absence of insulin, intracellular Lcn2 protein levels were higher in adipocytes cultured in low-glucose DMEM compared to those in high-glucose DMEM (Fig 2B), while Lcn2 secretion was not significantly affected. The addition of insulin led to a marked increase in Lcn2 expression and secretion in a dose-dependent manner (Fig 2A). Interestingly, the effect of insulin was more significant in the presence of high glucose than low glucose (Fig 2A, 2B). This result is in line with a previous *ex vivo* study showing that insulin increased Lcn2 production and secretion in cultured adipose tissue

(Tan et al., 2009). Considering that insulin stimulates glucose uptake into adipocytes, we then addressed the question whether the effect of insulin on Lcn2 expression depends on glucose uptake and metabolism. Hence we substituted glucose with 3-O-methyl-d-glucose, a poorly metabolized analog of glucose, and performed the similar experiment. Interestingly, we found that the induction of Lcn2 expression by insulin was significantly abolished in DMEM containing 3-O-methyl-d-glucose (Fig 2C, 2D), suggesting that glucose metabolism is required for the insulin induction of Lcn2 expression and secretion.

Blocking NFκB signaling pathway reduces insulin-stimulated Lcn2 secretion in 3T3-L1 adipocytes

Previous studies have shown that Lcn2 promoter region contains NFκB binding sites (Shen et al., 2006); TNFα and LPS are the two strong inducers of Lcn2 expression in human neutrophils (Kjeldsen et al., 1994). Herein, we examined the effect of TNFα on Lcn2 expression and secretion in adipocytes. Consistent with the previous observations in human neutrophils, TNFα treatment for 24 hours significantly induced the expression and secretion of Lcn2 in a dose-dependent manner (Fig 2E). High glucose is known to induce inflammation and activate NFκB pathway in endothelial cells (Du et al., 1999; Morigi et al., 1998; Pieper and Riaz-ul-Haq, 1997) and vascular smooth muscle cells (Hattori et al., 2000; Yerneni et al., 1999). Our results shown above suggest that insulin stimulates Lcn2 expression and secretion maybe through the glucose-NFκB pathway. To test this hypothesis, we evaluated the consequences of blocking the transduction of NFκB and PI3K signaling pathway on Lcn2 expression and secretion induced by insulin and glucose.

Aspirin and wortmannin were used to inhibit the activation of NFκB and PI3K activation, respectively. Salicylic acid, the main metabolite of aspirin, has been shown to modulate NF-κB activation (McCarty and Block, 2006). Our results demonstrated that the treatment of 5mM aspirin for 24 hours significantly attenuated insulin-stimulated Lcn2 secretion, but increased basal intracellular Lcn2 expression (Fig 2F), suggesting that the effect of insulin and glucose on Lcn2 secretion is possibly mediated by inflammatory pathway.

Wortmannin, on the other hand, blocks insulin signaling pathway by inhibiting phosphatidylinositol 3-kinase (PI3K). As shown in Fig 2F, 24 hour-treatment of 100nM wortmannin didn't significantly affect insulin-stimulated Lcn2 expression or secretion, suggesting that insulin may regulate Lcn2 expression independent of PI3K pathway.

Fatty acids regulate Lcn2 expression in 3T3-L1 adipocytes

In addition to glucose, fatty acids are nutrient signals that play an important role in the control of gene expression. We next determined how different types of fatty acids regulate adipose Lcn2 expression and secretion. Differentiated 3T3-L1 adipocytes were treated with 250 μM palmitate (C16:0), 400 μM oleate (C18:1), or 400 μM eicosapentaenoic acid (EPA C20:5) in presence of 100 μM fatty acid-free BSA and 100nM insulin for various time periods. We found that intracellular and secreted Lcn2 was markedly increased after 12 hour-treatment of palmitate. Similarly, oleate and EPA also induced Lcn2 expression and secretion, although the effect of EPA was less significant compared with palmitate during 12 hour-treatment period (Fig 3A, 3B).

Phytanic acid is a branched chain fatty acid that is metabolized in the peroxisome. Twelve hour-treatment of 10μM phytanic acid markedly reduced intracellular and secreted Lcn2 in 3T3-L1 adipocytes (Fig 3C).

DISCUSSION

Accumulating evidence has linked Lcn2 to obesity, insulin resistance, inflammation, and metabolic diseases (Yan et al., 2007; Wang et al., 2007; Zhang et al., 2008; Law et al., 2010; Guo et al., 2010; Jin et al., 2011; Auguet et al., 2011; Jang et al., 2012). Knowing the regulation of Lcn2 expression could help understand the role of Lcn2 in the pathogenesis of metabolic diseases. However, most of previous studies examined the regulation of Lcn2 expression in non-adipose tissues (Garay-Rojas et al., 1996; Karlsen et al., 2010; Roudkenar et al., 2007; Shen et al., 2006; Sommer et al., 2009). The regulation of adipose Lcn2 expression has not been fully addressed. In this study, we investigated how metabolic challenges and nutrient signals regulate adipose LCN2 expression and secretion. We found that *Lcn2* gene expression was upregulated in adipose tissue of C57 male mice during acute cold exposure and 48 hour fasting. Additionally, we showed that Lcn2 protein expression and secretion was directly regulated by norepinephrine, insulin, glucose, and fatty acids in 3T3-L1 adipocytes.

It has been reported that thermal stress, including both cold and hot stress, could induce Lcn2 gene expression in liver, heart and kidney (Roudkenar et al., 2009), while the expression of Lcn2 in serum and adipose tissue in response to thermal stress was not examined in that study. Our results showed that the gene expression of Lcn2 was upregulated by cold stimulation in all adipose tissues examined, including BAT,

epididymal and inguinal adipose depots as well as liver. The results from 3T3-L1 adipocyte cultures demonstrated that NE treatment for 24 hours significantly increased the abundance of intracellular Lcn2 protein and slightly stimulated Lcn2 secretion in 3T3-L1 adipocytes. This result suggests that increased NE levels may be responsible in part for cold-induced Lcn2 expression in adipose tissues in vivo. However, changes in *Lcn2* gene expression in response to starvation were not consistent with that in Lcn2 protein expression. This discrepancy implies that there might be a post-translational mechanism for the regulation of Lcn2 protein stability and secretion.

In order to explore more evidence for linking Lcn2 to energy metabolism, we determined whether and how nutrient signals regulate Lcn2 expression in adipocytes. First, we examined Lcn2 protein expression and secretion in 3T3-L1 adipocytes under the conditions of low and high glucose in the presence or absence of insulin. Our results showed that insulin treatment for 24 hours significantly increased Lcn2 protein expression and secretion in 3T3-L1 adipocytes, which is consistent with a previous study showing that insulin increased Lcn2 production and secretion in cultured human omental adipose tissue explants (Tan et al., 2009). In the absence of insulin, the low concentration of glucose in the cultured medium led to an increase in intracellular Lcn2 protein levels when compared to the high glucose condition. The addition of insulin dramatically increased Lcn2 protein expression and secretion under both the low and high glucose condition; the insulin effect on the induction of Lcn2 expression and secretion was more prominent in the presence of high concentration of glucose. These results suggest that the effect of insulin on Lcn2 expression is glucose-dependent. To further prove this

hypothesis, we designed an experiment to examine the insulin effect on Lcn2 expression in the presence of 3-O-methyl-d-glucose. Interestingly, insulin-stimulated Lcn2 secretion was blunted by substituting glucose with 3-O-methyl-d-glucose, suggesting that the effect of insulin was partially dependent on glucose metabolism. Wortmannin is known to inhibit insulin signaling transduction responsible for GLUT4 translocation thereby glucose uptake by blocking PI3K-Akt2 pathway activity in adipocytes. More interestingly, blocking PI3K by Wortmannin didn't significantly affect insulin-stimulated Lcn2 protein expression and secretion. All the data together suggest that glucose metabolism in adipocytes rather than just simple glucose uptake is important for mediating insulin regulation of Lcn2 expression and secretion. We further speculate that insulin-stimulated glucose catabolism and possibly ROS production may be attributed to the eventual induction of Lcn2 expression and secretion. Therefore, the detailed molecular signaling pathways mediating insulin regulation of adipose Lcn2 expression and secretion deserve further investigation.

Previous studies have demonstrated that NFκB is a downstream target of Akt activation induced by anti-apoptotic signals such as PDGF in fibroblasts (Ozes et al., 1999; Romashkova and Makarov, 1999). Since NFκB binding site exists in the promoter region of Lcn2, and Lcn2 expression is strongly induced by TNFα and LPS, it is reasonable to speculate that insulin induces Lcn2 expression may be through promoting glucose catabolism (oxidation) and ROS production thereby NFκB activation. Indeed, our results that the insulin stimulation of Lcn2 expression and secretion was significantly

attenuated when NFκB pathway activation was blocked by aspirin support the above hypothesis.

In addition, we looked into the effect of fatty acids (saturate fatty acid, monounsaturated fatty acid and polyunsaturated fatty acid) on Lcn2 expression and secretion in adipocytes. We found that all of three types of fatty acids (palmitate, oleate, and EPA) upregulated Lcn2 expression and secretion in 3T3-L1 adipocytes. However, phytanic acid, a branched fatty acid, significantly reduced Lcn2 protein expression and secretion after 12-hour treatment. Phytanic acid has several unique features. Firstly, unlike other types of fatty acids, phytanic acid cannot undergo β-oxidation in mitochondria due to the presence of the first methyl-group at the 3-position. Instead it is metabolized by α-oxidation in the peroxisome and converted into pristanic acid. Pristanic acid undergoes several rounds of β-oxidation to form medium chain fatty acids which are finally metabolized in mitochondria. Secondly, phytanic acid has been reported to enhance insulin-independent glucose uptake in primary rat hepatocytes (Heim et al., 2002), while other types of fatty acids inhibited glucose uptake (Boden, 2001). Thirdly, phytanic acid and its metabolites have been reported to activate retinoid X receptor (RXR) (Kitareewan et al., 1996) and PPARα (Ellinghaus et al., 1999), promoting peroxisomal and mitochondrial fatty acid oxidation (Gloerich et al., 2005; Hashimoto et al., 2006). Lastly, phytanic acid has been indicated to be positively associated with energy expenditure as an efficient inducer of UCP1 expression and brown adipocyte differentiation (Schluter et al., 2002a; Schluter et al., 2002b). All of the above aspects,

such as peroxisome activity, fatty acid oxidation, energy expenditure, may be associated with the unique regulatory effect of phytanic acid on Lcn2 expression.

In summary, we have demonstrated that Lcn2 expression and secretion in adipocytes is highly regulated by metabolic challenges and nutrient signals. Cold stimulation and fasting increase *Lcn2* gene expression in BAT and WAT in mice. In 3T3-L1 adipocytes, Lcn2 protein expression and secretion are directly regulated by metabolic hormones and nutrient signals. NE stimulates Lcn2 protein expression and secretion. Moreover, insulin stimulates Lcn2 protein expression and secretion in the glucose- and NFκB-dependent manner. Additionally, TNFα, palmitate, oleate, and EPA are all the inducers of Lcn2 expression and secretion. Further studies are needed on the detailed mechanism for the regulation of Lcn2 expression in adipocytes, which will help understand better the role of Lcn2 in the pathogenesis of metabolic diseases.

Figure 1A

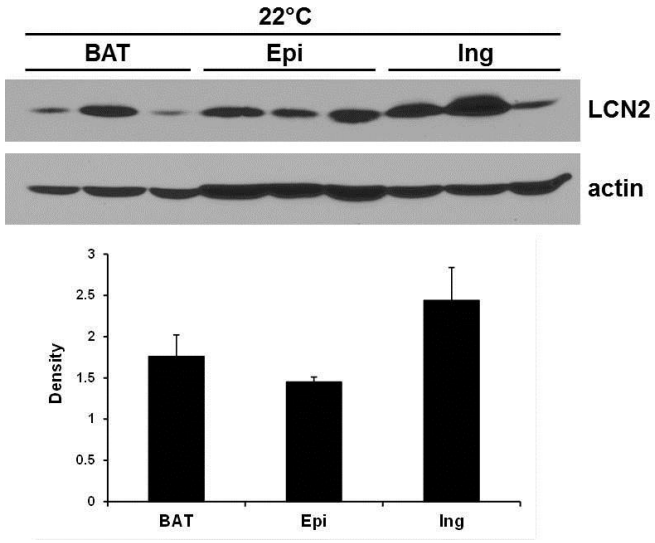

Figure 1A. The expression of Lcn2 in brown adipose tissue (BAT), epididymal adipose tissue (Epi), and inguinal adipose tissue (Ing) of C57/BL6 mice. Adipose tissues were isolated from mice at the age of 12 weeks. Protein levels of Lcn2 and actin were determined by immune-blotting.

Figure 1B

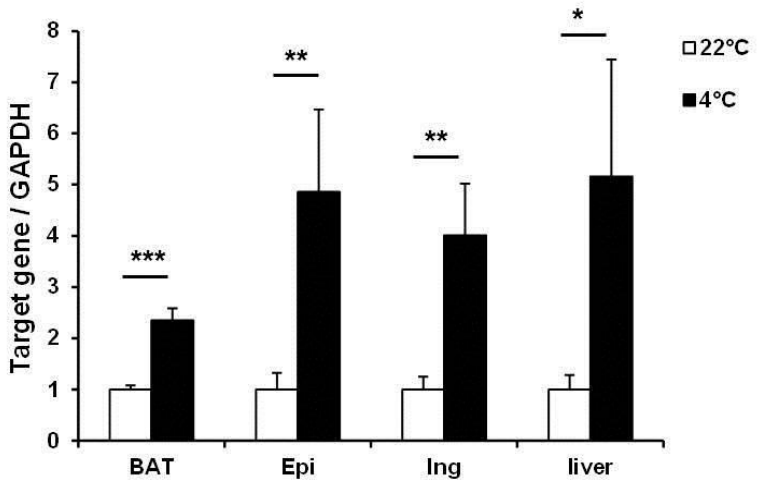

Figure 1B. *Lcn2* gene expression was upregulated by cold stimulation. C57/BL6 mice at the age of 12 weeks were exposed to 22 ℃ (n=6) or 4 ℃ (n=4) for 5 hours. Total RNA was extracted from BAT, Epi, Ing, and liver. The gene expression of *Lcn2* was determined by real-time RT-PCR. The expression levels in cold-adapted mice were normalized to the levels in mice exposed at 22 ℃ and shown as fold changes. The results represented for two independent experiments. * $p<0.05$, ** $p<0.01$, *** $p<0.001$.

Figure 1C

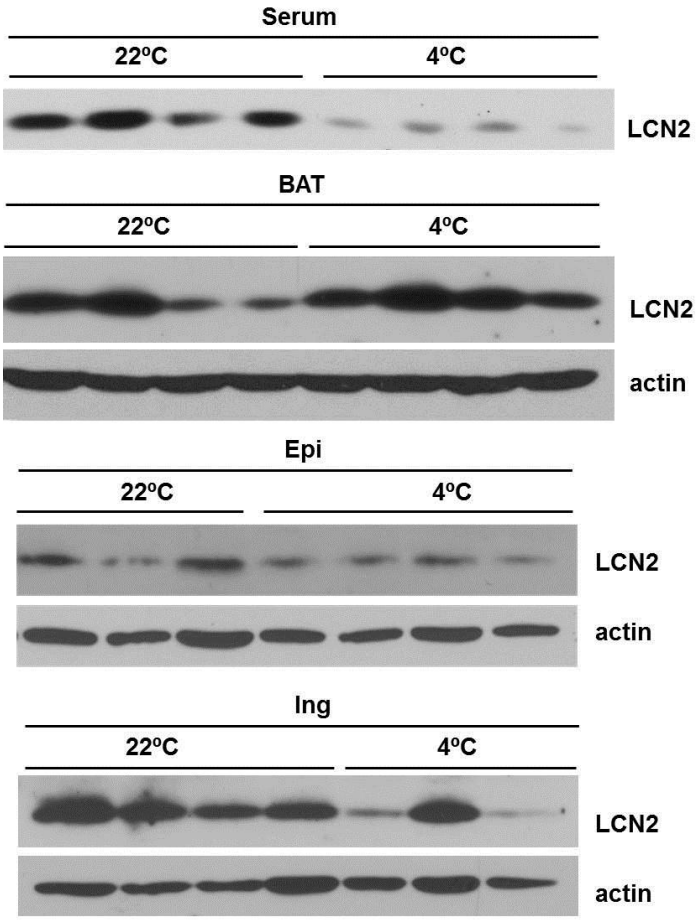

Figure 1C. Lcn2 protein levels were regulated by cold stimulation. C57/BL6 mice at the age of 12 weeks were exposed to 22 ℃ or 4 ℃ for 5 hours. Protein levels of Lcn2 were determined in serum, BAT, Epi and Ing by immune-blotting.

Figure 1D

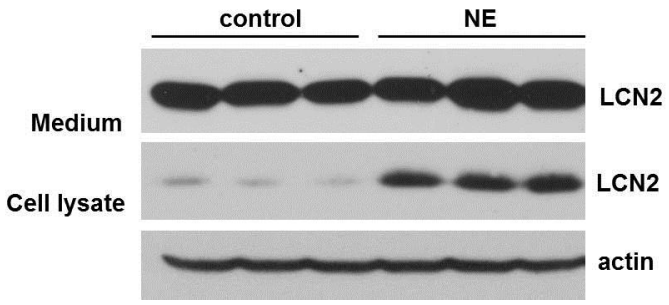

Figure 1D. Norepinephrine increased Lcn2 expression in 3T3-L1 adipocytes. 3T3-L1 cells on day 7 of differentiation were treated with or without 1 μM norepinephrine (NE) for 24 hours. Conditional media and cells were collected to determine Lcn2 protein levels by immune-blotting. The results represented for three independent experiments.

Figure 1E

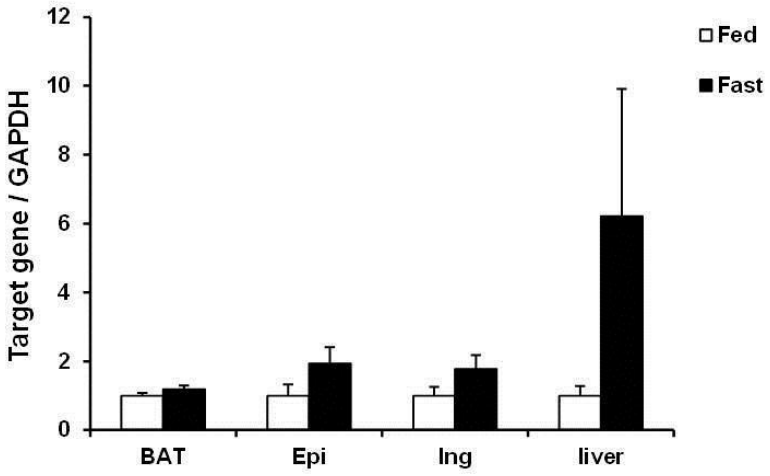

Figure 1E. *Lcn2* gene expression was regulated by starvation. C57/BL6 mice at the age of 12 weeks were sacrificed at fed state (n=6), or at fast state when they were starved for 48 hours (n=4). Total RNA was extracted from BAT, Epi, Ing, and liver. The gene expression of *Lcn2* was determined by real-time RT-PCR. The expression levels in mice at fast and re-fed state were normalized to the levels in mice at fed state, shown as fold changes. The results represented for two independent experiments.

Figure 1F

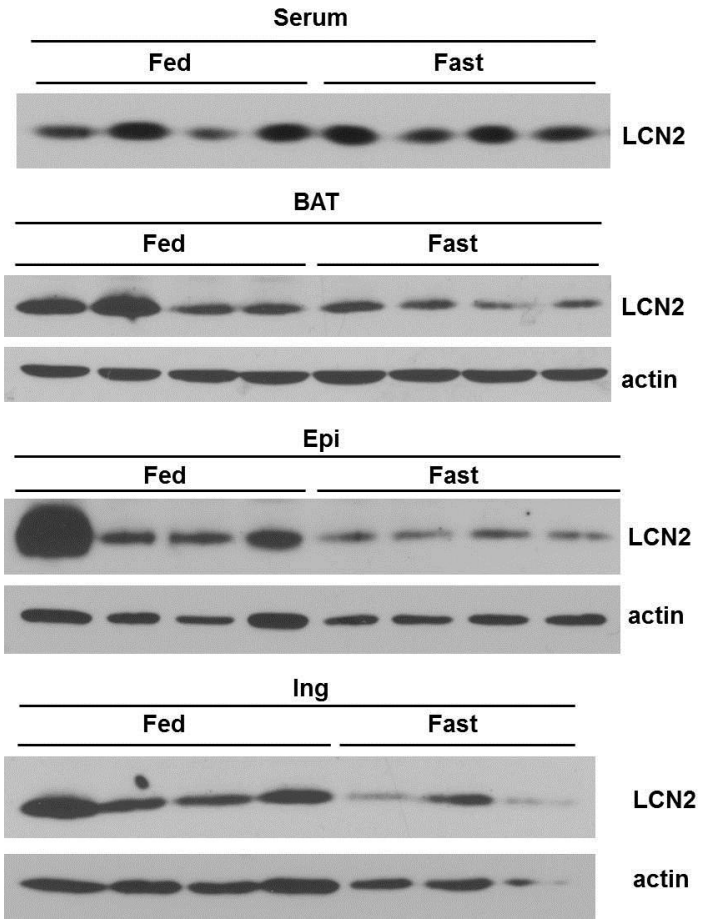

Figure 1F. Lcn2 protein expression was regulated by starvation. C57/BL6 mice at the age of 12 weeks were sacrificed at fed state or at fast state when they were starved for 48 hours. Protein levels of Lcn2 were determined in serum, BAT, Epi and Ing by immune-blotting.

Figure 2A

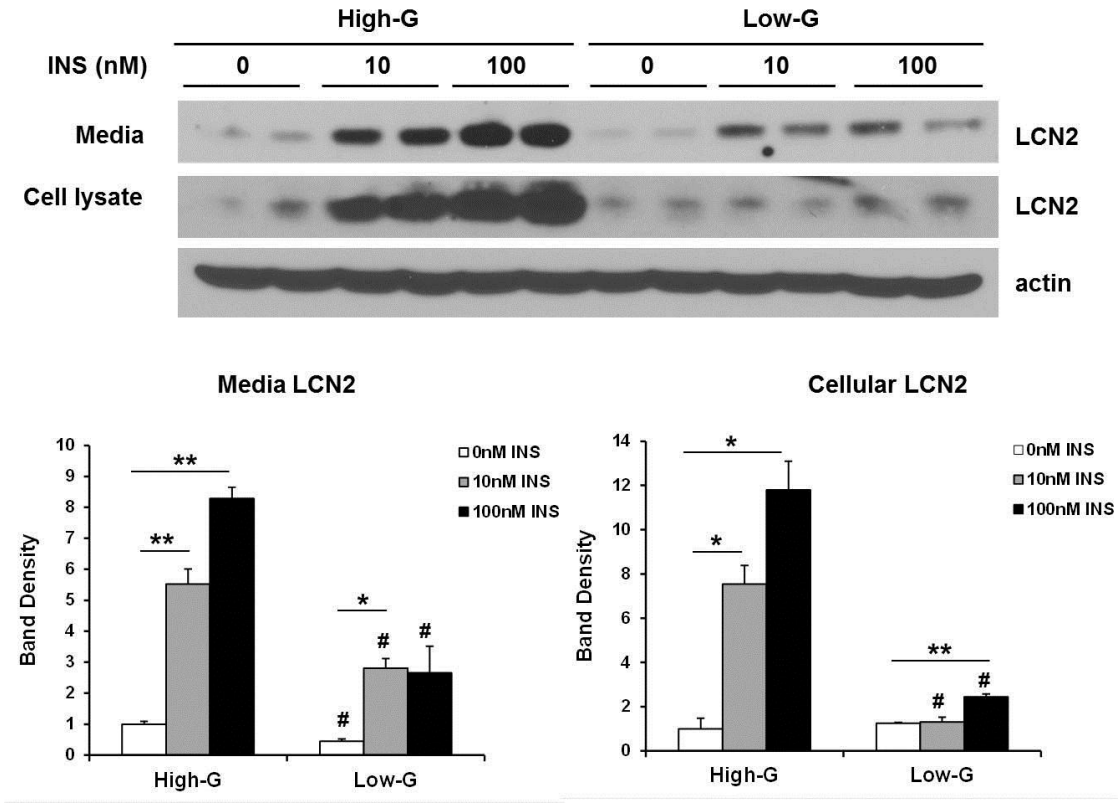

Figure 2A. Lcn2 expression and secretion was upregulated by insulin in a dose-dependent manner in 3T3-L1 adipocytes. On day 7 of 3T3-L1 cell differentiation, culture media were either maintained in DMEM containing high concentration of glucose (4.5g/L) or switched to DMEM containing low concentration of glucose (1g/L). Insulin was added at different concentrations as indicated. Conditional media and cells were collected after 24 hours to determine Lcn2 protein levels by immune-blotting. Lower panels was the quantification of band density, shown as mean ± SE. *or # $p<0.05$, ** $p<0.01$. *Comparison between insulin treatments. # Comparison between glucose treatments.

Figure 2B

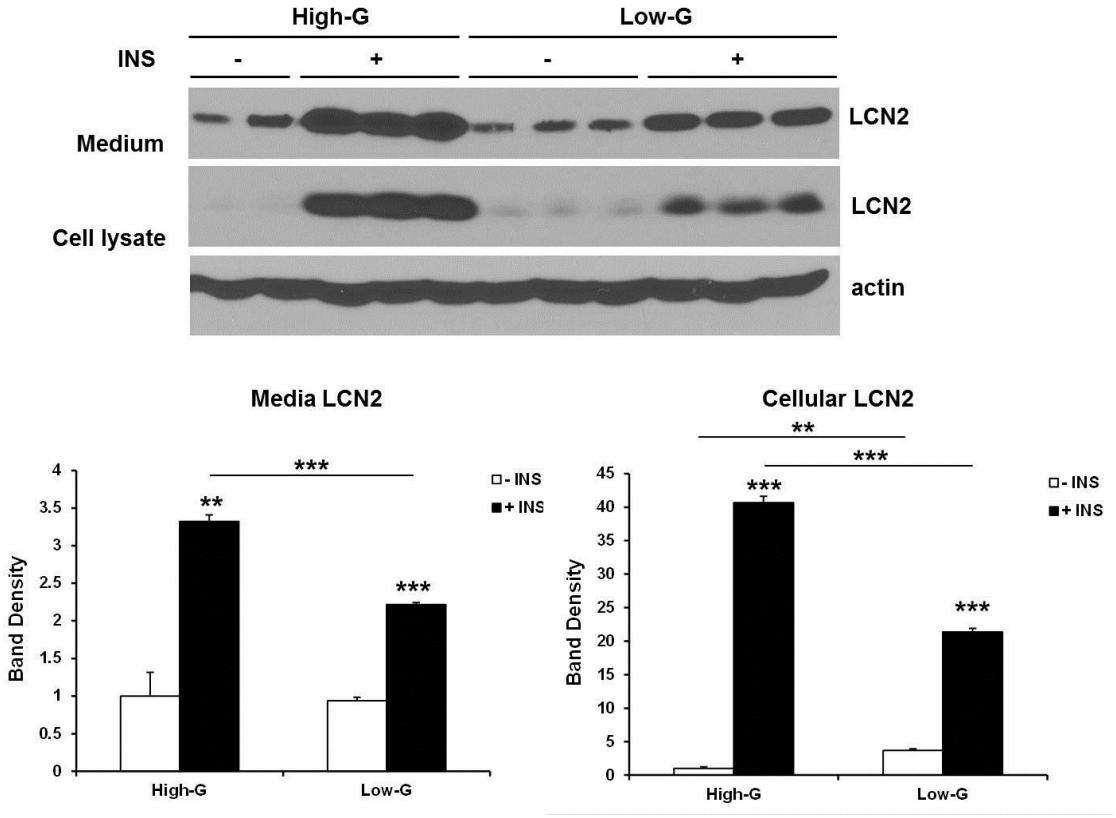

Figure 2B. Lcn2 expression and secretion was upregulated by insulin in 3T3-L1 adipocytes. On day 7 of 3T3-L1 cell differentiation, culture media were maintained as high-glucose DMEM or switched to low-glucose DMEM. 100nM insulin was added in indicated samples. Conditional media and cells were collected after 24-hour treatment to determine Lcn2 protein levels by immune-blotting. The results represented for three independent experiments. Lower panels was the quantification of band density in the blots, shown as mean ± SE. ** $p<0.01$, *** $p<0.001$.

Figure 2C

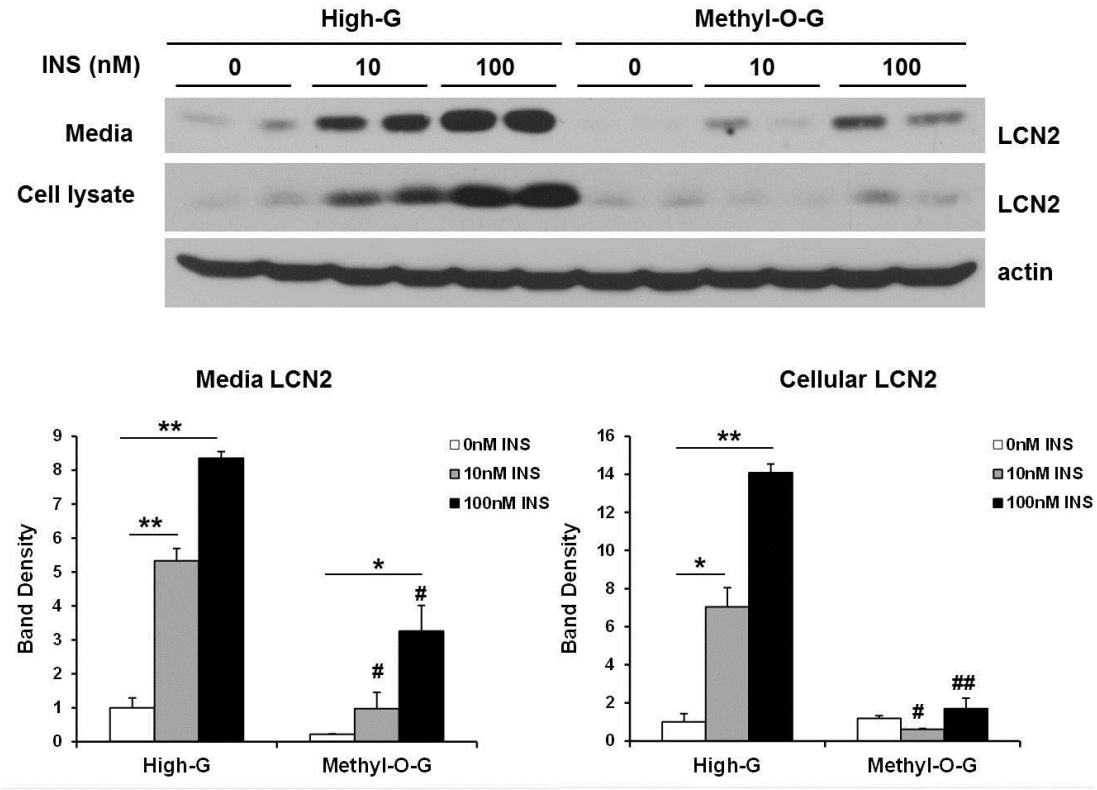

Figure 2C. 3-O-methyl-d-glucose (Methyl-O-G) abolished insulin-stimulated Lcn2 expression and secretion in 3T3-L1 adipocytes. On day 7 of 3T3-L1 cell differentiation, culture media were changed to high-glucose DMEM containing 4.5g/L glucose or DMEM containing 1g/L glucose and 3.5g/L 3-O-methyl-d-glucose. Insulin was added at different concentrations as indicated. Conditional media and cells were collected after 24 hours to determine Lcn2 protein levels by immune-blotting. Lower panels was the quantification of band density, shown as mean ± SE. *or # $p<0.05$, **or ## $p<0.01$. *Comparison between insulin treatments. # Comparison between glucose treatments.

Figure 2D

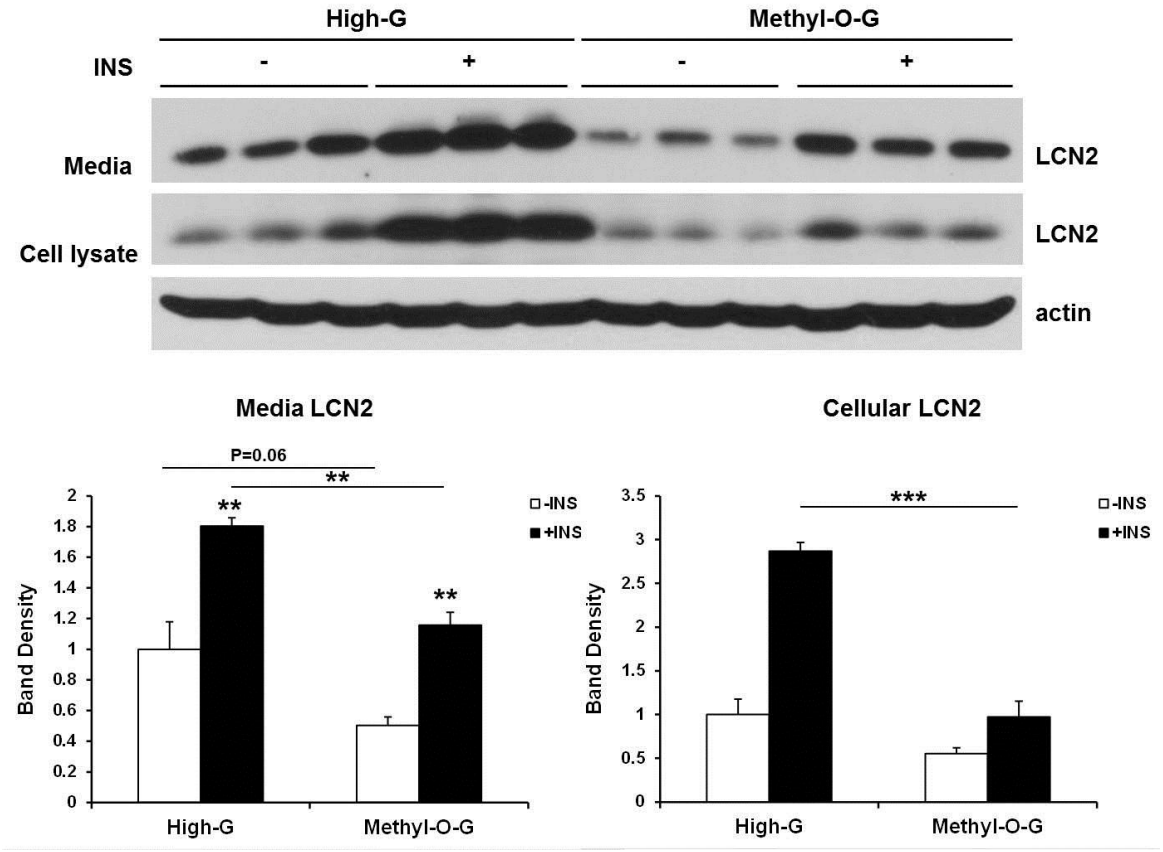

Figure 2D. 3-O-methyl-d-glucose abolished insulin-stimulated Lcn2 expression and secretion in 3T3-L1 adipocytes. On day 7 of 3T3-L1 cell differentiation, culture media were changed to high-glucose DMEM containing 4.5g/L glucose or DMEM containing 1g/L glucose and 3.5g/L 3-O-methyl-d-glucose. 100nM insulin was added in indicated samples during the 24-hour treatment. Conditional media and cells were collected to determine Lcn2 protein levels. The results represented for two independent experiments. Lower panels was the quantification of band density in the blots, shown as mean ± SE. ** $p<0.01$, *** $p<0.001$.

Figure 2E

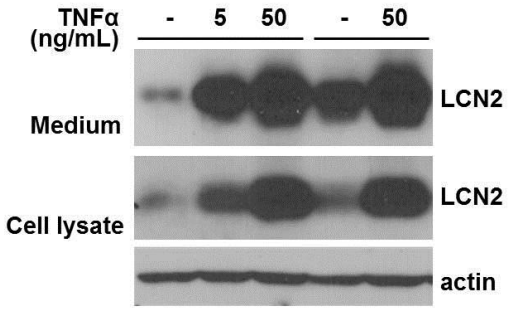

Figure 2E. Lcn2 expression and secretion was stimulated by TNFα in 3T3-L1 adipocytes. 3T3-L1 cells on day 8 of differentiation were starved in DMEM containing 1mg/mL glucose and 0.5% BCS for 12 hours, followed by treatment with TNFα at indicated concentrations for 24 hours. Conditional media and adipocytes were collected to determine Lcn2 protein levels by immune-blotting. The results represented for three independent experiments.

Figure 2F

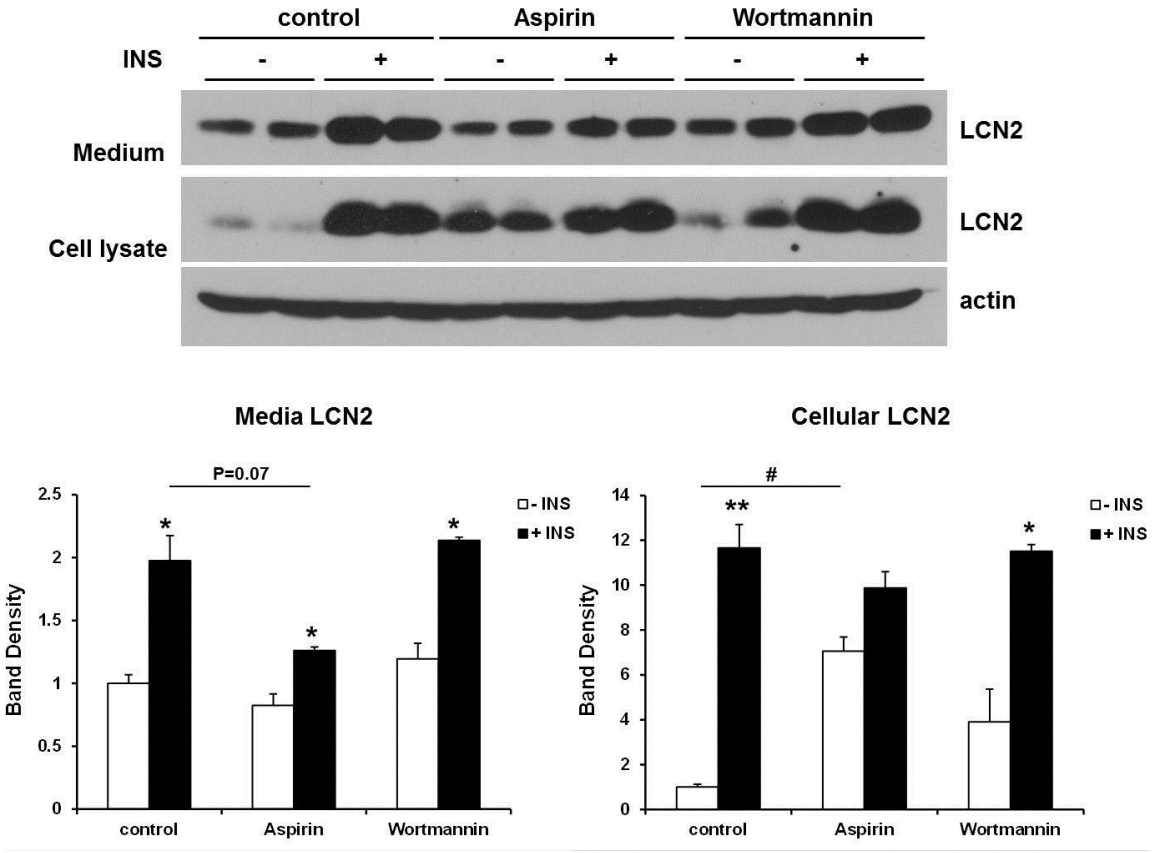

Figure 2F. Aspirin attenuated insulin-stimulated Lcn2 secretion in 3T3-L1 adipocytes. 3T3-L1 adipocytes on day 7 of differentiation were treated with 5mM aspirin or 100nM wortmannin in high-glucose DMEM for 24 hours. 100nM insulin was present in the samples as indicated. Conditional media and cells were collected to determine Lcn2 protein levels by immune-blotting. The results represented for three independent experiments. Lower panels was the quantification of band density in the blots, shown as mean ± SE. * $p<0.05$, ** $p<0.01$.

Figure 3A

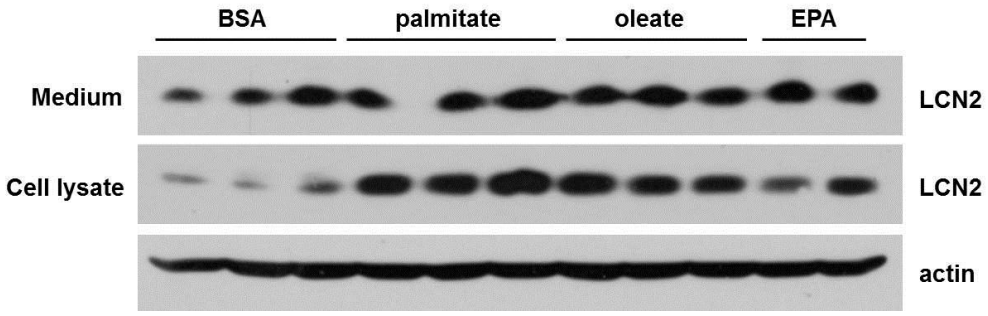

Figure 3A. The effect of 12-hour treatment of fatty acids on Lcn2 expression. 3T3-L1 cells were induced to differentiate into adipocytes. On day 7 of differentiation, cells were serum-free starved but incubated with 100nM insulin for overnight. Then the cells were treated with BSA/fatty acids in low-glucose media containing 5.5mM glucose in presence of 100nM insulin. The concentrations of fatty acids were as follows: 100 μM fatty acid-free BSA as control; 250 μM palmitate (palmitate:BSA=2.5:1); 400 μM oleate (oleate:BSA=4:1); 400 μM EPA (EPA:BSA=4:1). Conditional media and cells were collected after 12-hour treatment to determine Lcn2 protein levels by immune-blotting. The results represented for two independent experiments.

Figure 3B

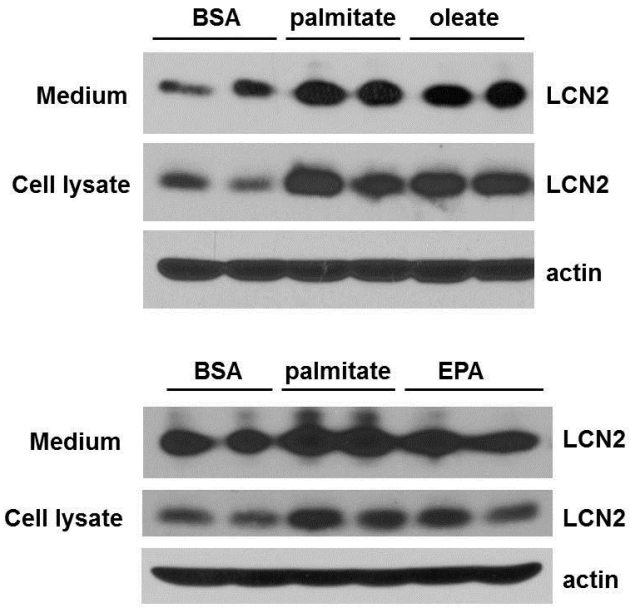

Figure 3B. The effect of 24-hour treatment of fatty acids on Lcn2 expression. 3T3-L1 adipocytes on day 7 of differentiation were incubated with 100nM insulin in serum-free DMEM for overnight. Then the cells were treated with 100 µM BSA plus 250 µM palmitate or 400 µM oleate or 400 µM EPA in low-glucose media in presence of insulin. Conditional media and cells were collected after 24 hours to determine Lcn2 protein levels by immune-blotting. The results represented for two independent experiments.

Figure 3C

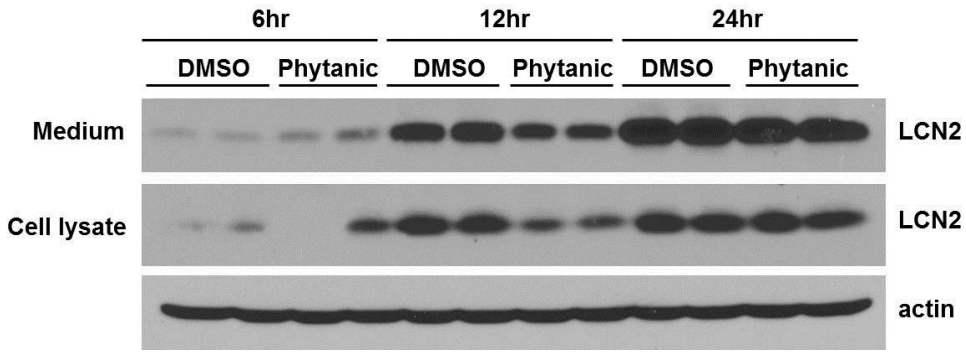

Figure 3C. The effect of phytanic acid on Lcn2 expression. 3T3-L1 adipocytes on day 7 of differentiation were starved in serum-free media in presence of 100nM insulin for overnight. Then the cells were treated with DMSO or 10μM phytanic acid for various time periods as indicated. Conditional media and cells were collected for determining Lcn2 protein levels by immune-blotting. The results represented for two independent experiments.

CHAPTER 3

THE ROLE OF LCN2 IN DIET-INDUCED OBESITY AND INSULIN RESISTANCE

This chapter is modified from two original publications:

Guo H, Jin D, Zhang Y, Wright W, Bazuine M, Brockman DA, Bernlohr DA, Chen X. (2010). *Diabetes*, 59(6):1376-85.

Jin D, Guo H, Bu SY, Zhang Y, Hannaford J, Mashek DG, Chen X. (2011). *FASEB J*, 25(2):754-64.

Guo H, Jin D, and Zhang Y equally contributed to the work published in *Diabetes*

Yuanyuan Zhang performed experiments from Fig 4C, 4D, 4F, 5A, 5C, 7A, 7B, and wrote the corresponding text sections.

SUMMARY

Lipocalin 2 (Lcn2) belongs to the lipocalin subfamily of low-molecular mass-secreted proteins that bind small hydrophobic molecules. Lcn2 has been recently characterized as an adipose-derived cytokine, and its expression is upregulated in adipose tissue in genetically obese rodents. The objective of this study was to investigate the role of LCN2 in diet-induced insulin resistance and metabolic homeostasis in vivo. We found that *Lcn2* KO mice were more susceptible to develop obesity, insulin resistance, dyslipidemia and fatty liver disease upon the HFD feeding. Additionally, we investigated the role of Lcn2 in PPARγ activation and function via assessing the insulin sensitization and fatty acid homeostasis of PPARγ agonist in HFD-induced obesity in *Lcn2* KO mice. We found that rosiglitazone (Rosi) significantly improved insulin sensitivity in *Lcn2* KO mice as effectively as in wild-type (WT) mice; unfed-state levels of blood glucose, free FAs, and triglycerides (TGs) were significantly reduced after a 25-d treatment of Rosi in *Lcn2* KO mice. However, Rosi action on fat deposition and FA homeostasis was altered; Rosi-induced body weight and subcutaneous fat gain and liver lipid accumulation were markedly lessened in *Lcn2* KO mice. We demonstrate that Lcn2 plays a critical role in lipid metabolism and metabolic homeostasis and that Lcn2 is a critical selective modulator of PPARγ activation and function in lipid homeostasis and energy expenditure.

INTRODUCTION

Adipose tissue plays a central role in the control of body weight homeostasis, inflammation, and insulin sensitivity by regulating lipid storage and releasing a variety of

adipokines/cytokines (Hajer et al., 2008; Waki and Tontonoz, 2007). Lipocalin 2 (Lcn2), also known as neutrophil gelatinase-associated lipocalin (NGAL), is a newly identified adipokine which belongs to the lipocalin subfamily (Yan et al., 2007; Zhang et al., 2008). Similar to other members in lipocalin family such as fatty acid binding proteins and retinol binding proteins, Lcn2 has a β-barrel motif which constitutes a lipid binding domain, indicating its capability of binding small hydrophobic molecules, such as retinoids, porphyrins, steroid, and fatty acids (LaLonde et al., 1994). Previous studies have shown that Lcn2 is able to bind bacterial ferric siderophores and functions in acute immune response to bacterial infection (Flo et al., 2004; Goetz et al., 2002). We and other groups have demonstrated that Lcn2 expression is upregulated in genetic and diet-induced obese rodents, while rosiglitazone (Rosi) administration significantly reduced Lcn2 expression in adipose tissue of obese animals (Wang et al., 2007; Zhang et al., 2008). Moreover, exogenous Lcn2 protein suppressed tumor necrosis factor α (TNFα) and lipopolysaccharide-induced chemokine production in cultured adipocytes and macrophages, revealing the anti-inflammatory function of Lcn2 (Zhang et al., 2008).

Peroxisome proliferator-activated receptor gamma (PPARγ) is a nuclear receptor that regulates fatty acid and glucose metabolism, especially in the adipose tissue. PPARγ recruits coactivators or corepressors to regulate gene transcriptions via transactivation or transrepression mechanism (Rosenfeld et al., 2006). The activation of PPARγ stimulates lipid uptake and adipogenesis in the adipose tissue, thus attenuating lipotoxicity and improving insulin sensitivity (Vasudevan and Balasubramanyam, 2004). Thiazolidinedione (TZD) drugs like Rosi are strong agonists of PPARγ; they exert insulin

sensitizing effects, ameliorate dyslipidemia and reduce inflammatory response by activating PPARγ. Meanwhile, TZD drugs also have long-term adverse effects, such as weight gain, fluid retention, and increased risk of heart failure (Guan et al., 2005; Lipscombe et al., 2007).

In this chapter, we investigated the metabolic consequences of Lcn2 deficiency in mice under regular chow diet (RCD) or HFD feeding conditions. We found that the ablation of Lcn2 profoundly exacerbated HFD-induced obesity, dyslipidemia and insulin resistance, indicating that Lcn2 is actively involved in lipid turnover and whole-body energy metabolism. We also examined the metabolic effects of Rosi in HFD-fed WT and *Lcn2* KO mice. Our results showed that the insulin-sensitizing effect of Rosi was retained, while Rosi-induced weight gain and lipid accumulation in liver and subcutaneous fat were markedly lessened in *Lcn2* KO mice.

RESULTS

Lcn2 KO mice are more susceptible to diet-induced obesity

WT and *Lcn2* KO mice were fed RCD or HFD for 12 weeks since the age of 3 weeks. As shown in Fig 4A-B, the body weight of *Lcn2* KO mice was significantly higher than that of WT mice on RCD or HFD. Correspondingly, the tissue weight of epididymal fat, inguinal fat, brown fat, and liver was all higher in HFD-fed *Lcn2* KO mice (Fig 4C-D). To investigate whether increased liver weight in *Lcn2* KO mice was associated with excess lipid accumulation, we measured triglyceride content in liver and

performed oil-red o staining in the liver section. As shown in Fig 4E-F, the liver of *Lcn2* KO mice demonstrated higher triglyceride content and larger lipid droplets in comparison with WT mice. The food intake or energy expenditure in WT and *Lcn2* KO mice didn't exhibit any significant difference as measured by indirect calorimetry (data not shown).

Lcn2 deficiency aggravates diet-induced dyslipidemia and insulin resistance

In order to investigate whether increased ectopic adiposity was associated with dyslipidemia or insulin resistance, we analyzed the serum parameters in WT and *Lcn2* KO mice. As shown in Table 1, serum glucose and insulin levels in *Lcn2* KO mice were significantly higher, while adiponectin levels were significantly lower compared with WT mice. Moreover, *Lcn2* KO mice on RCD had higher serum levels of triglycerides, cholesterol, and free fatty acids than WT (Table 2). Although HFD feeding did not further induce serum levels of triglyceride or cholesterol in *Lcn2* KO mice, it augmented LDL and β-hydroxybutyrate levels. All these data, combined with higher triglyceride content in liver, indicate that *Lcn2* KO mice on HFD developed dyslipidemia.

Next we performed glucose tolerance test (GTT) and insulin tolerance test (ITT) on WT and *Lcn2* KO mice at the age of 16 weeks to further assess systemic insulin sensitivity in the absence of Lcn2. As show in Fig 5A-D, *Lcn2* KO mice were more glucose intolerant and insulin resistant than WT mice upon HFD feeding, suggesting that HFD-induced insulin resistance was exaggerated by Lcn2 deficiency.

TZD rescues diet-induced dyslipidemia and insulin resistance in *Lcn2* KO mice

Previously we have shown that adipose PPARγ expression was decreased in the absence of Lcn2 (Zhang et al., 2008). Considering that PPARγ is a critical regulator for fatty acid and glucose metabolism in the adipose tissue, while *Lcn2* KO mice developed insulin resistance and dyslipidemia, we hypothesized that LCN2 was important for the full action of PPARγ in the improvement of the diabetic state. To test this hypothesis, we examined the metabolic effect of PPARγ agonist in HFD-fed *Lcn2* KO mice.

TZD is a class of medications used in the treatment of type II diabetes. They exert insulin sensitizing effects, ameliorate dyslipidemia and reduce inflammatory response by activating PPARγ (Vasudevan and Balasubramanyam, 2004). We treated HFD-fed WT and *Lcn2* KO mice with Rosi, a derivative of TZD, by oral gavage. GTTs and ITTs were performed after 14 and 20 days of Rosi treatment respectively. As shown in Fig 6A-D, Rosi effectively improved glucose intolerance and insulin resistance in both WT and *Lcn2* KO mice, indicating that Lcn2 deficiency didn't affect the insulin-sensitizing effect of Rosi.

Lcn2 deficiency diminishes the effects of Rosi on weight gain and lipid accumulation

Some side effects of TZD have been documented as a result of increased uptake and storage of fatty acids, such as weight gain, increased subcutaneous fat mass, liver lipid accumulation, and fluid retention. Consistent with previous studies, we observed that Rosi administration significantly increased body weight, as well as the tissue weight of inguinal fat pad and BAT in WT mice (Fig 7A-B). Interestingly, Rosi-induced weight gain was attenuated in *Lcn2* KO mice (Fig 7A). Meanwhile, the increase in inguinal fat

mass was also abolished; liver weight was even significantly reduced by Rosi treatment in *Lcn2* KO mice (Fig 7B). Consistently, liver triglyceride content in WT mice showed a 2-fold increase after Rosi treatment, which was not observed in *Lcn2* KO mice (Fig 7C). Furthermore, we measured the in vivo incorporation of [^{3}H] H_2O into fatty acids in the adipose tissue of HFD-fed WT and *Lcn2* KO mice. As shown in Fig 7D, Rosi significantly increased the level of ^{3}H-labeled fatty acids in epididymal adipose tissue of WT mice, but marked reduced the synthesis of ^{3}H-labeled fatty acids in *Lcn2* KO mice, indicating that Lcn2 deficiency completely blocked or even reversed the effect of Rosi on *de novo* lipogenesis in the adipose tissue. In conclusion, these results clearly demonstrated that Rosi-induced weight gain and lipid accumulation in liver and adipose tissue were abolished in the absence of Lcn2, indicating the regulatory role of Lcn2 in PPARγ-mediated anabolic metabolism.

DISCUSSION

We showed that lack of LCN2 in mice potentiates HFD-induced obesity, dyslipidemia, fatty liver, glucose intolerance, and insulin resistance; TZD improved glucose homeostasis and systemic insulin sensitivity in HFD-fed Lcn2 KO mice without increasing weight gain and subcutaneous fat mass as compared with WT mice. Therefore, we conclude that LCN2 plays a critical role in lipid metabolism and diet-induced obesity and insulin resistance, possibly through the modulation of PPARγ activity.

Lcn2 KO mice gained more body weight than WT mice with HFD feeding; the increased body weight may come from increased fat mass as well as enlarged organs

(Fig5C-D). On one hand, *Lcn2* KO mice possessed larger adipocytes in epididymal and inguinal adipose tissue than WT mice on RCD, as measured by Multisizer Analysis (data not shown). On the other hand, *Lcn2* KO mice had a higher level of lipid accumulation in liver than WT mice, as demonstrated by the oil red O staining. All these data indicate that Lcn2 deficiency interferes with lipid metabolism. Indeed, dyslipidemia is another prominent feature perceived in *Lcn2* KO mice, which is likely due to the impaired regulation of lipid metabolism in adipose tissue and liver in *Lcn2* KO mice. We showed that *Lcn2* KO mice on an RCD had higher serum triglycerides levels than WT mice, but the serum triglyceride levels in HFD-fed *Lcn2* KO mice were lower as compared with WT mice (Table 2). The lower serum triglycerides could be due to the increased triglycerides synthesis and decreased VLDL (or triglyceride) secretion into the circulation as a result of fatty liver in HFD-fed *Lcn2* KO mice. This explanation is strengthened by a previous study in liver insulin receptor KO mice, which also exhibited hepatic insulin resistance and significantly decreased serum triglyceride levels (Biddinger et al., 2008).

In most cases, the administration of full PPARγ agonist like Rosi promotes lipid uptake and storage in the adipose tissue, improves systemic insulin sensitivity, reduces inflammation, and inevitably increases fat mass and body weight. Previous studies have demonstrated that TZD administration stimulates fat gain selectively in subcutaneous regions in humans (Mori et al., 1999; Smith et al., 2005), which was consistent with what we observed in WT mice on Rosi treatment (Fig 7B). Interestingly, the insulin-sensitizing effect of Rosi was retained in *Lcn2* KO mice, but the side effect of Rosi on body weight and fat mass was abolished (Fig 6). This result suggested that adipogenesis and insulin

sensitivity are differentially regulated by PPARγ activation. Indeed, some of previous studies support the idea that PPARγ can be partially activated. For example, phosphorylation of PPARγ at serine 273 by protein kinase cdk5 didn't alter its adipogenic capacity, but led to dysregulation of multiple genes associated with insulin sensitivity (Choi et al., 2010). The author concluded that partial PPARγ agonists may exert insulin-sensitizing effect without altering the adipogenic function of PPARγ. Another example is the development of non-TZD selective partial agonists of PPARγ. MBX-102, for example, retains effective anti-diabetic properties without inducing weight gain or lipid accumulation, through its weak transactivation but strong transrepression activity of PPARγ (Gregoire et al., 2009). Therefore, it is likely that Lcn2 may interfere with PPARγ activation at the level of the recruitment of coactivators/corepressors. In the absence of Lcn2, PPARγ is only partially or selectively activated by TZD.

In summary, we found that Lcn2 deficiency potentiated diet-induced obesity, dyslipidemia and insulin resistance in mice. Rosi administration exerted insulin-sensitizing effect but failed to induce weight gain or subcutaneous fat-mass increase in HFD-fed *Lcn2* KO mice. Our data provided new insight into the role of LCN2 in the regulation of PPARγ activation and lipid homeostasis. In this manner, LCN2 may be a potential therapeutic target for controlling obesity-associated type II diabetes and metabolic complications.

Figure 4A

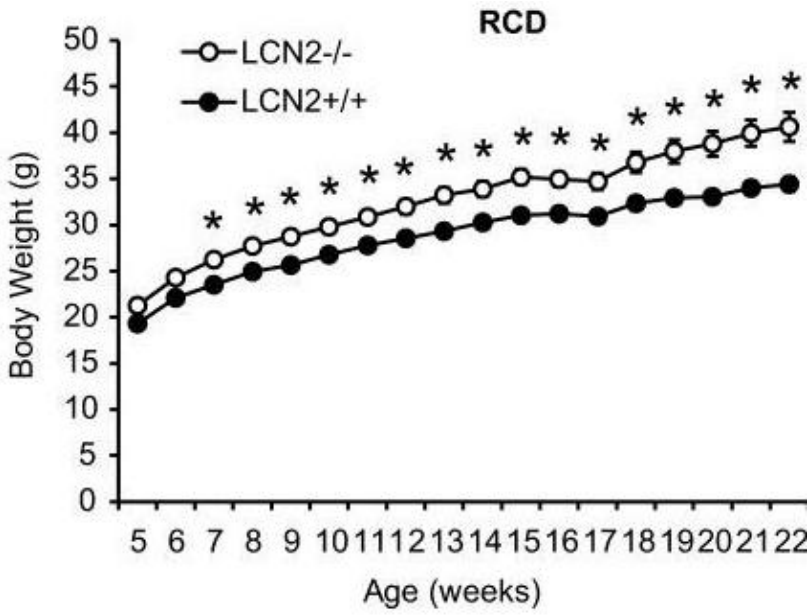

Figure 4A. Growth curve of WT and *Lcn2* KO mice on RCD (n=13). * $p<0.05$

Figure 4B

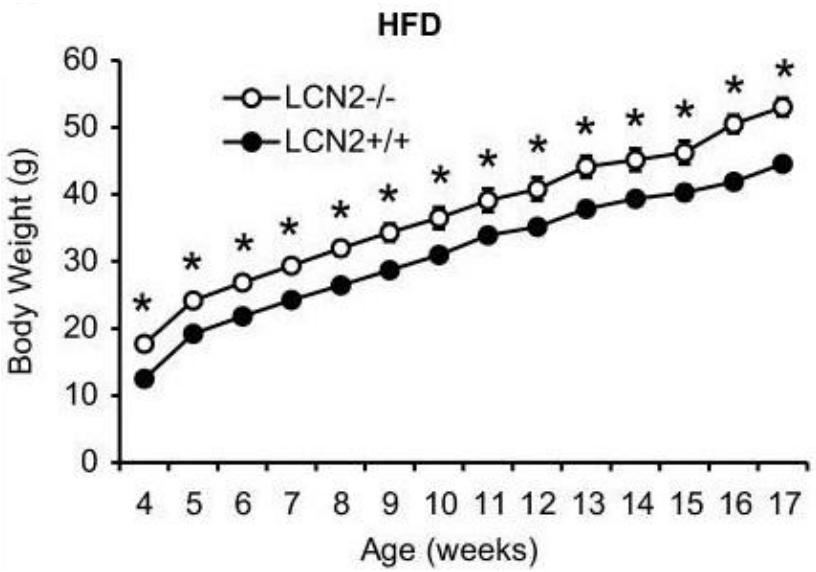

Figure 4B. Growth curve of WT and *Lcn2* KO mice on HFD (n=10-14). * $p<0.05$

Figure 4C

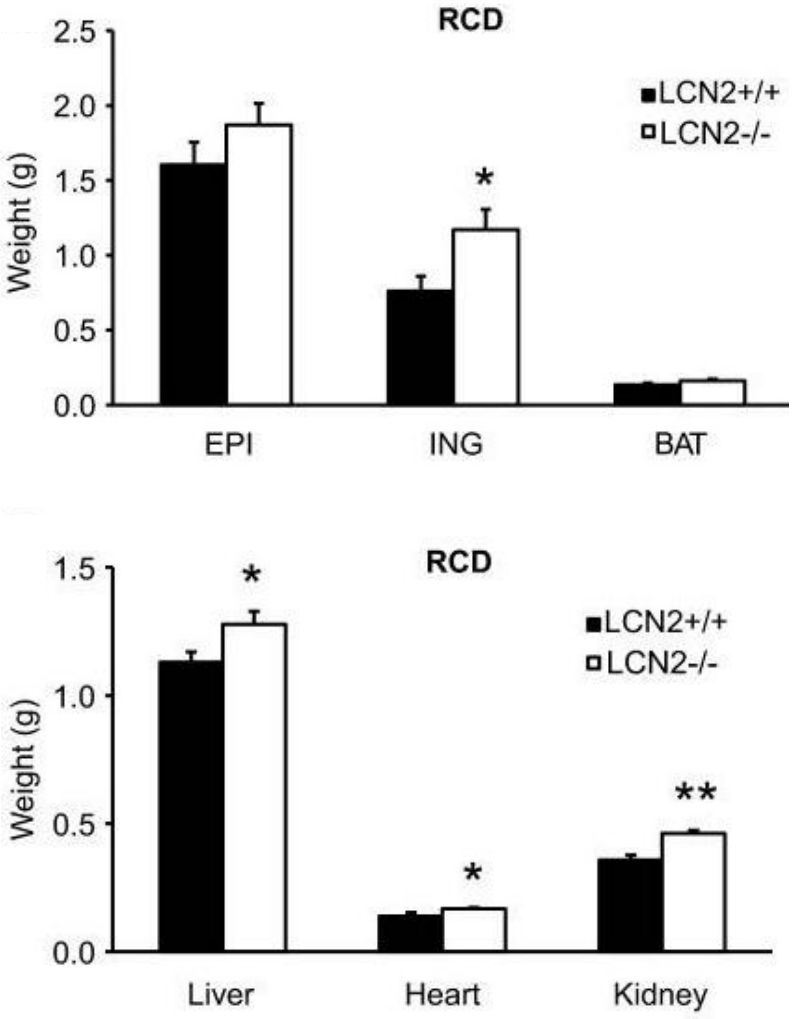

Figure 4C. Tissue weight of WT and *Lcn2* KO mice on RCD at the age of 30 weeks. The data were represented as mean ± SE.* $p<0.05$, ** $p<0.01$.

Figure 4D

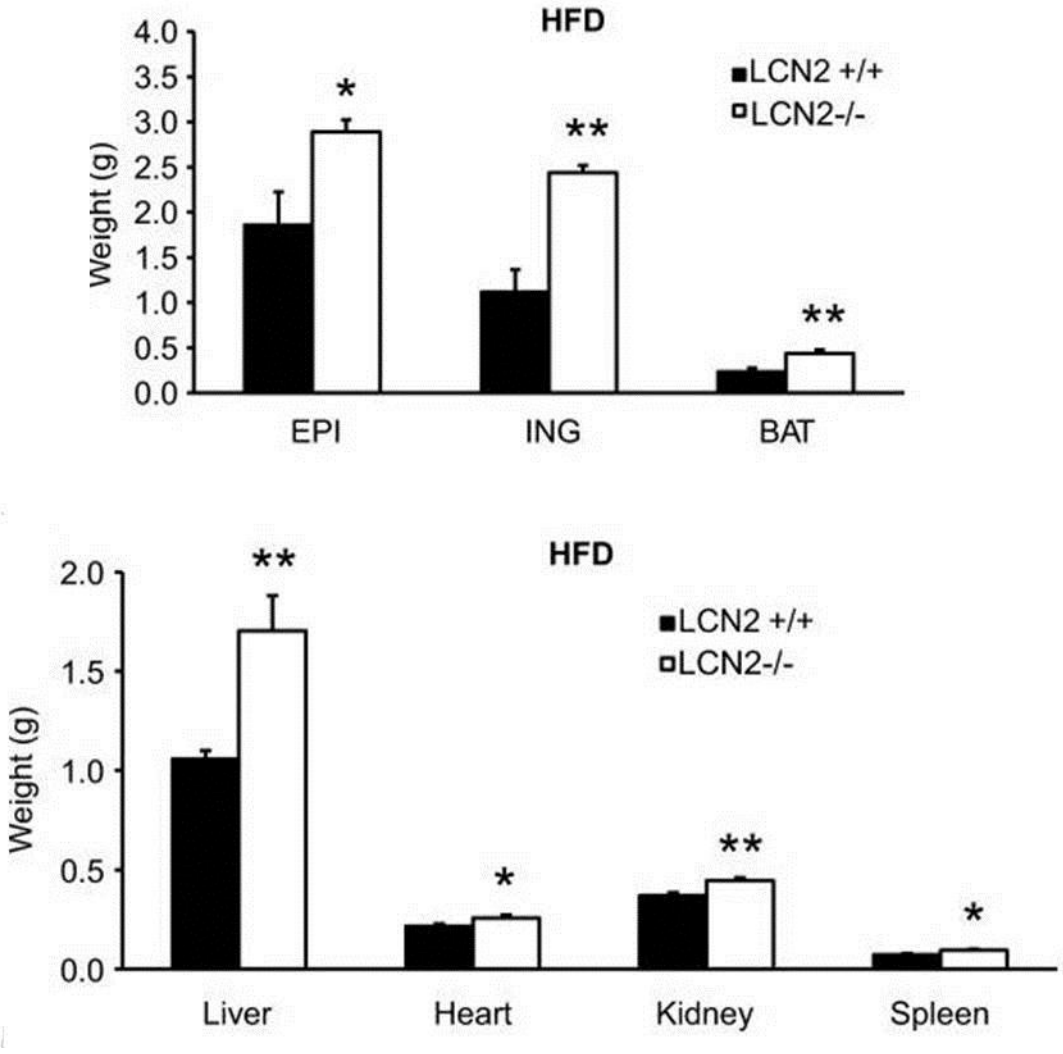

Figure 4D. Tissue weight of WT and *Lcn2* KO mice on HFD at the age of 16 weeks. The data were represented as mean ± SE.* $p<0.05$, ** $p<0.01$.

Figure 4E

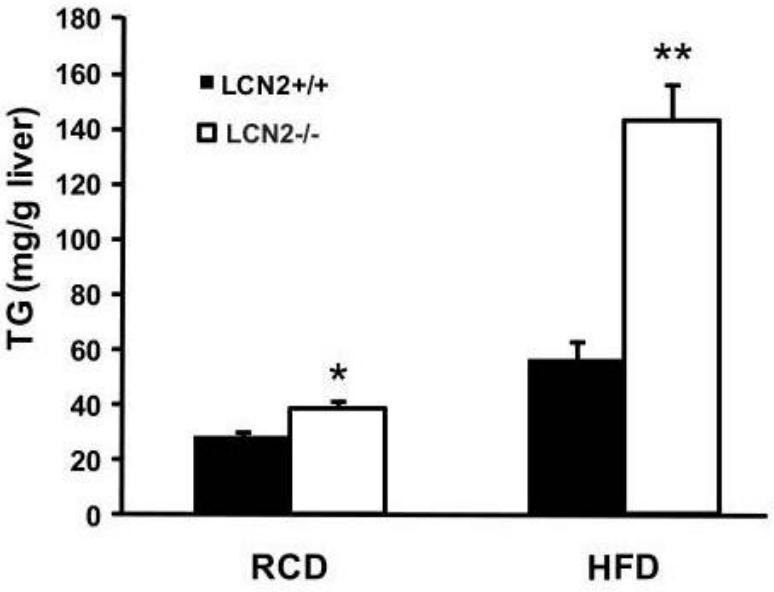

Figure 4E. Liver triacyglyceride content in WT and *Lcn2* KO mice on RCD at the age of 30 weeks (n=6-8) and on HFD at the age of 16 weeks (n=11). The data were represented as means ± SE. * $p<0.05$, ** $p<0.01$.

Figure 4F

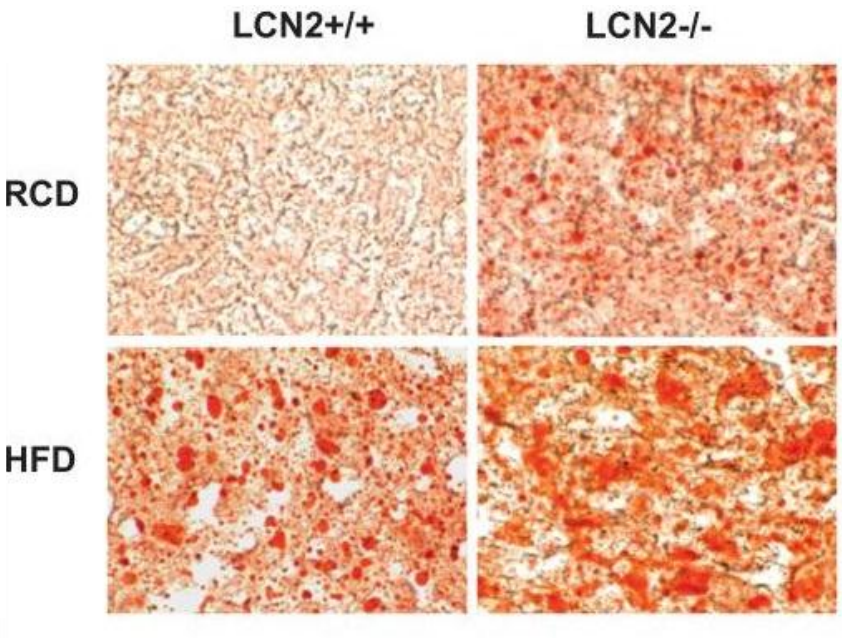

Figure 4F. Oil-red O staining of liver section of WT and *Lcn2* KO mice on RCD (30 weeks old) and HFD (16 weeks old).

Figure 5A

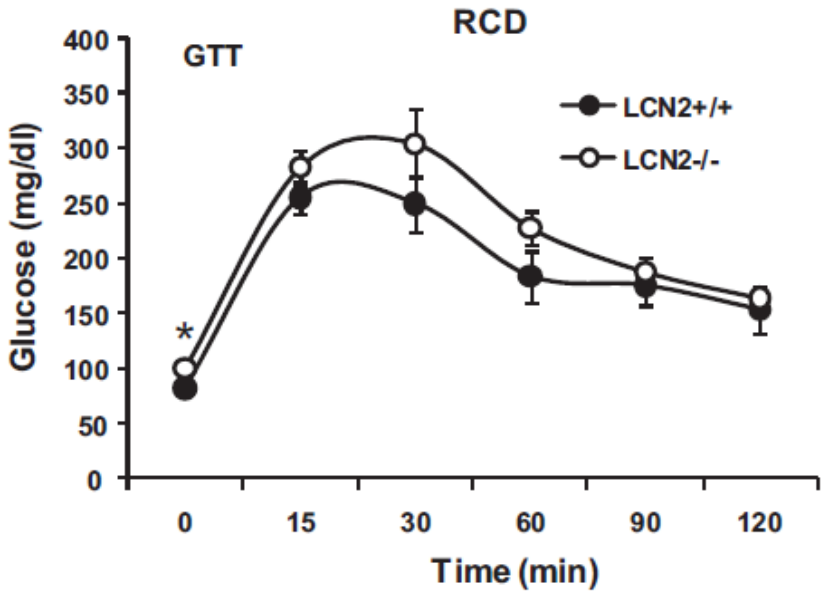

Figure 5A. Assessment of glucose tolerance in WT and *Lcn2* KO mice on RCD at the age of 28-29 weeks (n=10–12). Data were represented as means ± SE. Experiments were repeated on two independent sets of mice, yielding similar results. * $p<0.05$.

Figure 5B

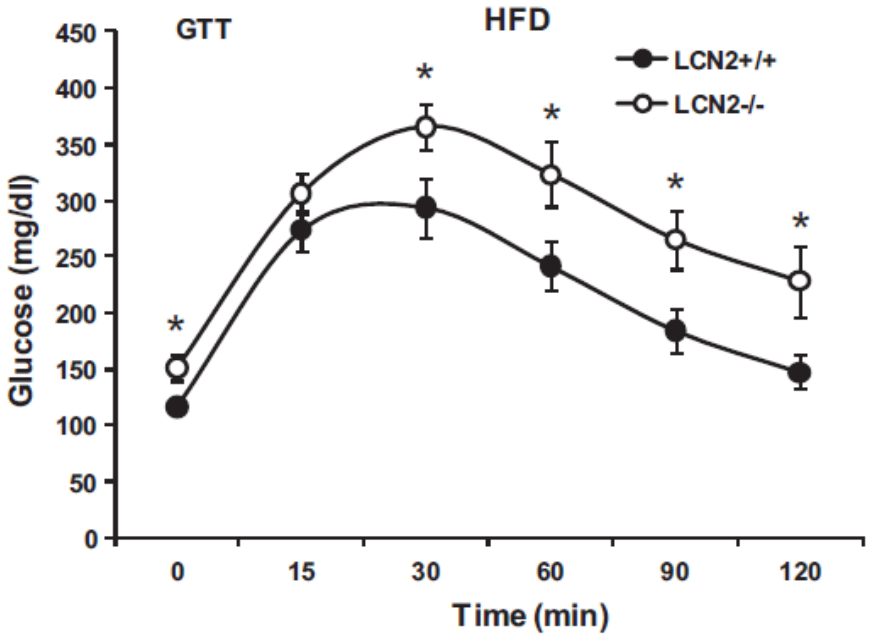

Figure 5B. Assessment of glucose tolerance in WT and *Lcn2* KO mice on HFD at the age of 14-15 weeks (n=10–12). Data were represented as means ± SE. Experiments were repeated on two independent sets of mice, yielding similar results. * $p<0.05$.

Figure 5C

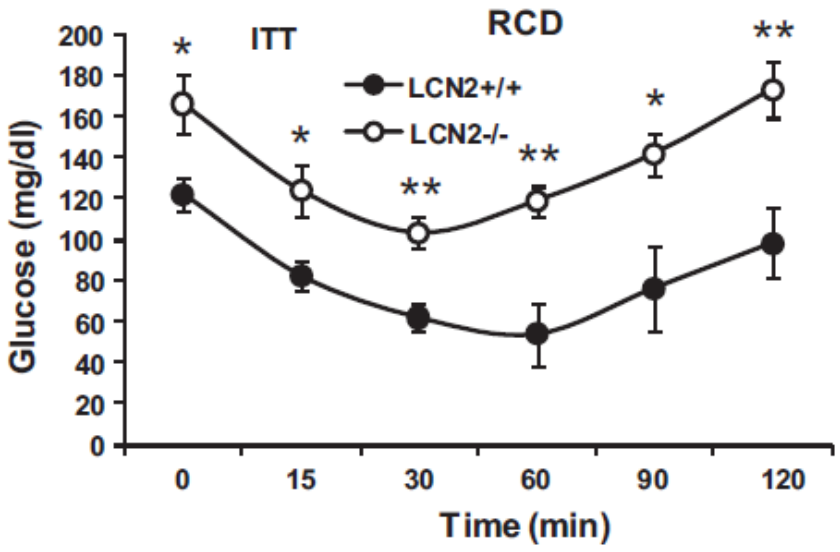

Figure 5C. Assessment of systemic insulin sensitivity in WT and *Lcn2* KO mice on RCD at the age of 28-29 weeks (n=10–12). Data were represented as means ± SE. Experiments were repeated on two independent sets of mice, yielding similar results. * $p<0.05$, ** $p<0.01$.

Figure 5D

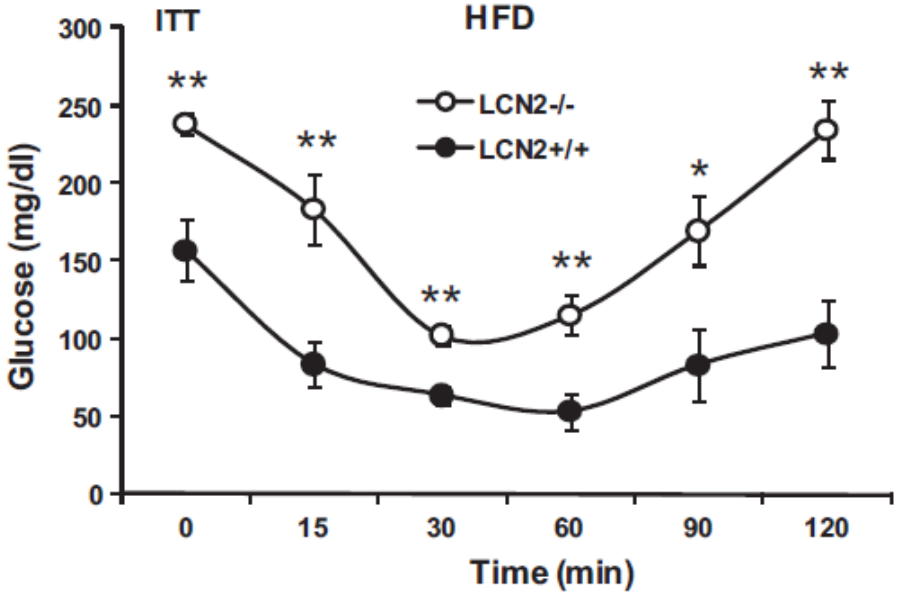

Figure 5D. Assessment of systemic insulin sensitivity in WT and *Lcn2* KO mice on HFD at the age of 14-15 weeks (n=10–12). Data were represented as means ± SE. Experiments were repeated on two independent sets of mice, yielding similar results. * $p<0.05$, ** $p<0.01$.

Figure 6A

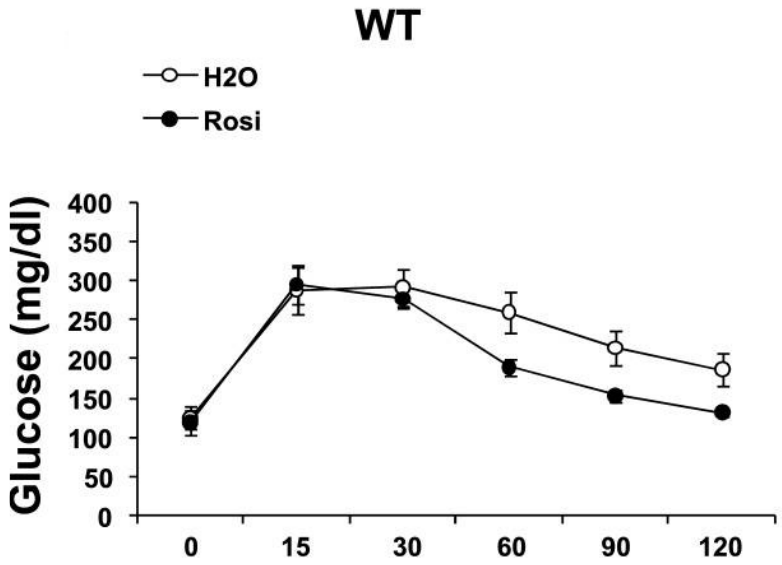

Figure 6A. Glucose tolerance tests in the HFD-fed WT mice treated with H_2O or Rosi at the age of 19-20 weeks (n=6-8). Data were represented as means ± SE.

Figure 6B

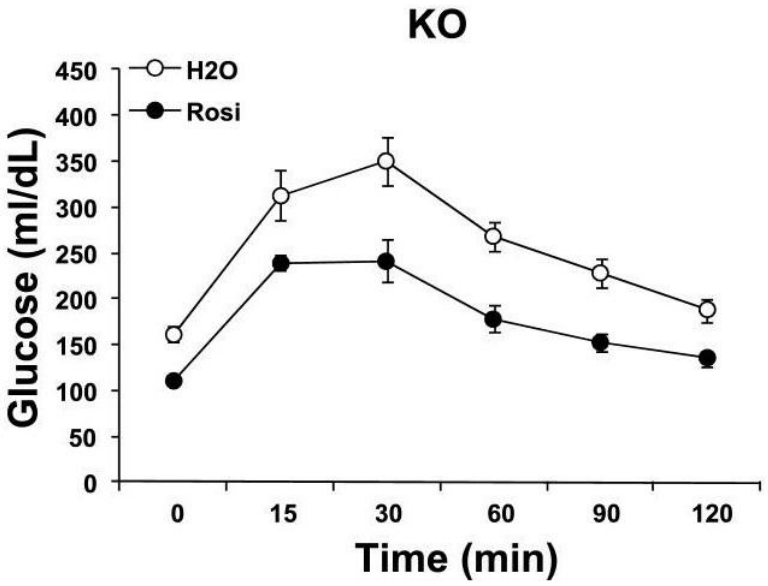

Figure 6B. Glucose tolerance tests in the HFD-fed *Lcn2* KO mice treated with H_2O or Rosi at the age of 19-20 weeks (n=6-8). Data were represented as means ± SE.

Figure 6C

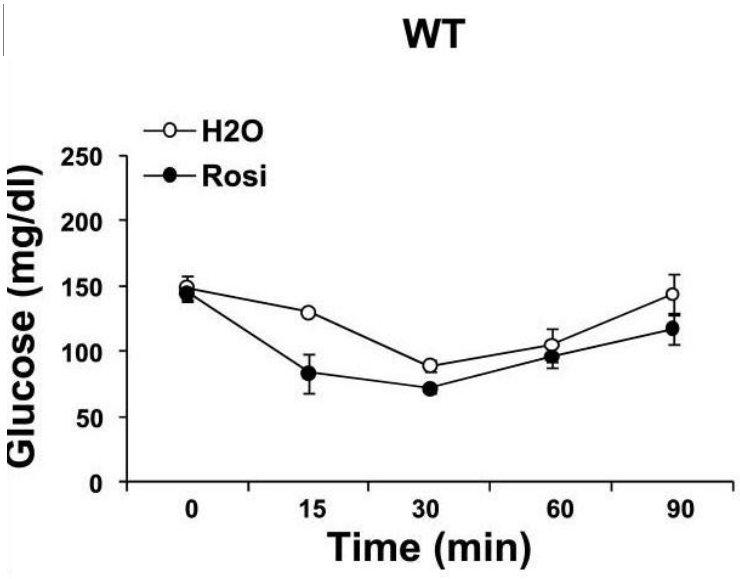

Figure 6C. Insulin tolerance tests in the HFD-fed WT mice treated with H_2O or Rosi at the age of 19-20 weeks (n=6-8). Data were represented as means ± SE.

Figure 6D

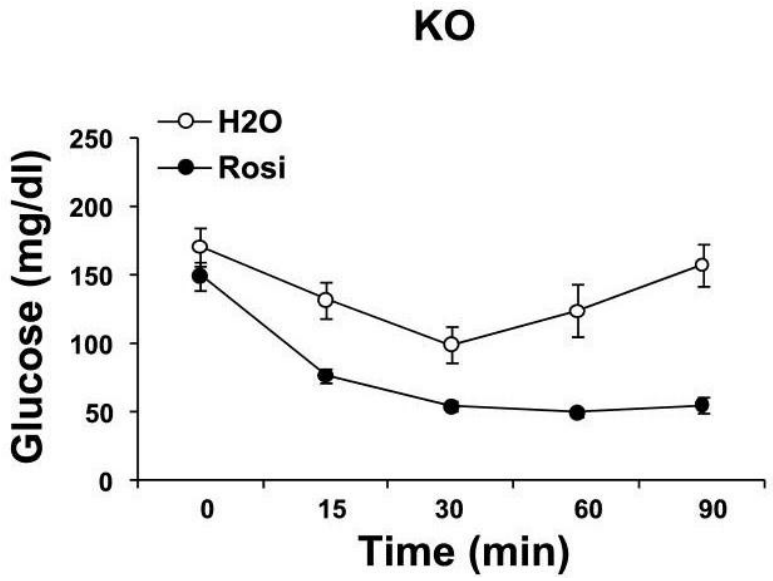

Figure 6D. Insulin tolerance tests in the HFD-fed *Lcn2* KO mice treated with H_2O or Rosi at the age of 19-20 weeks (n=6-8). Data were represented as means ± SE.

Figure 7A

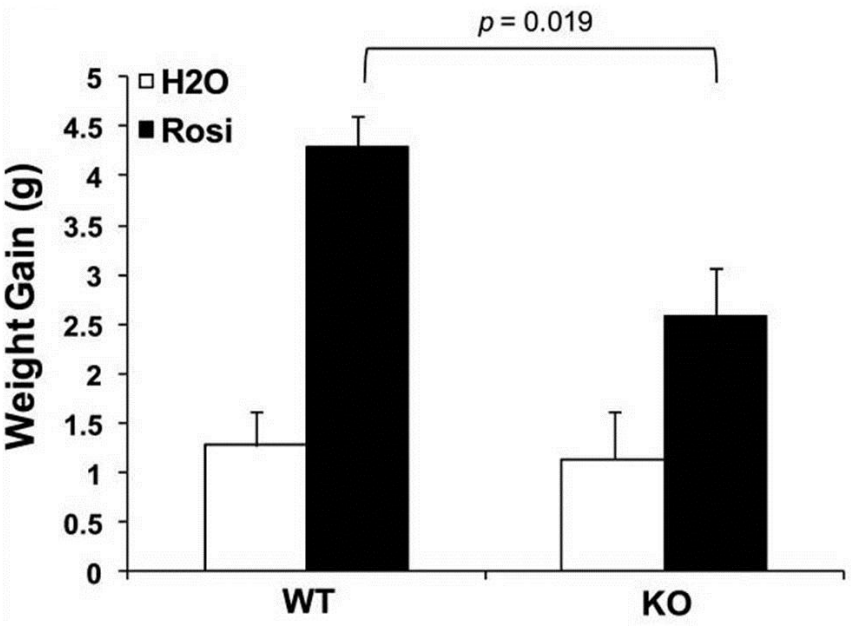

Figure 7A. Body weight gain in the HFD-fed WT and *Lcn2* KO mice treated with H_2O or Rosi (n=13-16). Weight gain between the age of 4 weeks and the age of 19 weeks was calculated and normalized to the weight gain in the H_2O-treated group. Data were represented as means ± SE.

Figure 7B

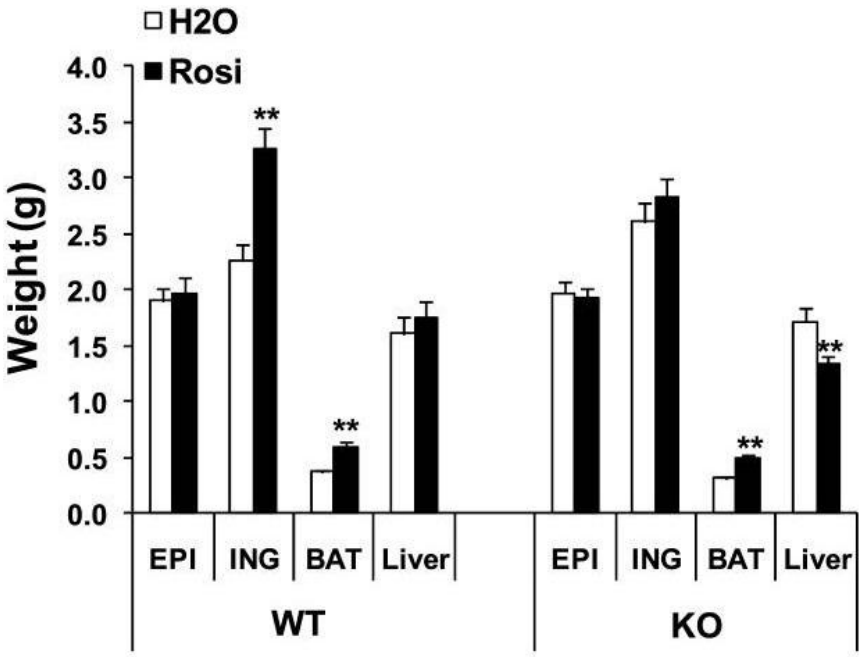

Figure 7B. Tissue weight in the HFD-fed WT and *Lcn2* KO mice treated with H_2O or Rosi (n=13-16). Data were represented as means ± SE. ** $p<0.01$.

Figure 7C

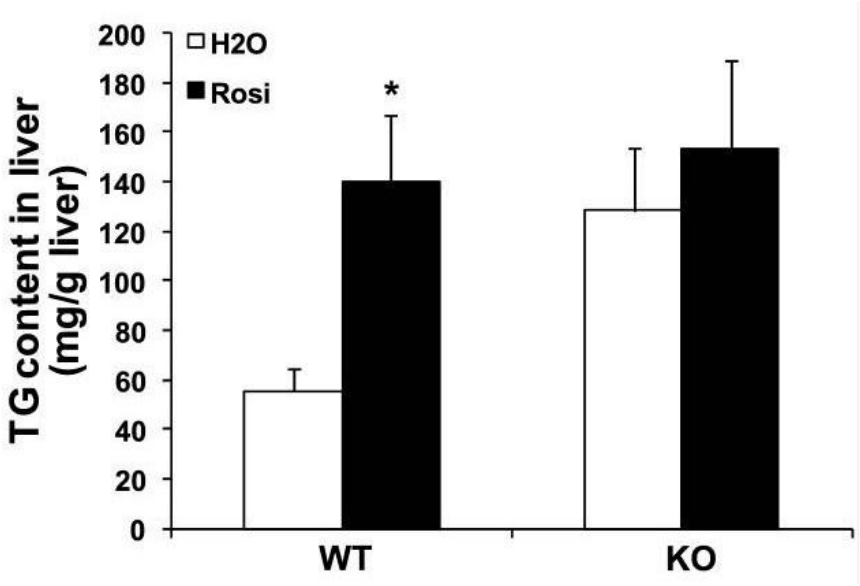

Figure 7C. Triglyceride content in liver of the HFD-fed WT and *Lcn2* KO mice treated with H_2O or Rosi (n=13-16). Data were represented as means ± SE. * $p<0.05$.

Figure 7D

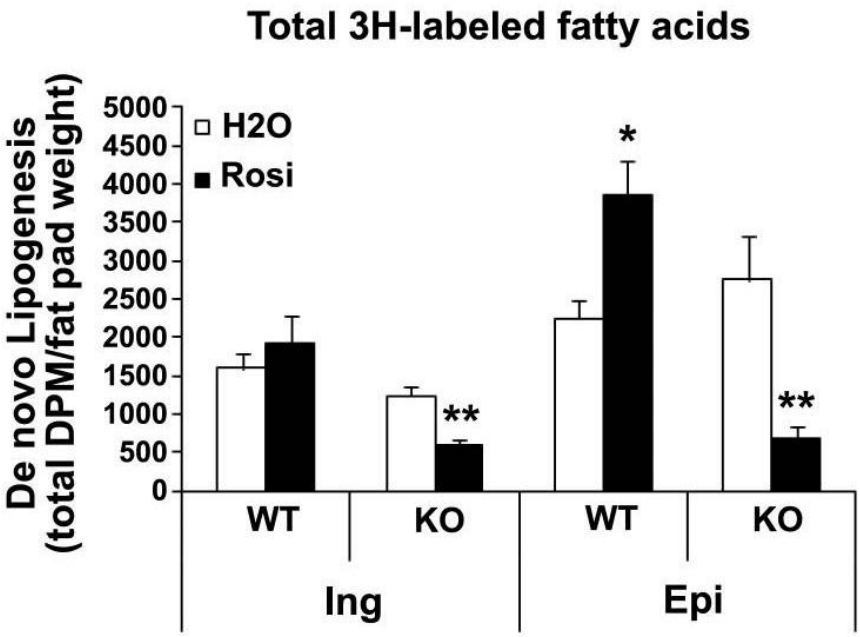

Figure 7D. De novo lipogenesis in HFD-fed WT and *Lcn2* KO mice at the age of 14 weeks (n=5). ^{3}H-labeled fatty acids present in adipose tissue were measured after an injection of [^{3}H] H_2O. Data were represented as mean ± SE. * $p<0.05$, ** $p<0.01$ vs. H_2O-treated group.

Table 1

Serum metabolic parameters in wild-type and *LCN2*$^{-/-}$ mice

Genotype	Diet	Glucose (mg/ml)	Insulin (ng/ml)	Leptin (ng/ml)	Adiponectin (μg/ml)	Plasminogen activator inhibitor-1 (ng/ml)
Wild type	RCD	82.33 ± 3.27	0.56 ± 0.15	3.33 ± 1.56	14.78 ± 1.85	3.59 ± 0.51
LCN2$^{-/-}$	RCD	100.38 ± 4.99*	0.79 ± 0.11	3.06 ± 0.95	15.46 ± 1.02	3.22 ± 0.62
Wild type	HFD	157.10 ± 19.55	1.85 ± 0.36	24.23 ± 3.86	16.50 ± 0.34	2.83 ± 0.42
LCN2$^{-/-}$	HFD	238.13 ± 6.45†	3.02 ± 0.57†	16.62 ± 2.07	13.50 ± 0.88†	3.43 ± 0.79

Data are means ± SE. Measurements were performed on 6-h–fasted mice fed an RCD and HFD (n = 9–11).

$^{*}P < 0.01$ vs. wild-type on an RCD;

$^{\dagger}P < 0.01$ vs. wild-type on an HFD.

Table 2

Plasma lipid profile in wild-type and LCN2-null mice

Genotype	Diet	Triglycerides (mg/dl)	Cholesterol (mg/dl)	HDL direct (mg/dl)	LDL direct (mg/dl)	Nonesterified fatty acids (mEq/l)	β-Hydroxybutyrate (mmol/l)
Wild type	RCD	89.76 ± 3.39	168.14 ± 5.56	85.26 ± 3.59	7.07 ± 0.29	1.31 ± 0.03	0.36 ± 0.03
$LCN2^{-/-}$	RCD	100.07 ± 4.05	191.82 ± 6.17*	94.99 ± 4.75	6.71 ± 0.38	1.58 ± 0.07	0.27 ± 0.05
Wild type	HFD	110.23 ± 3.34	194.72 ± 4.59	90.5 ± 2.23	6.74 ± 0.33	1.23 ± 0.07	0.39 ± 0.04
$LCN2^{-/-}$	HFD	99.34 ± 1.78	197.26 ± 14.82	86.63 ± 2.79	17.38 ± 3.19†	1.11 ± 0.04	0.48 ± 0.02†

Data are means ± SE. Measurements were performed on 6-h–fasted mice fed an RCD and HFD (n = 9–11).

*P < 0.01 vs. wild-type on an RCD;

†P < 0.01 vs. wild-type on an HFD.

CHAPTER 4

THE ROLE OF LCN2 IN ADAPTIVE REMODELING AND THERMOGENIC ACTIVATION OF BROWN ADIPOSE TISSUE

This chapter is modified from the manuscript:

Yuanyuan Zhang, Hong Guo, Mara G Mashek, DonSanjiv Ariyakumar, Anibal G. Armien, David A Bernlohr, Douglas G Mashek and Xiaoli Chen. (2013) *to be submitted*

Yuanyuan Zhang performed experiments from Fig 8A-F, 9A-H, 10A, 10C-D, 10G, 11A-E, 12A-G, and wrote the corresponding text sections.

SUMMARY

Lipocalin 2 (Lcn2) is a recently identified adipokine playing an important role in innate immunity, inflammation, and insulin resistance. Herein we report that Lcn2 has a critical role in adaptive remodeling and thermogenic activation of brown adipose tissue (BAT). *Lcn2* KO mice were sensitive to acute cold exposure, and developed significantly hypothermia, hypoglycemia, liver glycogen depletion, and hyperlactatemia after 4 hour exposure to 4℃. Nevertheless, *Lcn2* KO mice had a normal central thermoregulation as evidenced by normal catecholamine release and lipolytic activity in response to cold stimulation. Further studies showed that Lcn2 deficiency reduces the efficiency of cold-induced mitochondrial oxidation of lipids and blunts cold-induced UCP1 activation and expression of thermogenic (PGC-1α and PRDM16) and angiogenic (VEGF-A) genes, leading to lipid accumulation and thermogenic dysfunction of brown adipocytes. This cold-intolerant phenotype was fully prevented by PPARγ agonist administration to *Lcn2* KO mice. All of these data demonstrate that Lcn2 deficiency impairs cold-induced BAT remodeling and thermogenic activation. This impairment is possibly attributed to the defective activation of PPARγ, suggesting a potential role of Lcn2 in activating this nuclear receptor.

INTRODUCTION

Adipose tissue plays a central role in metabolic homeostasis, inflammation, and insulin resistance. The main functions of WAT are to regulate lipid storage and mobilization, glucose homeostasis, and inflammation. Many WAT functions that

influence whole-body metabolism are exerted by adipose-derived adipokines and cytokines (Ouchi et al., 2011; Waki and Tontonoz, 2007). As opposed to WAT, BAT has long been known to be important in small mammals and human newborns for body temperature maintenance and energy expenditure via UCP1-mediated non-shivering thermogenesis (Cannon and Nedergaard, 2004). In recent years, the discovery of metabolically active BAT in adult humans has suggested a potential alternative mechanism for metabolic regulation (Cypess et al., 2009; Nedergaard et al., 2007; Saito et al., 2009; van Marken Lichtenbelt et al., 2009; Virtanen et al., 2009; Zingaretti et al., 2009). Cold exposure actives BAT leading to increased glucose uptake and oxidative metabolism (Ouellet et al., 2012). Changes in BAT activity may also influence whole-body energetics. Obese subjects have reduced thermogenic activity, showing no or little BAT activity when exposed to cold (Vijgen et al., 2011) and BAT activity is negatively correlated with BMI and body fat mass (Vijgen et al., 2011; Vijgen et al., 2012). In obese animals, brown adipocytes are enlarged with lipids and metabolically inactive. More importantly, BAT activation has a significant influence on glucose and lipid homeostasis (Bartelt et al., 2011). Thus, activating BAT function is an attractive therapeutic approach for obesity and obesity-related metabolic complications.

UCP1-mediated heat production is the primary mechanism of BAT thermogenic activity. Multiple metabolic processes determine the efficiency of heat production from BAT thermogenesis, that is, fuel mobilization from storage tissues to BAT, lipolysis and lipogenesis in BAT, intracellular delivery of substrates (fatty acids) from lipid droplets to peroxisome and mitochondria for oxidation, and UCP1-mediated proton leak and heat

production. These metabolic processes become highly active during cold adaptation. Both fatty acid synthesis and oxidation are simultaneously increased in BAT, which constitutes a feed-forward cycle and continuously provides substrates for thermogenesis during cold adaptation (Trayhurn, 1981). More significantly, both acute and chronic exposure to cold environment (4 ℃) cause an increase in oxygen consumption by two to four fold in rodents (DAVIS et al., 1960; DEPOCAS et al., 1956). To meet the increased O_2 consumption during cold exposure, vascularization of BAT is increased, which is an important remodeling process for activating non-shivering thermogenesis of BAT. This process is primarily mediated by vascular endothelial growth factor (VEGF), which can be induced by thermogenic O_2 consumption (hypoxia) (Ferrara, 2004) and norepinephrine (Fredriksson et al., 2000). The induction of VEGF during cold stimulation is to increase capillary permeability, allowing plasma triglycerides to leave the capillaries and increasing O_2 delivery (Asano et al., 1997; Bartelt et al., 2011; Fredriksson et al., 2005). The cold-induced activation of thermogenic metabolic processes is regulated by neural, hormonal, and nutrient signals. Although the major pathways mediating BAT thermogenic activation have been extensively documented, the molecular details of how these pathways are regulated and what factors are involved remain largely unknown.

Lipocalin2 (Lcn2), also named as neutrophil gelatinase-associated lipocalin (NGAL), is a newly identified adipokine with abundant expression in adipose tissue (Yan et al., 2007; Zhang et al., 2008). As a member of the multigene family of up and down β-barrel proteins, Lcn2 has structural similarity to other member proteins; fatty acid binding proteins (FABPs) and retinol binding proteins (RBPs) (LaLonde et al., 1994). Lcn2

contains a lipid binding domain constituted by eight stranded antiparallel β-barrel, which confers to Lcn2 the ability to bind small hydrophobic molecules, such as retinoid, steroid, and fatty acids (LaLonde et al., 1994). We have recently characterized Lcn2 as a critical regulator of energy metabolism, glucose and lipid homeostasis, and insulin resistance (Guo et al., 2010; Guo et al., 2012; Jin et al., 2011). In our previous publications, we also reported that *Lcn2* KO mice exhibit cold-intolerance during acute cold exposure (Guo et al., 2010). However, how Lcn2 regulates the metabolic processes thereby affecting the efficiency of BAT thermogenic activity remains elusive. Here we report that Lcn2 is essential for adaptive remodeling and thermogenic activation of BAT during cold exposure. Lcn2 deficiency reduces the efficiency of cold-induced mitochondrial oxidation of lipids and blunts cold-induced UCP1 activation and VEGF-A expression, leading to brown adipocyte hypertrophy and dysfunction. All of these defects are associated with a potential role of Lcn2 as a binding protein of lipid ligands for activating nuclear receptors such as PPARγ.

RESULTS

Lcn2 deficiency impairs BAT thermogenic activation by cold stimulation

Lcn2 KO mice displayed cold sensitive and failed to maintain their body temperature when acutely exposed to 4℃ (Fig 8A). After 4-hour cold exposure, the levels of serum glucose were unaltered in WT mice, but were markedly reduced in *Lcn2* KO mice (Fig 8B). In contrast, serum lactate levels were significantly increased in *Lcn2* KO mice compared to WT controls (Fig 8C). Serum fatty acid levels did not differ

between the two genotypes (Fig 8D). The assessment of glycogenolysis and gluconeogensis demonstrated that *Lcn2* KO mice had significantly lower liver glycogen content than WT mice after 4-hour cold exposure (Fig 8E). As shown in Fig 8F, the mRNA expression levels of gluconeogenic genes glucose-6-phosphatase (G6Pase), but not phosphoenolpyruvate carboxykinase 1 (PEPCK1) in liver were increased in WT and *Lcn2* KO mice to a similar extent in response to cold stimulation.

Lcn2 KO mice exhibit normal sympathetic nervous system activation during cold exposure

The sympathetic nervous system (SNS) plays a key role in mediating central control of thermogenesis, primarily promoting glucose uptake and UCP1 expression in BAT as well as lipolysis in BAT and WATs to meet the increased energy demand during cold adaptation (Cannon and Nedergaard, 2004). We therefore determined SNS activation in response to cold stimulation in *Lcn2* KO mice. After 4-hour exposure to 4℃, *Lcn2* KO mice released similar or even higher levels of catecholamine compared to WT mice as determined by serum levels of noradrenaline and adrenaline (Fig 9A). The mRNA expression of β3 adrenergic receptor (*ADRB3*), thyroid hormone receptor α (*Thra*), and thyroid hormone receptor β (*Thrb*) in BAT was also normal in *Lcn2* KO mice after cold exposure (Fig 9B). Then we further evaluated lipolysis in adipose tissue in response to β-adrenergic signaling activation after cold stimulation. As shown in Fig 9C, HSL phosphorylation at Ser563 in BAT and WAT was induced by cold at the similar level between two genotypes or even more significantly stimulated in *Lcn2* KO mice. The

basal levels of glycerol release from BAT and WAT explants isolated from *Lcn2* KO mice were slightly lower than those from WT mice, while FFA release was not different between WT and *Lcn2* KO mice (Fig 9D, 9E). Similar results were observed in primary differentiated brown adipocytes (Fig 9F). Furthermore, TAG hydrolase activity (Fig 9G) and ATGL protein expression (Fig 9H) in BAT were not changed in *Lcn2* KO mice under either normal or cold exposure condition. In the analysis of lipogenic gene expression, there was no significant difference in the mRNA levels of fatty acid synthase (FAS), stearoyl-CoA desaturase 1 (SCD1), and fatty acid elongase 3 (ELOVL 3) in BAT between WT and *Lcn2* KO mice in either the normal or cold condition (data not shown).

SV-differentiated brown adipocytes have decreased fatty acid oxidation with Lcn2 deficiency

The above results have indicated that Lcn2 deficiency doesn't significantly affect the mobilization and provision of substrates including both glucose and fatty acids. We then determined the efficiency of substrate utilization, particularly fatty acid oxidation in *Lcn2* KO mice. As shown in Fig 10A, the oxygen consumption of mitochondria isolated from BAT and liver was not different between WT and *Lcn2* KO mice under the normal conditions or upon exposure to 4℃ for 3 hours. Besides, we determined the oxidation of ^{14}C-labeled fatty acids in primary differentiated brown adipocytes to evaluate the capacity of mitochondrial oxidation. Fig 10B showed that Lcn2 KO brown adipocytes had lower capability to oxidize oleate from either exogenous (pulse) or endogenous

(chase) sources compared with WT brown adipocytes, suggesting that Lcn2 deficiency affects oxidative capacity of brown adipocytes.

Lcn2 deficiency leads to inefficient mitochondrial oxidation *in vivo* and the development of hypertrophic brown adipocytes during cold exposure

To provide insights into the mitochondrial oxidative capacity *in vivo*, we performed electron transmission microscopy for mitochondrial biogenesis in BAT. Electron microscopy of BAT from the mice exposed to 4 ℃ for 4 h showed that *Lcn2* KO mice had normal morphology of mitochondria, but large lipid droplets in brown adipocytes, which is in line with lighter colored BAT (Fig 10C) and the higher TG contents of BAT in *Lcn2* KO mice compared to WT controls (Fig 10D). Moreover, Lcn2 KO brown adipocytes have increased lipid area (data not shown) and decreased mitochondria number per cell area (Fig 10F), which may result from the hypertrophy of brown adipocytes in *Lcn2* KO mice as the diameter of Lcn2 KO brown adipocytes was markedly increased when compared with that of WT cells (Fig 10E). This may also be associated with reduced mitochondrial biogenesis as evidenced by decreased expression of Nrf1 and Cox4 in Lcn2 KO BAT under the cold-stimulated condition (Fig 10G). Thus, the decreased mitochondria number per cell area indicates that the overall mitochondrial oxidative capacity is reduced in Lcn2 KO BAT.

Lcn2 deficiency reduces UCP1 protein and thermogenic gene expression in BAT during cold exposure

UCP1-mediated uncoupling of oxidative phosphorylation from ATP production, dissipating the energy as heat is the last and key step controlling thermorgenesis. We examined the expression of UCP1 and thermogenic genes, the markers of metabolically active BAT, to indicate if Lcn2 deficiency affects the cold activation of functional brown adipocyte recruitment in *Lcn2* KO mice. Compared to WT mice, the UCP1 protein levels were not significantly altered in Lcn2 KO BAT under the normal physiological condition. However, we discovered that the cold-induced UCP1 expression was significantly attenuated in Lcn2 KO BAT (Fig 11A). Additionally, the mRNA levels of PGC-1α (Fig 11B) and PRDM16 (Fig 11C) were markedly lower in BAT of *Lcn2* KO mice than that of WT mice after 4-hour cold exposure.

Lcn2 deficiency eliminates cold-induced VEGF-A and HIF-1α expression in BAT

As an angiogenic factor, VEGF plays a key role in adipose tissue angiogenesis and remodeling under both normal and disease states (Hausman and Richardson, 2004; Zhang et al., 1997). VEGF expression is upregulated in BAT in response to cold exposure (Fredriksson et al., 2005). The increased VEGF expression by cold stimulation is to ensure the delivery of adequate amount of lipid fuels and O_2 to BAT for thermogenesis. The regulation of VEGF expression involves hypoxia-dependent (via HIF-1α) (Ferrara, 2004) and hypoxia-independent (via β-adrenergic stimulation) mechanisms (Fredriksson et al., 2000). In this study, we found that the mRNA expression levels of VEGF-A were significantly lower in BAT of Lcn2 KO than that of WT mice (Fig 11D). After cold exposure to 4 ℃ for 4 hour, the mRNA expression of VEGF-A

(Fig 11D) and HIF-1α (Fig 11E) genes was upregulated in BAT of WT mice; however, this cold-induced expression of VEGF-A and HIF-1α was completely diminished in BAT of *Lcn2* KO mice. Our data support that the impaired adaptive remodeling of BAT contributes to the mechanism for reduced thermogenic programming and cold intolerance in *Lcn2* KO mice.

PPARγ agonist reverses adaptive thermo-dysregulation in *Lcn2* KO mice

As described early, Lcn2 has structural characteristics of binding lipophilic molecules such as fatty acids and retinoids. We hypothesized that Lcn2 may serve as an important carrier of lipid ligands responsible for activating nuclear receptors. UCP1 and VEGF-A are the responsive genes of PPARγ and RAR/RXR activation, and their expression is upregulated by PPARγ ligands (Digby et al., 1998; Gealekman et al., 2008; Kelly et al., 1998). Decreased expression of UCP1 and VEGF-A during cold exposure in *Lcn2* KO mice suggests that the activation of PPARγ or RAR/RXR may be impaired and contributes to the dysregulation of adaptive remodeling and thermogenic activation of BAT in *Lcn2* KO mice. To prove this hypothesis, mice were first treated with Rosiglitazone (10mg/kg/day), the synthetic ligand for PPARγ, via oral gavage for 25 days, followed by 5 hour exposure to 4 ℃. As shown in Fig 12A, Rosiglitazone (Rosi) treatment did not change body temperature during cold exposure in WT mice, but completely reversed cold-intolerance in *Lcn2* KO mice. Rosi treatment also led to the significant improvement of serum parameters in *Lcn2* KO mice, such as increased liver glycogen content (Fig 12B), serum glucose levels (Fig 12C), and decreased serum lactate

(Fig 12D) and free fatty acid levels (Fig 12E). Moreover, the mRNA expression of PGC-1a, PRDM16, Nrf-1, and Cox4 were significantly upregulated by Rosi treatment in Lcn2 KO BAT under cold condition (Fig 12F-G). All these data suggest that the impaired PPARγ activation is the primary cause for the reduced thermogenesis in *Lcn2* KO mice.

DISCUSSION

Here we show that Lcn2 has a critical new role in adaptive remodeling and thermogenic activation of BAT through a mechanism involving the modulation of lipid-mediated nuclear receptor signaling activation. In mice lacking Lcn2, cold stress fails to efficiently stimulate mitochondrial oxidation of fatty acids in BAT. This promotes non-oxidized fatty acids, to the pathway of reesterification into triglycerides leading to the increased accumulation of large lipid droplets and brown adipocyte dysfunction in *Lcn2* KO mice upon cold stimulation. More importantly, Lcn2 is essential for cold-stimulated remodeling of BAT such as vascularization, mitochondrial biogenesis, and functional brown adipocyte recruitment. We also demonstrate that Lcn2 regulates PPARγ signaling activation.

The SNS plays a key role in central regulation of adaptive thermogenesis and metabolic adaptation. However, Lcn2 deficiency does not seem to affect the SNS activation and lipolytic response of BAT and WATs to cold stimulation. Lipid turnover in BAT is highly active during cold adaptation; both triglyceride synthesis and breakdown are upregulated to meet the increasing demand for energy (Trayhurn, 1981). *Lcn2* KO mice displayed only a slight reduction in basal lipolysis (glycerol release) of tissue

explants and cultured adipocytes. As indicated by the mRNA expression of lipogenic genes FASN and SCD-1, lipogenesis is not significantly changed in BAT of *Lcn2* KO mice. However, we found that *Lcn2* KO mice fail to develop metabolically active and thermogenically functional BAT in response to cold, as evidenced by enlarged brown adipocytes filled with large lipid droplets and increased triglyceride content. Apparently, subtle changes in lipolysis and lipogenesis are unlikely to be the main mechanism contributing to BAT hypertrophy and dysfunction in *Lcn2* KO mice. We then examined the downstream thermogenic pathways of lipoysis, i.e. fatty acid oxidation in *Lcn2* KO mice. The mitochondrial number per cell area was significantly reduced in Lcn2 KO BAT, which results from the combination of enlarged lipid droplets, thereby causing brown adipocyte hypertrophy, and decreased mitochondrial biogenesis also contributing to the reduced efficiency of fatty acid oxidation in Lcn2 KO BAT during cold exposure.

We also show that Lcn2 deficiency significantly blunts cold-induced increase in UCP1 protein abundance, thermogenic genes PGC-1α and PRDM16, suggesting that thermogenic signaling pathways are dysregulated in BAT of *Lcn2* KO mice. We found that the sympathetic and thyroid hormonal signaling in *Lcn2* KO mice remains intact as supported by the normal levels of catecholomine release and HSL phosphorylation in WATs and BAT and the normal mRNA expression of β3 adrenergic receptor and thyroid hormone receptors in BAT in response to cold stimulation. During the cold-induced thermogenic process, the rapid lipid oxidation in BAT leads to a vast demand for O_2 and lipid delivery to this tissue. Thus, the angiogenesis in BAT is increased by cold stimulation to meet the increase requirement for blood supply (Foster and Frydman, 1978;

Foster and Frydman, 1979; Smith and Horwitz, 1969). VEGF, an angiogenic factor, is highly abundant in BAT; the acute induction of VEGF-A expression by cold stimulation and NE suggest its role in regulating vascular permeability for the delivery of plasma lipids to BAT during cold exposure (Asano et al., 1997; Fredriksson et al., 2005). Thus, the vascular permeability is another critical and controlling process for BAT thermogenic activation. However, our results of significantly lower levels of VEGF-A expression in BAT during cold exposure suggest that this remodeling process was significantly impaired in *Lcn2* KO mice.

We next sought to explore the possible mechanism for the role of Lcn2 in adaptive remodeling and thermogenic activation of BAT. Due to the structural property, Lcn2 has been speculated as a binding protein for lipophilic molecules or lipid ligands, suggesting that Lcn2 is involved in modulating activation of nuclear receptors such as PPARs. PPARγ/α is mainly responsive to lipolytic signals released from lipolysis which is activated by the sympathetic and β-adrenergic receptor signaling pathway. As we anticipated, Rosi, which is a synthetic ligand for PPARγ was able to fully reverse the cold intolerant phenotype of *Lcn2* KO mice. This result indicates that PPARγ activation is defective in *Lcn2* KO mice, but Lcn2 is not required for Rosi action. These data suggest that Lcn2 is an important, but perhaps not direct regulator of PPARγ.

In summary, herein we discovered a novel role for Lcn2 in adaptive remodeling and thermogenic activation of BAT as a potential regulator of lipid and retinoid signaling and its regulated activity of lipid-sensing nuclear receptors, specifically PPARγ. Mice lacking Lcn2 display impaired BAT remodeling and thermogenic activation in response

to cold, including mitochondrial biogenesis and oxidation, peroxisomal oxidation, UCP1-mediated uncoupling, and VEGF mediated vascular permeability. Lcn2 is essential for lipid/retinoid-modulated nuclear receptor activation. The detailed mechanism in this regard warrants further investigation.

Figure 8A

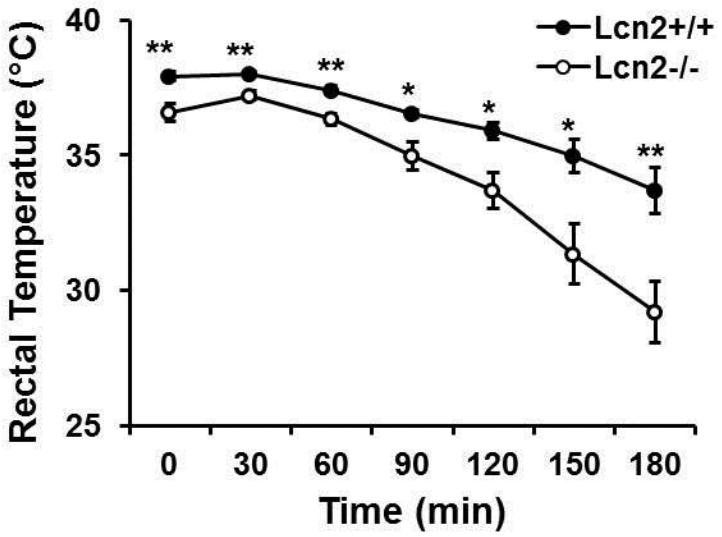

Figure 8A. Body temperature in WT and *Lcn2* KO mice during acute cold exposure (n = 9-12). WT and *Lcn2* KO mice at the age of 14 weeks were exposed to 4°C for 4 hours. Rectal temperature was measured every 30 minutes as indicated. Experiments were repeated on two to four independent sets of mice, yielding similar results. The data were presented as mean ± SE. * $p<0.05$; ** $p<0.01$. * Comparison between genotypes.

Figure 8B

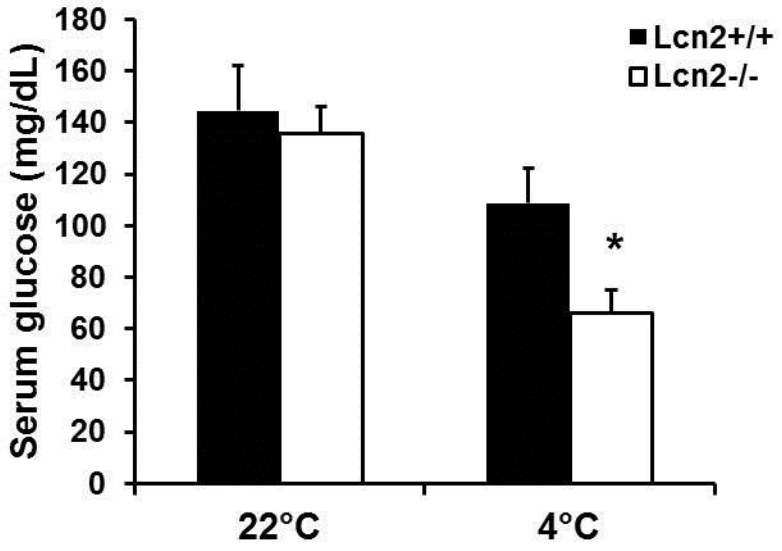

Figure 8B. Serum glucose levels in WT and *Lcn2* KO mice at 22^0C or after exposed to 4^0C for 4 hours (n = 5-8). The data were presented as mean ± SE. * $p<0.05$. * Comparison between genotypes.

Figure 8C

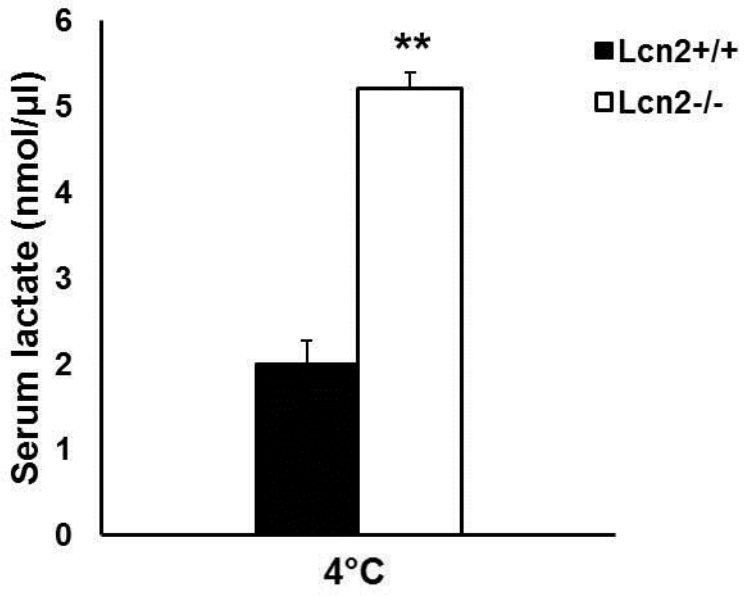

Figure 8C. Serum lactate levels in WT and *Lcn2* KO mice after exposed to 4^0C for 4 hours (n = 5-8). The data were presented as mean ± SE. **p<0.01. * Comparison between genotypes.

Figure 8D

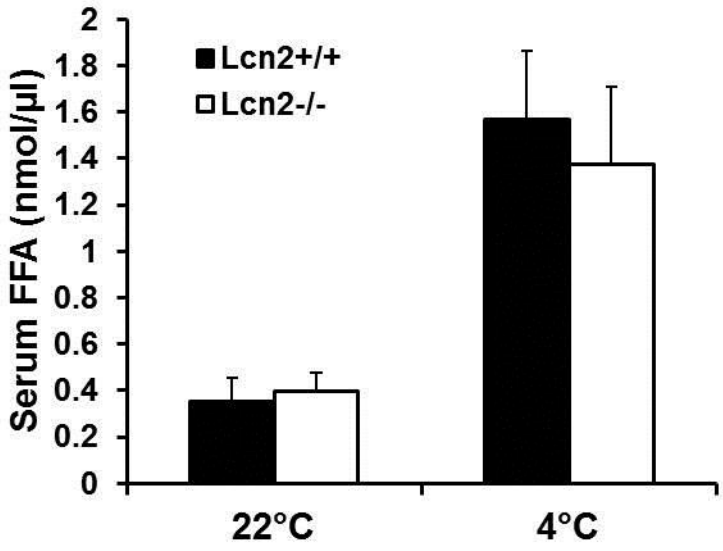

Figure 8D. Serum fatty acid levels in WT and *Lcn2* KO mice at 22°C or after exposed to 4°C for 4 hours (n = 5-8). The data were presented as mean ± SE.

Figure 8E

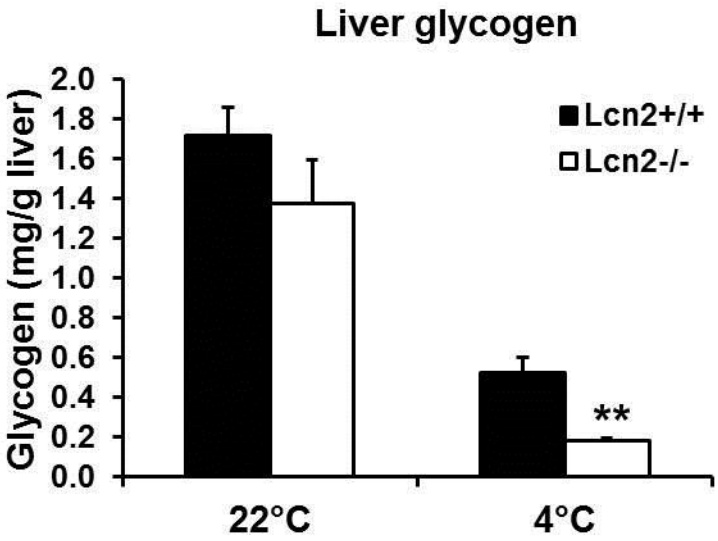

Figure 8E. Liver glycogen content in WT and *Lcn2* KO mice at 22^0C or after exposed to 4^0C for 4 hours (n = 5-7). The data were presented as mean ± SE. **p<0.01. * Comparison between genotypes.

Figure 8F

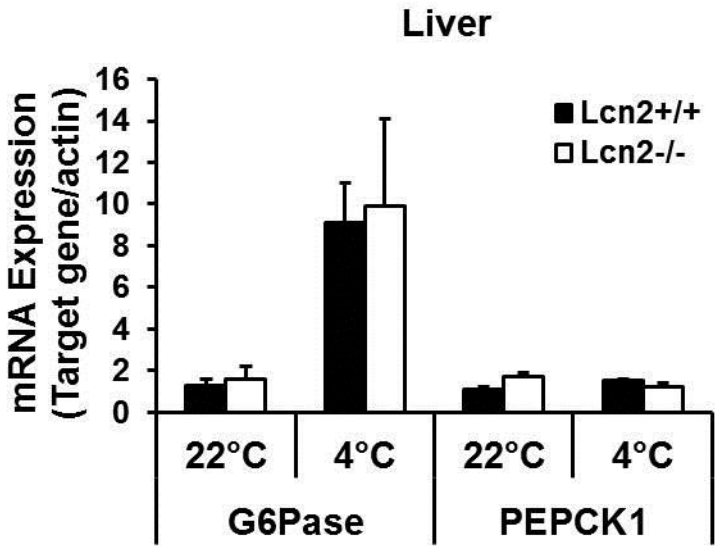

Figure 8F. mRNA expression levels of gluconeogenic genes in liver (n = 5-7). The data were presented as mean ± SE.

Figure 9A

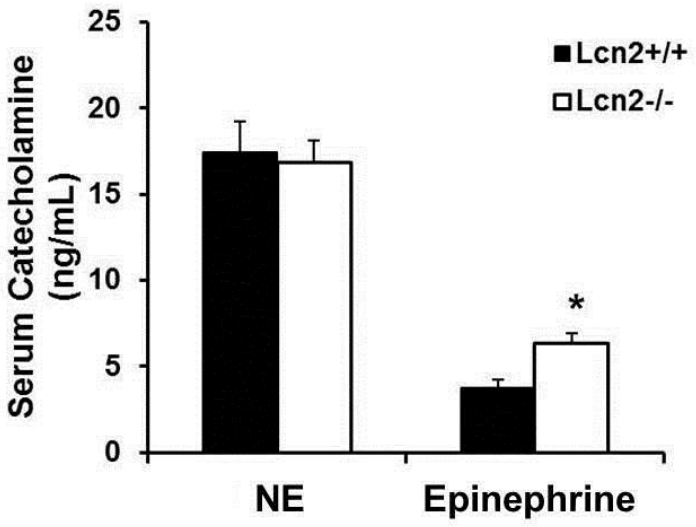

Figure 9A. Serum catecholamine levels in WT and *Lcn2* KO mice after exposed to 4^{o}C for 4 hours (n = 7-9). The data were presented as mean ± SE. * $p<0.05$. * Comparison between genotypes.

Figure 9B

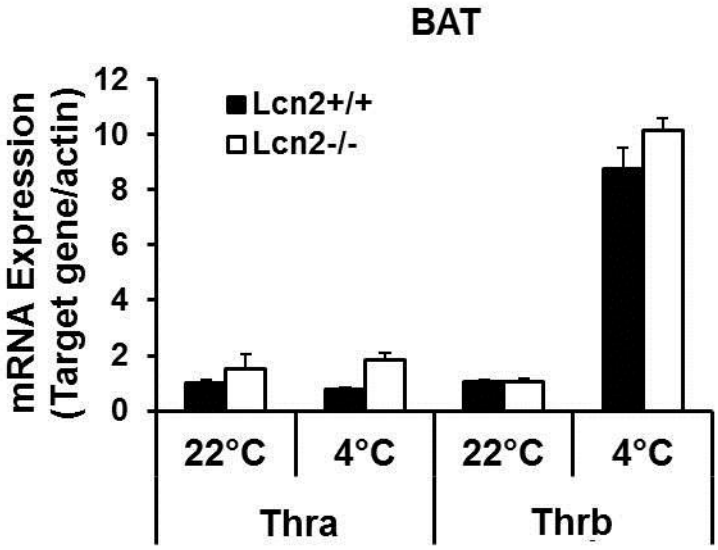

Figure 9B. mRNA expression levels of thyroid hormone receptor α (Thra) and thyroid hormone receptor β (Thrb) in BAT of mice (n = 5-7). The data were presented as mean ± SE.

Figure 9C

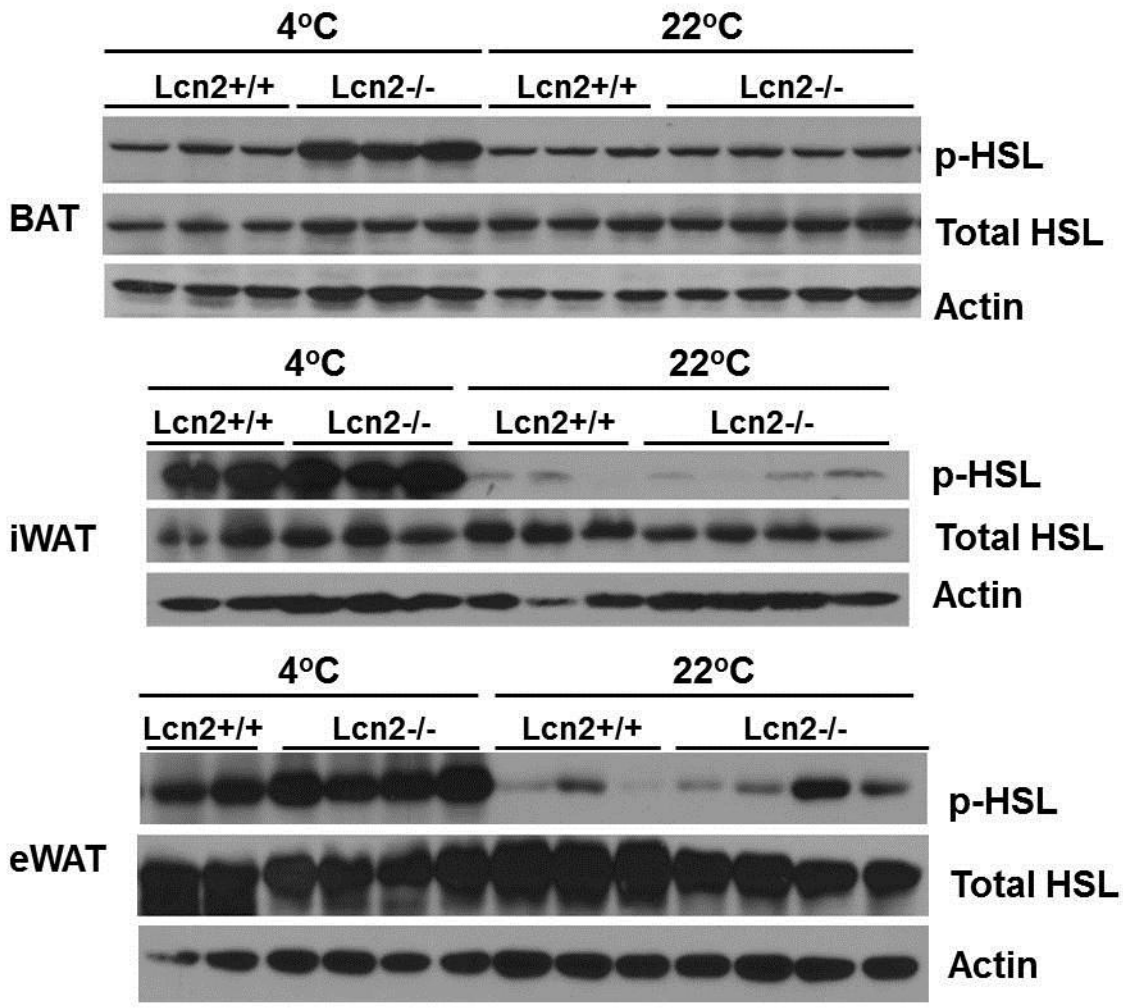

Figure 9C. HSL phosphorylation at Ser563 in BAT and WATs of WT and *Lcn2* KO mice during cold exposure. Each lane represented for one mouse.

Figure 9D

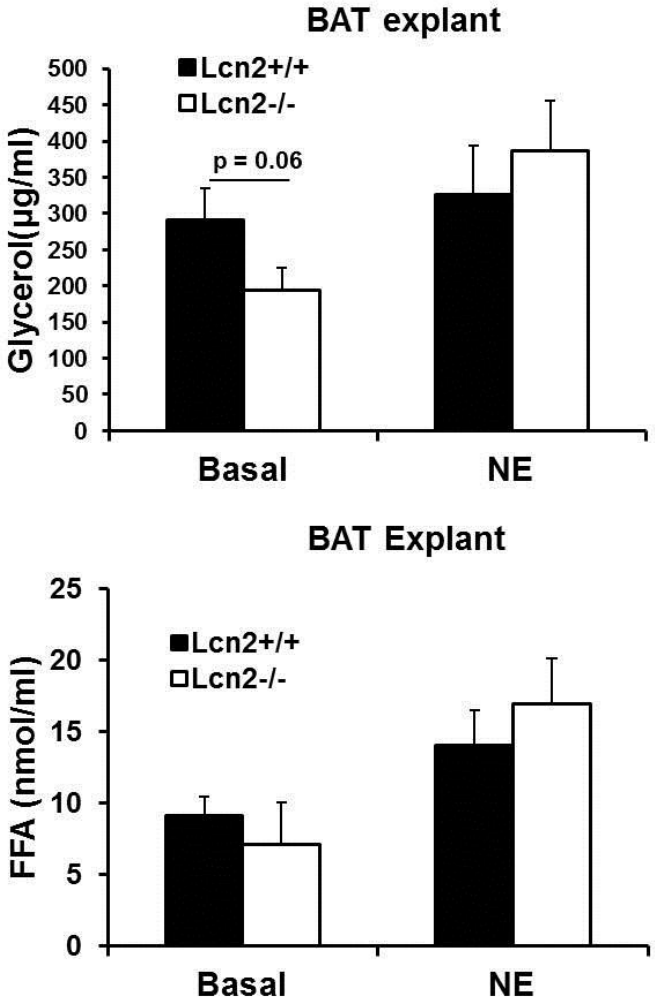

Figure 9D. Glycerol and fatty acid release from BAT explants in response to norepinephrine (NE). BAT explants were isolated from WT and *Lcn2* KO mice and pre-cultured in KRH buffer with 0.5% fatty acid-free BSA for 2 hours. Then the media was refreshed with or without 1μM NE. The media was collected for determining glycerol and fatty acid levels after 2 hour-treatment. The data were presented as mean ± SE.

Figure 9E

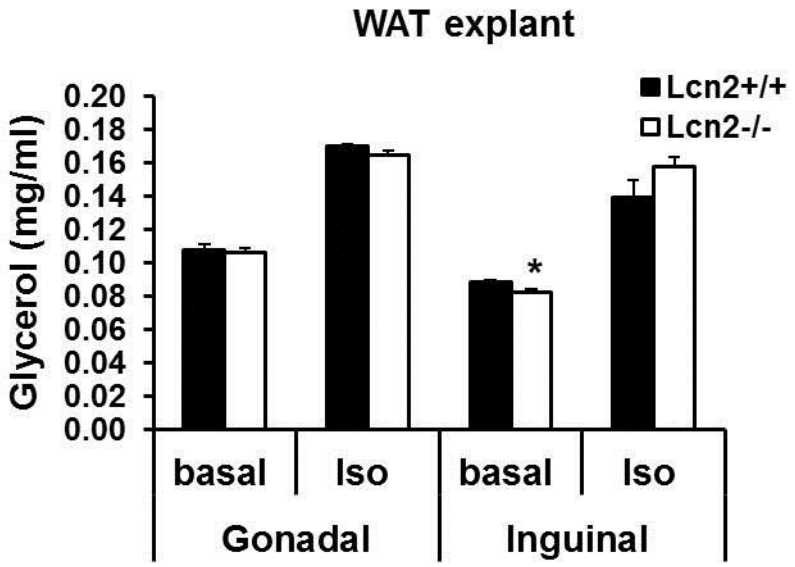

Figure 9E. Glycerol release from WAT explants in response to isoproterenol. WAT explants were isolated from WT and *Lcn2* KO mice and pre-cultured in KRH buffer with 0.5% fatty acid-free BSA for 2 hours. Then the media was refreshed with or without 1μM isoproterenol. Glycerol levels were determined in media after 2 hour-treatment. The data were presented as mean ± SE. * $p < 0.05$. * Comparison between genotypes.

Figure 9F

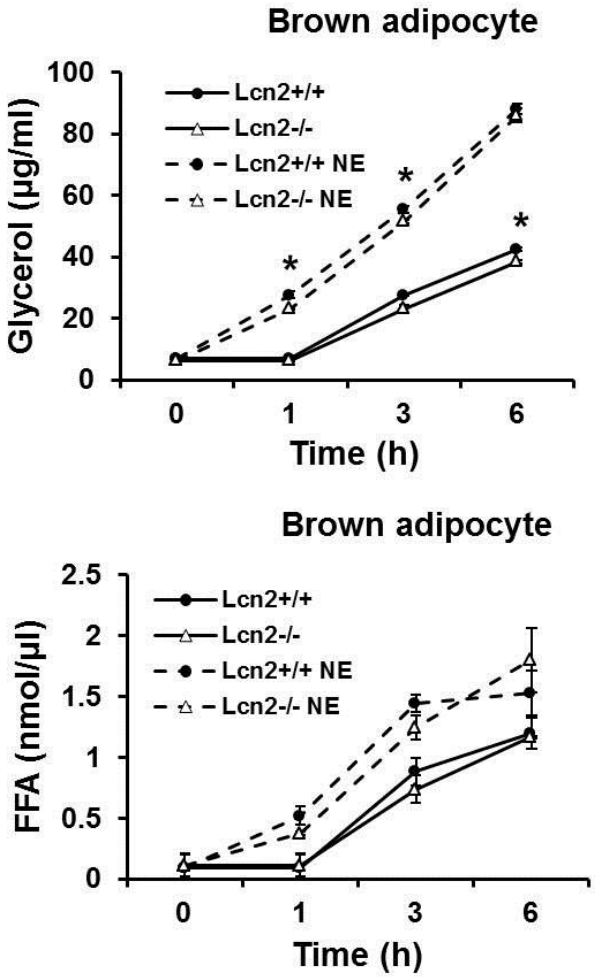

Figure 9F. Glycerol and fatty acid release from SV-differentiated brown adipocytes. Differentiated brown adipocytes were starved in high-glucose DMEM with 2% BSA for 6 hours; then the media was refreshed with or without 1µM NE. Media was collected at indicated time points for determining glycerol and fatty acid levels. The data were presented as mean ± SE. * $p < 0.05$. * Comparison between genotypes.

Figure 9G

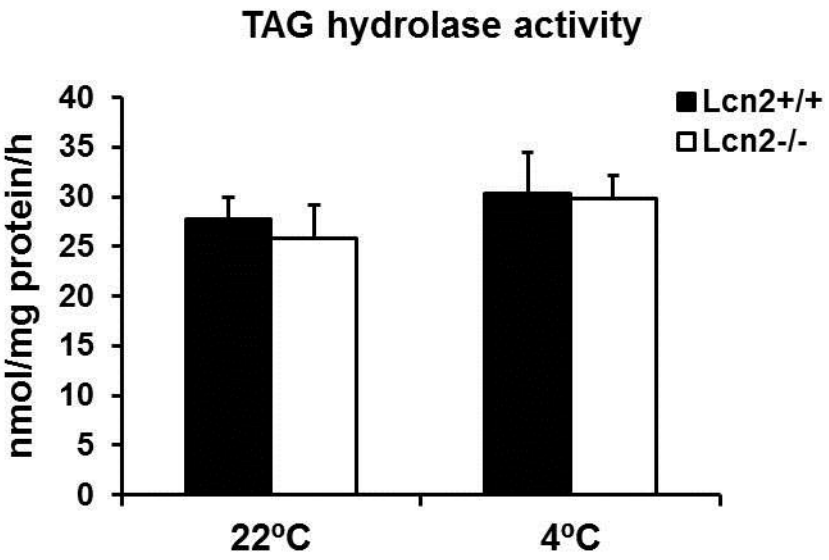

Figure 9G. Triglyceride hydrolase activity in BAT (n = 6-7). The data were normalized to protein content, presented as mean ± SE.

Figure 9H

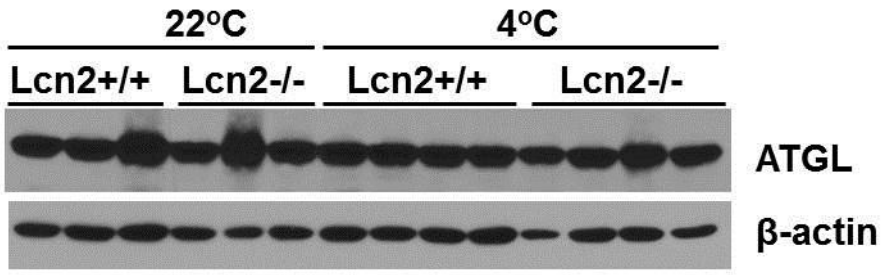

Figure 9H. The protein levels of ATGL in BAT of WT and *Lcn2* KO mice at 22^0C or after exposed to 4^0C for 4 hours. Each lane represented for one mouse.

Figure 10A

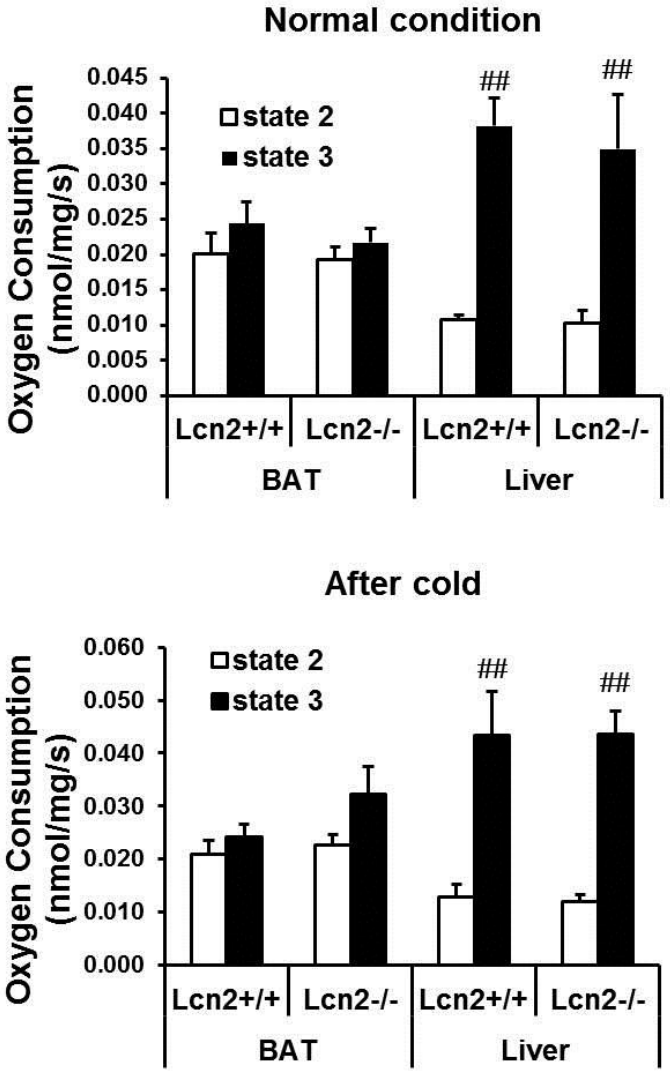

Figure 10A. Oxygen consumption of mitochondria isolated from BAT and liver of mice under the normal condition (n = 9) and exposed to 4 ˚C for 3 hours (n = 6). State 2: mitochondrial respiration in response to glutamate and malate. State 3: mitochondrial respiration in response to ADP. The data were presented as mean ± SE. ## $p < 0.01$. #Comparison between treatments.

Figure 10B

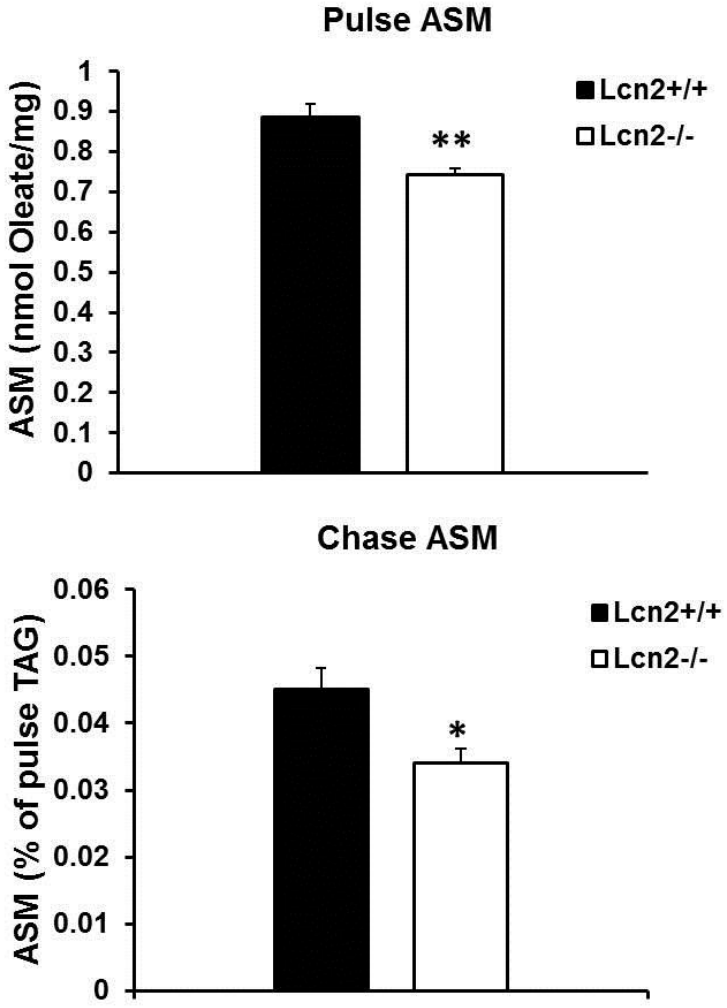

Figure 10B. Oxidation of ^{14}C-labled oleate in SV-differentiated brown adipocytes during pulse and chase phase. ASM: acid soluble metabolites. * $p < 0.05$. * Comparison between genotypes.

Figure 10C

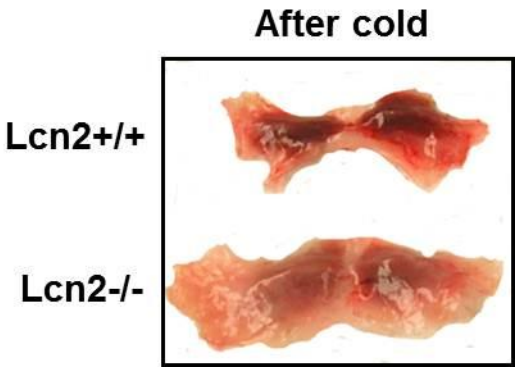

Figure 10C. Brown adipose tissue from WT and *Lcn2* KO mice exposed to 4 ℃ for 4 hours.

Figure 10D

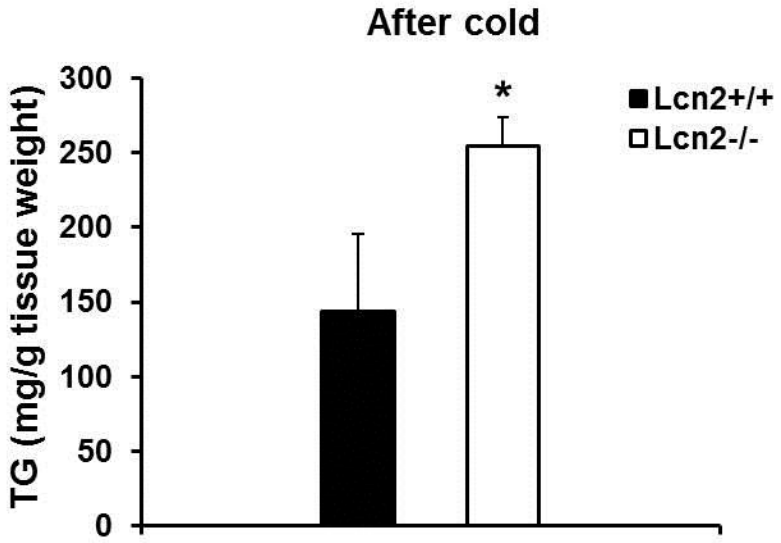

Figure 10D. Triglyceride content of BAT in WT and *Lcn2* KO mice after cold exposure (n = 6). The data were normalized to tissue weight, presented as mean ± SE. * $p < 0.05$. * Comparison between genotypes.

Figure 10E

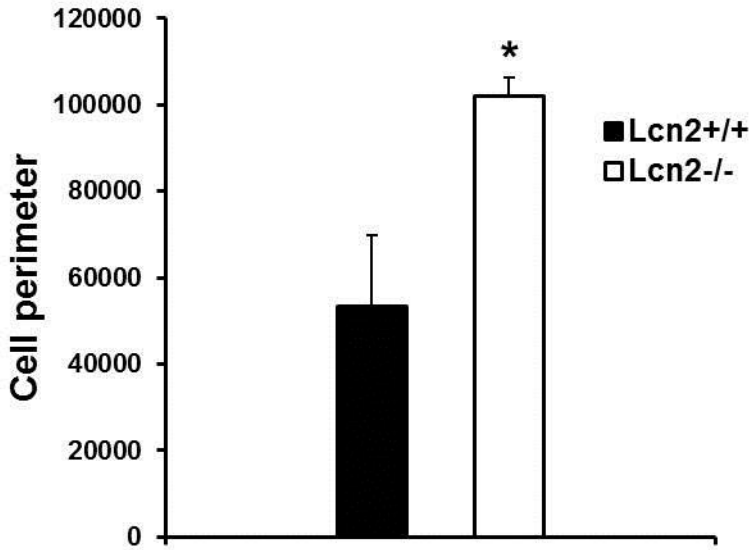

Figure 10E. Quantitative analysis of perimeter of brown adipocytes from mice exposed to 4℃ for 4 h (n = 4). The data were presented as mean ± SE. * $p < 0.05$. * Comparison between genotypes.

Figure 10F

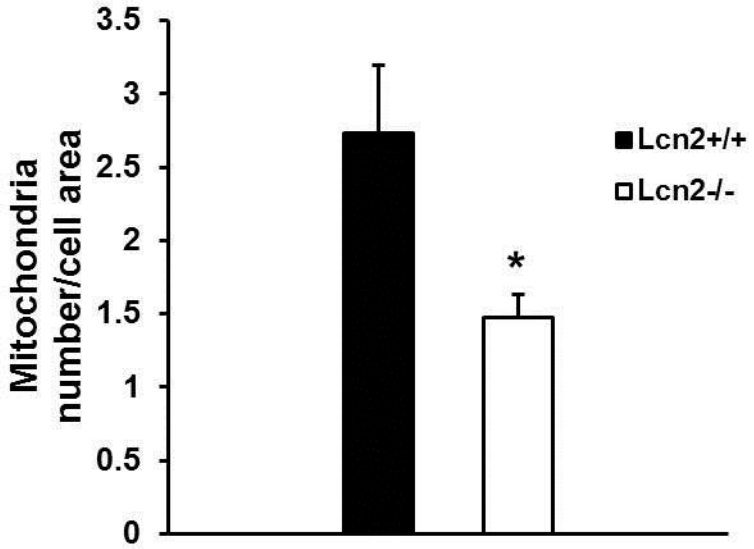

Figure 10F. Quantitative analysis of mitochondria number per cell area from mice exposed to 4 ℃ for 4 h (n = 4). The data were presented as mean ± SE. * $p < 0.05$. * Comparison between genotypes.

Figure 10G

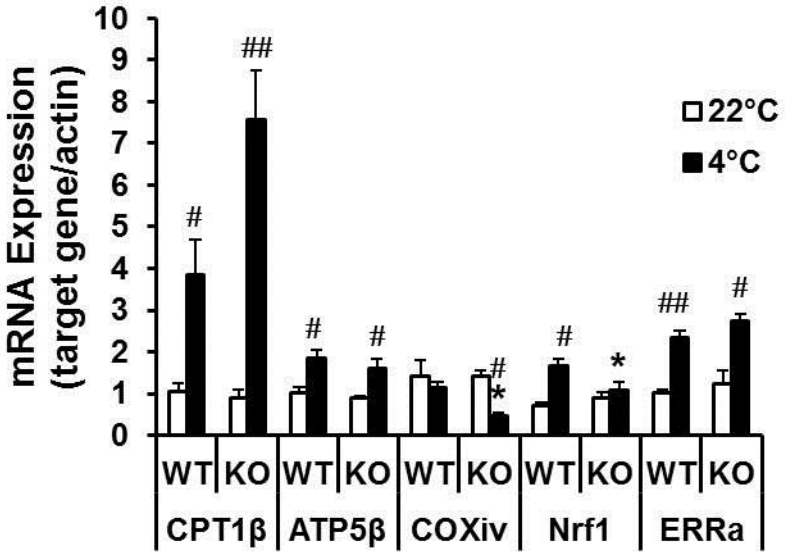

Figure 10G. The mRNA expression of mitochondrial genes in BAT of mice (n = 4-6). The data were presented as mean ± SE. * or # $p < 0.05$; ** or ## $p < 0.01$. * Comparison between genotypes. # Comparison between treatments.

Figure 11A

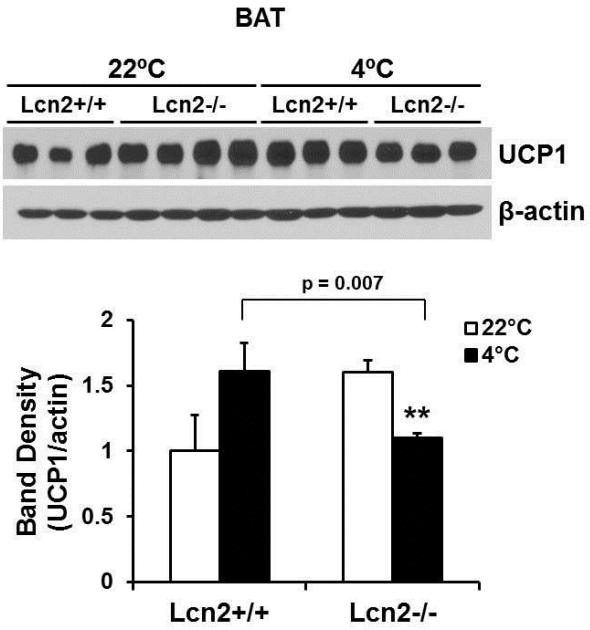

Figure 11A. Cold-induced UCP1 protein expression in BAT of WT and *Lcn2* KO mice. ** $p < 0.01$. * Comparison between genotypes.

Figure 11B

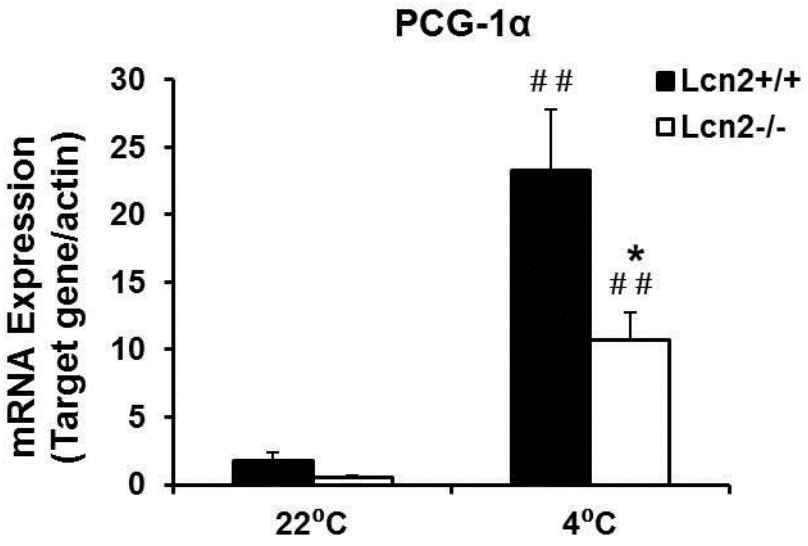

Figure 11B. Cold-induced mRNA expression of PGC-1α (n = 4-5). The data were presented as mean ± SE. * $p < 0.05$; ## $p < 0.01$. * Comparison between genotypes. #Comparison between treatments.

Figure 11C

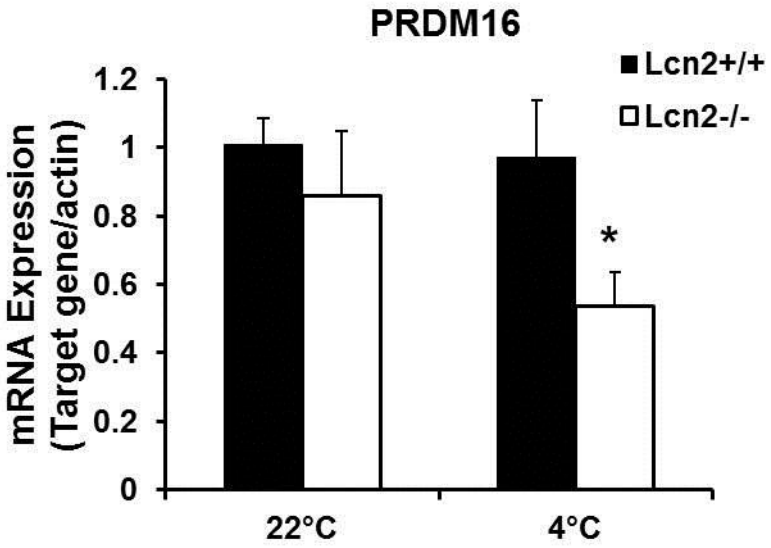

Figure 11C. Cold-induced mRNA expression of PRDM16 (n = 4-5). The data were presented as mean ± SE. * $p < 0.05$. * Comparison between genotypes.

Figure 11D

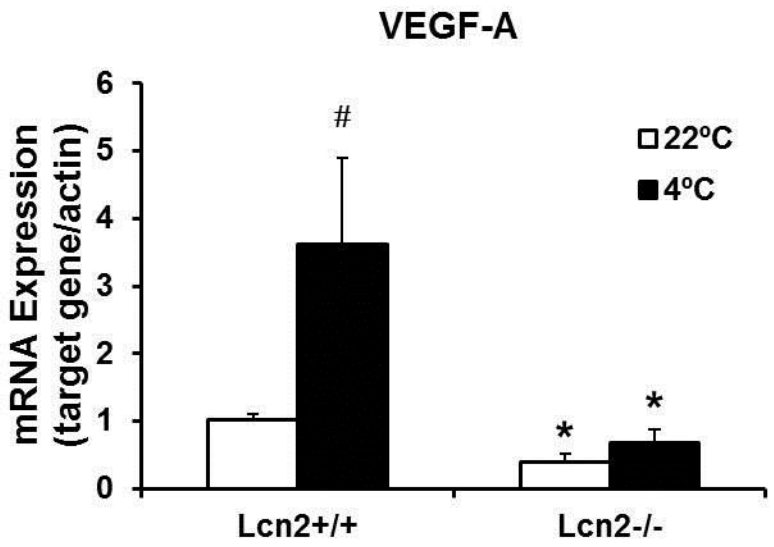

Figure 11D. mRNA expression of VEFG-A in BAT of mice (n = 4). The data were presented as mean ± SE. * or # $p < 0.05$. * Comparison between genotypes. #Comparison between treatments.

Figure 11E

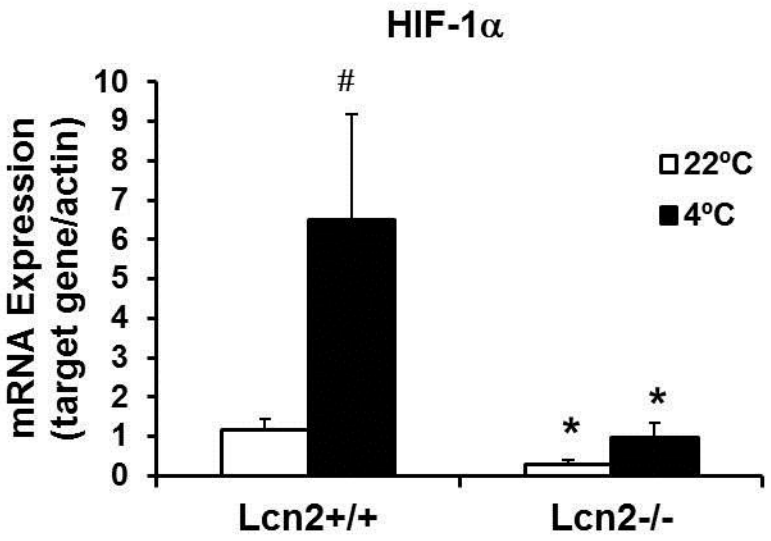

Figure 11E. mRNA expression of HIF-1α in BAT of mice (n = 4). The data were presented as mean ± SE. * or # $p < 0.05$. * Comparison between genotypes. #Comparison between treatments.

Figure 12A

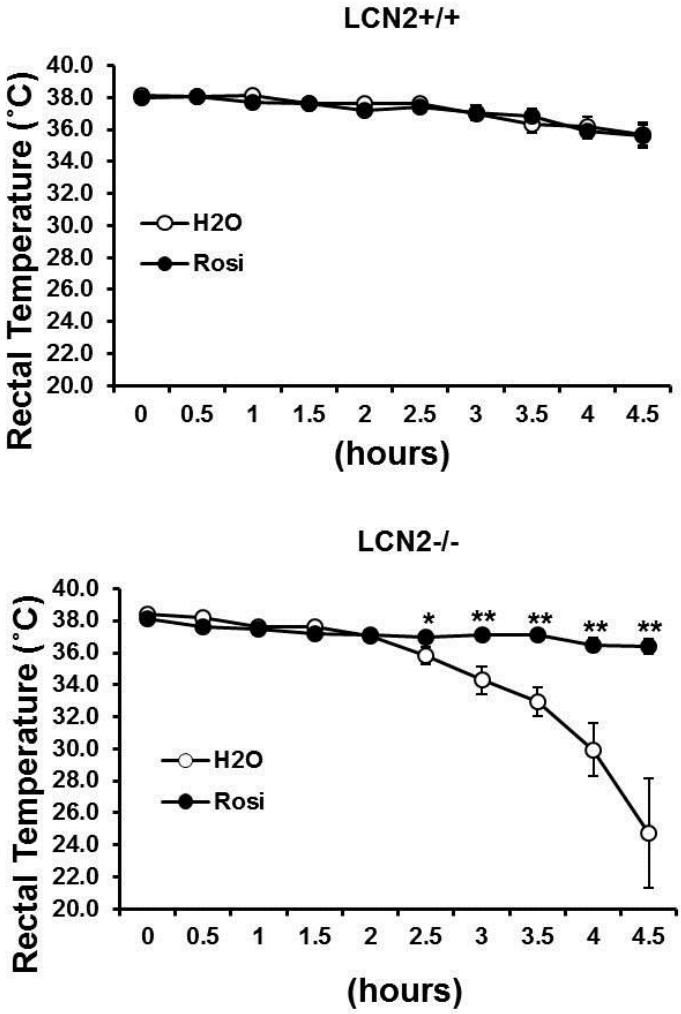

Figure 12A. Body temperature of WT and *Lcn2* KO mice with or without Rosi treatment (n = 5). * $p < 0.05$; ** $p < 0.01$.

Figure 12B

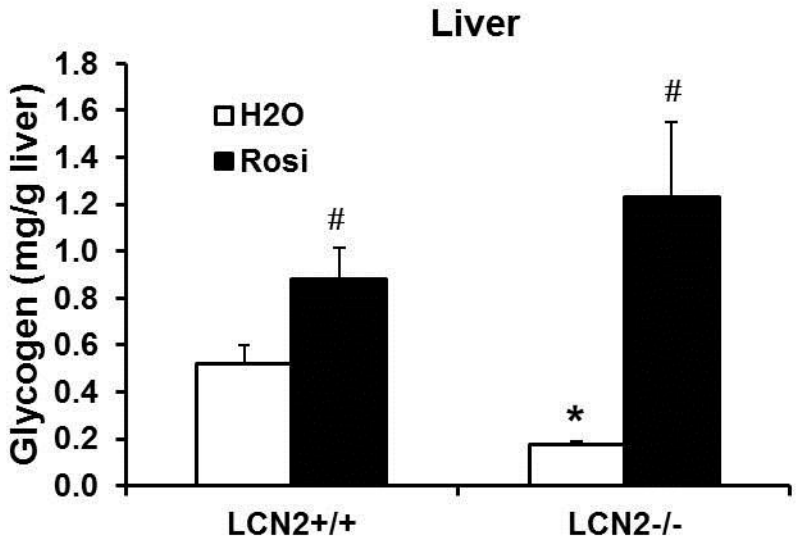

Figure 12B. Liver glycogen content in mice with and without Rosi treatment (n = 4-5). The data were presented as mean ± SE. * or # $p < 0.05$. * Comparison between genotypes. # Comparison between treatments.

Figure 12C

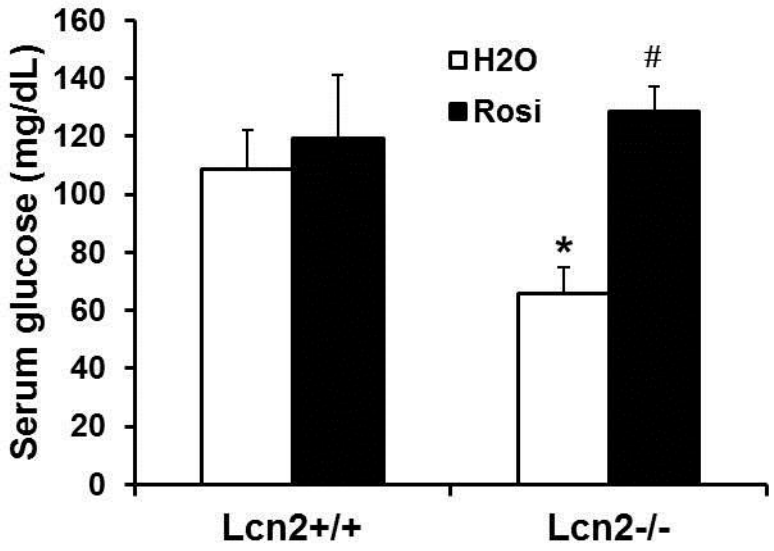

Figure 12C. Serum glucose levels in mice with and without Rosi treatment (n = 4-5). The data were presented as mean ± SE. * or # $p < 0.05$. * Comparison between genotypes. # Comparison between treatments

Figure 12D

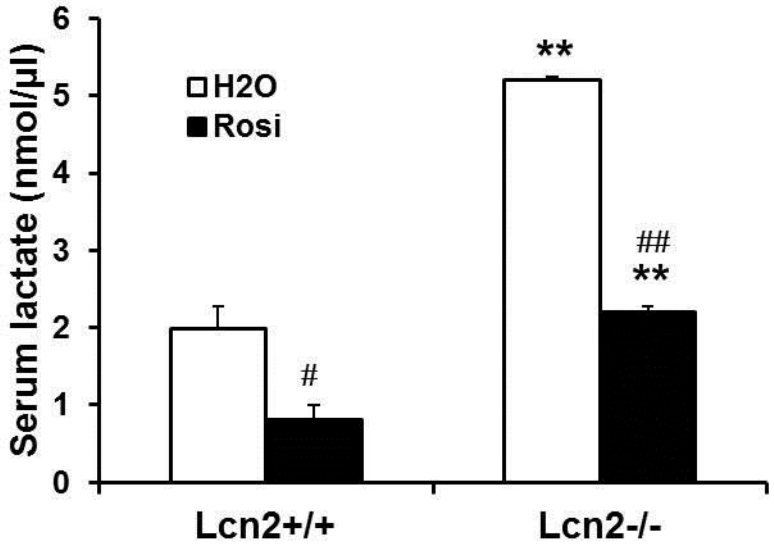

Figure 12D. Serum lactate levels in mice with and without Rosi treatment (n = 4-5). The data were presented as mean ± SE. * or # $p < 0.05$; ** or ## $p < 0.01$. * Comparison between genotypes. # Comparison between treatments.

Figure 12E

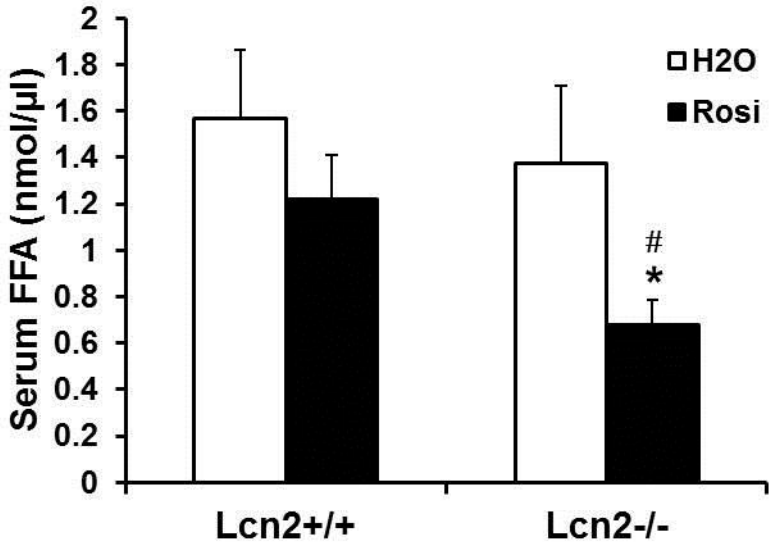

Figure 12E. Serum fatty acid levels in mice with and without Rosi treatment (n = 4-5). The data were presented as mean ± SE. * or # $p < 0.05$. * Comparison between genotypes. # Comparison between treatments.

Figure 12F

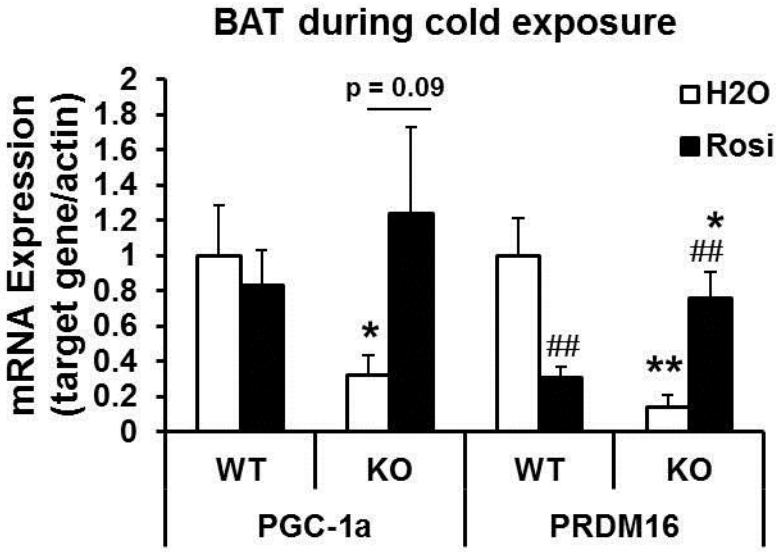

Figure 12F. mRNA expression of thermogenic genes PGC-1α and PRDM16 in BAT (n = 4-5). The data were presented as mean ± SE. * or # $p < 0.05$; ** or ## $p < 0.01$. *Comparison between genotypes. # Comparison between treatments.

Figure 12G

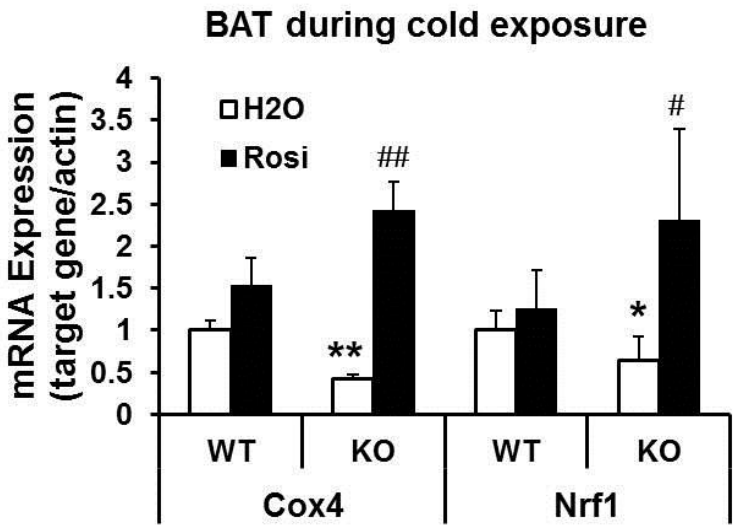

Figure 12G. mRNA expression of Cox4 and Nrf1 in BAT (n = 4-5). The data were presented as mean ± SE. * or # $p < 0.05$; ** or ## $p < 0.01$. * Comparison between genotypes. # Comparison between treatments

SUMMARY

In the thesis, we investigated the metabolic regulation and function of an adipose tissue-derived cytokine - Lcn2. We found that adipose Lcn2 expression is regulated by metabolic challenges and nutrient signals. *Lcn2* mRNA expression is significantly upregulated during fasting and cold exposure in mice, while changes in Lcn2 protein expression are depot-dependent. Insulin stimulates Lcn2 expression and secretion in adipocytes, possibly by increasing glucose uptake and metabolism and activating inflammatory signaling pathway (Fig 13A). In addition, fatty acids induce Lcn2 protein expression and secretion in adipocytes. These results suggest that the regulation of adipose Lcn2 expression involves multiple signaling pathways. Further studies are needed to determine which pathways or transcriptional factors dominantly regulate adipose Lcn2 expression and secretion. Moreover, we explored the metabolic consequences of Lcn2 deficiency in mice. We found that Lcn2 deficiency not only potentiates diet-induced obesity, dyslipidemia, fatty liver disease, and insulin resistance, but also impaired cold-induced adaptive thermogenesis in mice. Interestingly, all these metabolic defects in *Lcn2* KO mice can be effectively improved by the administration of PPARγ agonist. Since the structure of Lcn2 indicates that it may serve as a putative transporter for small hydrophobic molecules, we speculate that Lcn2 may regulate the action of its ligands, which links to the activation of PPARγ possibly via an unknown mechanism (Fig 13B). However, the ligands of Lcn2 have not been discovered yet. Hence, the detailed mechanism for Lcn2-mediated PPARγ activation needs to be

addressed in the future research. Overall, our results indicate that Lcn2 plays a critical role in lipid homeostasis and thermogenic activation via a possible mechanism of modulating PPARγ activation.

Figure 13A

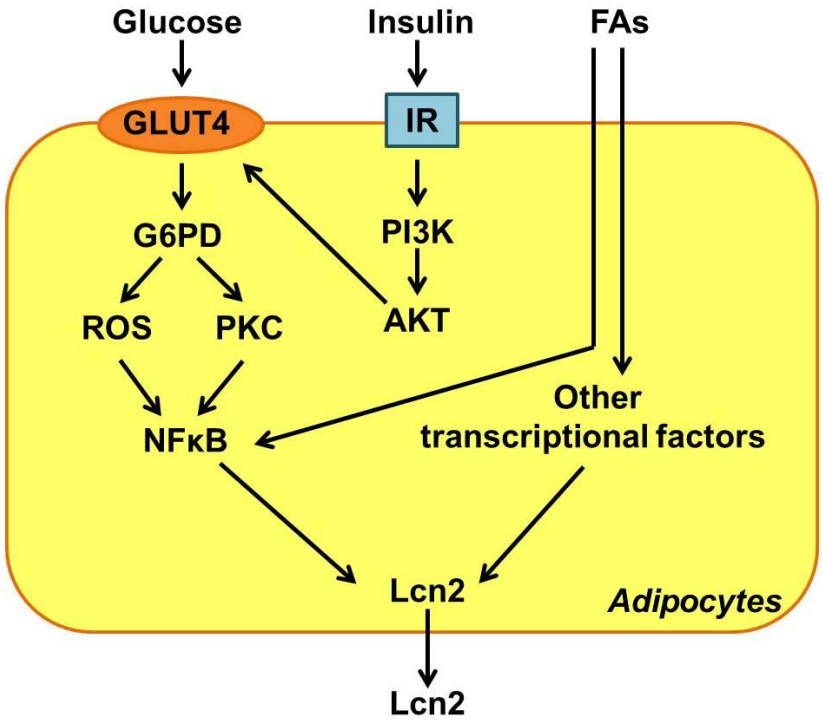

Figure 13A. The model of the regulation of Lcn2 expression and secretion in 3T3-L1 adipocytes.

Figure 13B

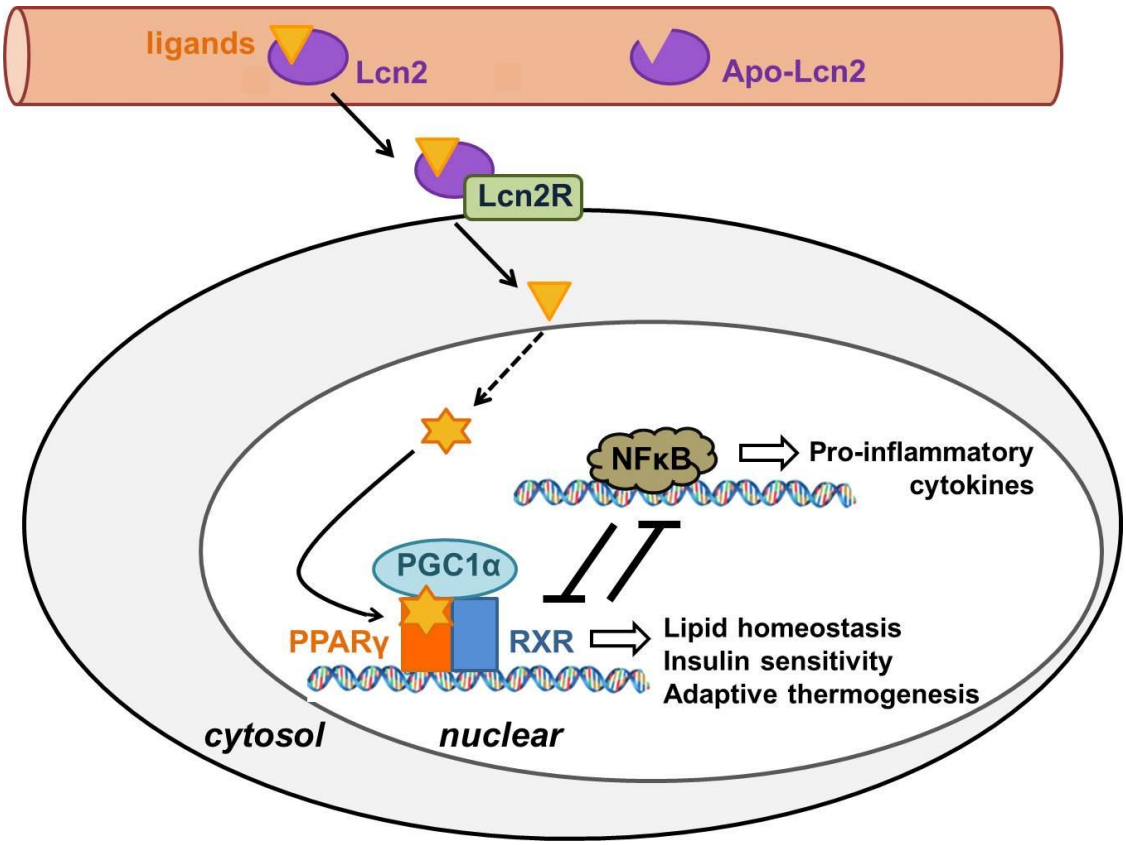

Figure 13B. The model of Lcn2-mediated PPARγ activation.

MATERIALS AND METHODS

Animal studies

Male C57BL/6 mice were obtained from the Jackson Laboratory (Bar Harbor, ME). *Lcn2* KO mice were provided by Dr. Alan Aderem (Institute for Systems Biology, Seattle, WA), which were originally generated by Dr. Shizuo Akira (Research Institute for Microbial Diseases, Osaka University, Osaka, Japan). *Lcn2* KO mice were generated by injecting gene targeted embryonic stem cells from mouse strain 129 into C57BL/6 blastocysts, as previously described (Flo et al., 2004). Male C57BL/6 WT mice and *Lcn2* KO mice were maintained at 70 ℉ on a 12:12h light-dark cycle. Animal handling followed National Institutes of Health guidelines, and experimental procedures were approved by the University of Minnesota Animal Care and Use Committee. Age matched male WT and *Lcn2* KO mice were fed a high-fat diet (fat calories: 60%) obtained from Bio-Serv (F3282; New Brunswick, NJ) at the age of 3 weeks and sacrificed at the age of 16 weeks for experiments. In the HFD-related rosiglitazone study, WT and *Lcn2* KO mice were fed an HFD at the age of 3 weeks; they were subjected to oral gavage of rosiglitazone (10mg/kg body weight/day) for 25 days after the development of obesity and insulin resistance in response to HFD preloading for 14 weeks. In the fasting study, C57BL/6 mice on a regular chow diet at the age of 14 weeks were fasted for 48 hours and sacrificed, while mice in the re-feed group had the access to food for overnight after 48-hour starvation before sacrifice. In the cold adaptive study, mice on the regular chow diet were exposed to 4 ℃ for 5 hours, with free access to water. Mice were individually housed and had no access to food during the whole period of cold exposure. Rectal

temperature of mice was measured every 30 minutes using the Micro Therma Thermometer (Braintree Scientific, Braintree, MA). After cold exposure, the mice were sacrificed immediately; blood and tissue samples were collected for various assessments. In the cold-related rosiglitazone study, WT and *Lcn2* KO mice at 10 weeks of age were subjected to oral gavage of rosiglitazone (10mg/kg body weight/day) for 2 weeks, followed by the exposure to 4℃ for 5 hours as described above.

Metabolic studies

Mice were fasted for 12 hours for glucose tolerance tests (GTTs) and for 6 hours for insulin tolerance tests (ITTs). GTTs and ITTs were conducted by intraperitoneal injection of glucose (1 mg/g body weight) or insulin (0.75 units/kg body weight). Blood was collected via the tail vein at 0, 15, 30, 60, 90, and 120 minutes after the injection; blood glucose levels were measured using an Ascensia contour glucometer.

Cell Cultures

3T3-L1 cells were cultured in DMEM with 10% bovine calf serum (Sigma Aldrich, Saint Louis, MO) and 100 IU/ml penicillin/streptomycin (Invitrogen, Carlsbad, CA) until confluence. Two days after confluence, the cells were induced for differentiation with the differentiation cocktail containing 10% fetal bovine serum (JRH Biosciences, Inc., Lenexa, KS), 115 μg/ml methylisobutylxanthine (Sigma Aldrich, Saint Louis, MO), 1 μg/ml insulin (Sigma Aldrich, Saint Louis, MO), and 390ng/ml dexamethasone (Sigma Aldrich, Saint Louis, MO). The differentiation cocktail was replaced with DMEM

containing 10% fetal bovine serum, 100 IU/ml penicillin/streptomycin and 1 μg/ml insulin two days later. The cultures were continued for another 6 days. In general, 80% - 95% of cells differentiated into adipocytes. On day 8 of differentiation, adipocytes were starved in DMEM with 1 mg/ml glucose and 0.5% bovine calf serum for 12 hours, followed by the treatment with TNFα. For glucose and fatty acid treatment, cells were not starved; but insulin was removed on day 6 of differentiation to keep their sensitivity to insulin during the treatment. Both conditioned media and cells were collected for protein or RNA detection.

Isolation and differentiation of primary BAT stromal-vascular cells

Isolation of primary stromal-vascular (S-V) cells was performed as previously described (Xiang et al., 2007). BAT was removed from WT and *Lcn2* KO mice, minced and digested with Krebs-Ringer bicarbonate HEPES buffer (pH 7.4) containing 200nmol/L adenosine, 3.5% BSA, and 2mg/mL collagenase. After 1.5-hour digestion, tissue explants were separated by centrifuging at 1200rpm for 5 min. Floating adipocytes were removed, while the S-V cells in the lower phase were collected and washed with KRBH buffer twice. After the wash, S-V cells were plated on 6-well plate and cultured in DMEM media containing 20% fetal bovine serum (Sigma Aldrich, Saint Louis, MO) and 100IU/mL penicillin/streptomycin (Invitrogen, Carlsbad, CA) until confluence. Then the cells were treated with the differentiation cocktail consisted of DMEM, 10% fetal bovine serum (Sigma Aldrich, Saint Louis, MO), 100IU/mL penicillin/streptomycin (Invitrogen, Carlsbad, CA), 115 μg/ml methylisobutylxanthine (Sigma Aldrich, Saint Louis, MO), 1

μg/ml insulin (Sigma Aldrich, Saint Louis, MO), 100ng/ml dexamethasone (Sigma Aldrich, Saint Louis, MO), 125 μM indomethacin (Sigma Aldrich, Saint Louis, MO), and 1nM 3,3',5-triiodo-L-thyronine sodium (Sigma Aldrich, Saint Louis, MO). 3 days later, the differentiation cocktail was replaced with DMEM containing 10% fetal bovine serum, 100IU/mL penicillin/streptomycin, 1 μg/ml insulin, and 1nM 3, 3', 5-triiodo-L-thyronine sodium. The cultures were continued for another 6 days. On day 9 of differentiation, differentiated brown adipocytes were used for the experiments.

Lipolysis Assay for tissue explants and cultured cells

0.1g white adipose tissue or 0.05g brown adipose tissue were isolated from overnight-fasted mice, minced into small pieces, and washed twice with PBS. The minced tissues were cultured in KRH buffer (129mM NaCl, 5mM $NaHCO_3$, 4.8mM KCl, 1.2mM KH_2PO_4, 1mM $CaCl_2$, 1.2mM $MgCl_2$, 2.8mM glucose, 10mM HEPES, pH 7.4) for 2 hours to release free fatty acids and glycerol from the vessels that remained in tissue explants. After 2 hour-incubation, KRH buffer was replaced with fresh KRH buffer containing 2% fatty acid-free BSA and 0.1% glucose with or without 1 μM norepinephrine. Culture medium was collected after 2 hours of incubation. Free fatty acid and glycerol in the media were measured using Free Fatty Acid Quantification Kit (Biovision, Mountain View, CA) and Free Glycerol Reagent (Sigma Aldrich, Saint Louis, MO).

3T3-L1 adipocytes or SV-differentiated adipocytes were pre-incubated in KRH buffer containing 0.5% fatty acid-free BSA for 2 hours. Then the media was refreshed with or

withour 1 μM norepinephrine. The extracellular media was collected after 1 hour, 3 hours, and 6 hours of incubation and analyzed for fatty acid and glycerol release as described above.

Measurement of glucose, lactate, fatty acid and glycerol levels

Mice serum glucose levels were detected with Autokit Glucose (Wako Diagnostics, Richmond, VA). Lactate and fatty acid levels were determined with Lactate Assay Kit (Biovision, Mountain View, CA) and Free Fatty Acid Quantification Kit (Biovision, Mountain View, CA). Serum and media glycerol levels were detected with Free Glycerol Reagent (Sigma Aldrich, Saint Louis, MO).

Serum lipid profile and measurements of insulin and adipokines

The concentrations of triglycerides, cholesterol, LDL and HDL cholesterol, betahydroxybutyrate and non-esterified fatty acids in serum were measured using the Roche COBAS Mira Plus automated chemistry analyzer. Serum levels of insulin, leptin, and adiponectin are assayed using a double-antibody immunoassay kit and rat insulin standards (Linco Research, St. Louis, MO). All the above assays were performed by Yale Mouse Metabolic Phenotyping Center: Analytical Core.

Measurement of liver glycogen content

The measurement of tissue glycogen content was performed base on a previous report (Burcelin et al., 2004). Briefly, mice tissue samples were put in 1M NaOH at 55 ℃ and

votexed several times until completely dissolved. Then the samples were neutralized with 1M HCl and centrifuged at 12,000rpm for 10min. Supernatant was obtained and divided into two parts: Part I was treated with amyloglucosidase (Sigma Aldrich, Saint Louis, MO) at 37 ℃ for 2 hours; part II was put on ice without amyloglucosidase treatment. Glucose concentration in both parts were detected with Autokit Glucose (Wako Diagnostics, Richmond, VA). The glycogen content was determined by calculating the glucose released from glycogen breakdown, i.e. substrating the background glucose levels in part II from the glucose levels in part I.

Liver oil-red O staining

Liver were harvested from WT and *Lcn2* KO mice on a regular chow diet or high fat diet and fixed in phosphate-buffered 10% formaldehyde (pH 7.2) for minimum 4 hours. Then the supernatant was removed; tissue samples were incubated in 0.1M PBS with 5% sucrose for 2 hours, followed by the incubation in 0.1M PBS with 20% sucrose for overnight at 4 ℃. Then tissue samples were snapped frozen in O.C.T. (Optimal Cutting Temperature) medium. OCT embedded tissues were sectioned at a thickness of 8-10 microns and mounted on slides treated for adherence for oil-red O staining (Sigma-Aldrich, Milwaukee, WI).

Triglyceride content measurement

Lipid extraction was performed using Bligh-Dyer method as previously described (BLIGH and DYER, 1959). Around 100mg BAT was homogenized in water. An aliquot

of 20 μL homogenate was saved for measuring protein concentration; the rest of homogenate was transferred to a glass tube and mixed with chloroform and methanol (chloroform: methanol 2:1). Then the sample was centrifuged at 1700rpm for 5 minutes at 4 ℃; the lower chloroform phase was transferred to a new glass tube and dried down with nitrogen. Next the sample was resuspended in 1mL chloroform. An aliquot of 100 μL sample was dried down with nitrogen again and resuspended in 100 μL isopropanol alcohol with 1% triton X-100. The sample was kept at room temperature for at least 1 hour and vortexed occasionally to fully resuspend lipids. Triglyceride content was finally measured with the commercially available kit (Stanbo Laboratory, Boerne, TX, USA) and normalized to protein content.

Measurement of triglyceride hydrolase activity

TAG hydrolase assay was done based on the methods as previously described (Schweiger et al., 2008). Briefly, brown adipose tissue was isolated and homogenized on ice with a motor-driven teflon-glass homogenizer in lysis buffer (0.25M sucrose, 1mM EDTA, 1mM dithiothreitol, pH 7.0). Then the tissue was centrifuged at 1,000g for 15 min and then at 100, 000g for 1 hour to obtain the infranatant. 100ug of protein was incubated with hot TAG substrate at 37 ℃ for 1 hour. The reaction was terminated by adding methanol/chloroform/heptane (10:9:7) and the termination buffer (1M potassium carbonate, 1M boric acid, 1M potassium carbonate, pH 10.5) and centrifuged at 800g for 15 min. The radioactivity in 750uL of the upper phase was determined by scintillation counting.

Lipid profiling

Analysis of the composition of fatty acids was performed as previously described (Bu et al., 2009). Briefly, SV cells were isolated from BAT of WT and *Lcn2* KO mice and induced to differentiation. Lipids were extracted from differentiated brown adipocytes. Intracellular free fatty acids were seperated by TLC on 0.25 mm silica gel G plates in hexane:ethyl ether:acetic acid (80:20:1, v/v). Then isolated triglyceride fractions were methylated in 3N methanolic HCl at 100℃ for 90 min. The fatty acid methyl esters were extracted with hexane for gas chromatography analysis.

FA synthesis *in vivo*

WT and *Lcn2* KO mice on HFD at the age of 14 weeks were subjected to rosiglitazone treatment for 14 days by oral gavage. The rate of *de novo* lipogenesis was determined by measuring the newly synthesized FAs present in adipose tissue of these mice. One hour after intraperitoneal injection of 1 mCi of $[^3H]H_2O$ in saline, adipose tissue was removed, and total lipids were extracted from a 100mg portion of tissue in chlorform:methanol (2:1, v/v) (BLIGH and DYER, 1959). Samples were saponified in ethanolic KOH, and sterols were extracted with petroleum ether. Following acidification with acetic acid, FAs were extracted from the same samples with petroleum ether (Dietschy and Spady, 1984). Aliquots of 3H-labeled FAs were counted in a liquid scintillation counter (LS6000IC; Beckman Coulter, Fullerton, CA). The rate of FA synthesis was calculated as detections per minute (dpm) per whole fat pad.

Fatty acid oxidaiton in adipocytes

SV cells were isolated from BAT of WT and *Lcn2* KO mice and induced to differentiate into brow adipocytes as described above. Differentiated brown adipocytes were cultured in DMEM containing 5 mM glucose, 0.5% FBS and 50 uM L-carnitine overnight. The next morning the media was changed to serum free DMEM containing 5 mM glucose, 0.1% FA-free BSA and 1mM carnitine. After 2 hours, cells were exposed to 250 uM of either [1-^{14}C] oleate or palmitate for 90 minutes. One subset of wells were harvested to measure the radiolabel in the acid-soluble metabolite fraction (pulse); another set of wells were washed with PBS and incubated with label free media for 3 hours before quantifying the label in acid-soluble metabolites (chase). Lipids were extracted and fractionated; radioisotopes in the acid-soluble metabolites were quantified as previously described (Lewin et al., 2005).

Mitochondria isolation and respiration

The isolation of mitochondria and oxidative respiration were performed as previously described (Mogensen et al., 2007; Curtis et al., 2010). Briefly, BAT and liver were isolated from WT and *Lcn2* KO mice exposed at 22 ℃ or 4 ℃, washed and minced in Krebs-Ringer HEPES, and lysed with the isolation buffer (20mM Tris-HCl, 220mM mannitol, 70mM sucrose, 1mM EDTA, pH 7.4) using a Dounce homogenizer. The homogenate was centrifuged at 700g for 10 minutes to remove cell debris, nuclei and lipids. Then the supernatant was centrifuged at 9400g for 10 minutes to acquire

mitochondria pellet. Oxidative respiration was assessed using a FOXY-R Oxygen Sensor (Ocean Optics, Dunedin, FL). Isolated mitochondria were injected into 500uL respiration buffer (10 mM HEPES, pH 7.4, 125 mM KCl, 5mM $MgCl_2$, and 2mM K_2HPO_4) and incubated for 5 minutes. Then substrates were injected to reach a final concentration of 10mM glutamate and 5mM malate in order to stimulate state 2 respiration. Five minutes later, 0.5mM ADP was added to stimulate state 3 respiration. Finally, protein concentration of mitochondria pellet was measured with bicinchoninic acid method (Pierce, Rockford, IL), and the oxygen consumption rate was normalized to mitochondrial protein content.

Quantitative real-time RT-PCR

Total RNAs were extracted from mouse tissues or 3T3-L1 adipocytes using TRIzol reagent (Invitrogen, Carlsbad, CA) according to the manufacturer's instructions. After treatment with RQ1 DNase (Promega, Madison, WI), 1μg RNA were used to synthesize the cDNA in reverse transcription with 5μM oligo dT primer, 0.5mM dNTP, 20 units RNasin Ribonuclease Inhibitor (Promega, Madison, WI), 5mM DTT, and 100 units SuperScript® II Reverse Transcriptase (Invitrogen, Carlsbad, CA). Realtime-PCR was performed using SYBR GreenER qPCR SuperMix Universal kit (Invitrogen Carlsbad, CA) with an ABI 7500 Real Time PCR System (Applied Biosystems, Foster City, CA). Results were analyzed using the software supplied with the 7500 system and presented as levels of expression relative to that of controls after normalizing to β-actin or GAPDH

using ΔΔCt method. Statistical significance was determined by two-tailed Student's *t* test. Primer sequences were listed in Table 1.

Immunoblotting

Lysates of 3T3-L1 adipocytes were prepared in a lysis buffer containing 25 mM Tris-HCl pH 7.5, 0.5 mM EDTA, 25 mM sodium chloride, 10 mM sodium fluoride, 1mM sodium vanadate, 1% Nonidet P-40 and protease inhibitor cocktails (Diagnostic Roche, Branchburg, NJ). Tissue samples were homogenized and solubilized in RIPA buffer (Sigma, St. Louis, MO). The lysates were centrifuged at 12,000g for 10 minutes, and supernatants were collected. Protein concentrations of lysates were detected with bicinchoninic acid method (Pierce, Rockford, IL). The conditional media were concentrated with NANOSEP centrifugal device (Pall Life Sciences, East Hills, NY) and adjusted to the same volume among samples. Equivalent proteins were loaded and separated on SDS-PAGE and then electro-transferred to nitrocellulose membranes. Membranes were incubated with anti-LCN2 (R&D System, Minneapolis, MN), anti-UCP1, anti-HSL, anti-phospho-HSL (Ser563) (Cell Signaling Technology, Danvers, MA), and anti-actin antibodies after blocking with TTBS (20 mM Tris-HCl pH 7.5, 0.5 M NaCl, 0.1% Tween-20) containing 5% milk (Fisher Scientific, Pittsburgh, PA). Then the membranes were washed in TTBS and incubated with corresponding secondary antibodies conjugated to horseradish peroxidase (GE Healthcare Bio-Sciences Corp., Piscataway, NJ). The signals were detected by ECL plus Western Blotting Detection Reagents (GE Healthcare Bio-Sciences Corp., Piscataway, NJ).

Electron microscopy

Fixation for Electron Microscopy

One to two cubic millimeters brown adipose tissue from WT and *Lcn2* KO mice after 4h exposure to 4℃ were collected and fixed immediately in 1-2ml of 2.5 % glutaraldehyde (Electron Microscopy Sciences, Hatfield, PA, USA) in 0.1M sodium cacodylate (Electron Microscopy Sciences, Hatfield, PA, USA) buffer overnight at 4 ℃. Samples were washed three times with 0.1M sodium cacodylate buffer and post fixed with 1% Osmium tetroxide (Electron Microscopy Sciences, Hatfield, PA, USA) in 0.1M sodium cacodylate buffer. After three washes in distilled water, samples were dehydrated using a 25-100% acetone gradient and then infiltrated with 2:1 acetone: Embed 812 resin (Electron Microscopy Sciences, Hatfield, PA, USA) for 2 h and subsequently transferred to a 1:2 acetone: Embed 812 resin mixture for 2 hour. Finally, tissue sections were infiltrated with 100% resin and embedded in 100% resin, followed by the incubation at 58^{o}C for 24 h to polymerize the resin.

Sectioning

Embedded samples were trimmed and sectioned on a Leica UC6 Ultramicrotome (Leica Microsystems, Vienna, Austria). Thin sections (60-70 nm) were obtained and collected on a 200 mesh copper grid (Electron Microscopy Sciences, Hatfield, PA, USA) using a perfect loop (Electron Microscopy Sciences, Hatfield, PA, USA).

Staining

Grids were stained with 5% uranyl acetate for 20 minutes and Satos' lead citrate for 6 minutes. These sections were observed under JEOL 1200 EX II transmission electron microscope (JEOL LTD, Tokyo, Japan). Images were obtained using a Veleta 2K x2K camera with iTEM software (Olympus SIS, Munster, Germany).

Analysis

A qualitative and quantitative assessment was performed. All tissue sections were blindly examined; Criteria include mitochondrial size, shape, cryptation, and matrix densities as well as lipid droplets. For the quantitative analysis, 10 cells were randomly selected from each WT and Lcn2 KO samples (4 mice per genotype were included). Number of mitochondria and lipid droplets in each cell was tallied. Average areas of the mitochondria and lipid droplets were calculated from a total of 100 mitochondria. All the measurements were acquired using iTEM software (Olympus SIS, Munster, Germany). Dimensions were compared between both the wild type and knockouts.

Table 3. List of real-time PCR primer sequences

Accesion	Gene	Forward (5'----3')	Reverse (5'----3')
NM 007393	Actb	CCTAAGGCCAACCGTGAAAA	GAGGCATACAGGGACAGCACA
NM 013462	Adrb3	AGTGCAGGAGGAAGATGGAAACCA	AGTTACTGGAGACACCCGCTTGTT
NM 016774	Atp5b	GCAAGGCAGGGACAGCAGA	CCCAAGGTCTCAGGACCAACA
NM 009941	Cox4	ATGTCACGATGCTGTCTGCC	GTGCCCCTGTTCATCTCGGC
NM 009948	Cpt1b	TCTAGGCAATGCCGTTCAC	GAGCACATGGGCACCATAC
NM 007953	Esrra	GGAGGACGGCAGAAGTACAAA	GCGACACCAGAGCGTTCAC
NM 008084	Gapdh	TTGTGCAGTGCCAGCCTCGTC	GCGCCCAATACGGCCAAATCC
NM 010431	Hif1a	TCAAGTCAGCAACGTGGAAG	TATCGAGGCTGTGTCGACTG
NM 010938	Nrf1	TGGTCCAGAGAGTGCTTGTGAAG	GGAGGCTGAGGAACGATTTCTTG
NM 008904	Ppargc1a	ACCGTAAATCTGCGGGATGATGGA	AGTCAGTTTCGTTCGACCTGCGTA
NM 001177995	Prdm16	AAGCTGTGCATGGCTCGTGTTTAG	AGTCACCAGGAACTGTGGTCCATT
NM 178060	Thra	TTGCGAAGACCAGATCATCCT	GTGGGGCACTCGACTTTCAT
NM 001113417	Thrb	AAATCTCCATCCATCCTATTCC	CTTCCAAGTCAACCTTTCCA
NM 001025257	Vegfa	CACGACAGAAGGAGAGCAGAAGT	TTCGCTGGTAGACATCCATGAA

BIBLIOGRAPHY

Aigner, F., Maier, H.T., Schwelberger, H.G., Wallnofer, E.A., Amberger, A., Obrist, P., Berger, T., Mak, T.W., Maglione, M., Margreiter, R., Schneeberger, S., and Troppmair, J. (2007). Lipocalin-2 regulates the inflammatory response during ischemia and reperfusion of the transplanted heart. Am. J. Transplant. *7,* 779-788.

Akelma, A.Z., Abaci, A., Ozdemir, O., Celik, A., Avci, Z., Razi, C.H., Hizli, S., and Akin, O. (2012). The association of serum lipocalin-2 levels with metabolic and clinical parameters in obese children: a pilot study. J. Pediatr. Endocrinol. Metab. *25,* 525-528.

Akiyama, H., Tanaka, T., Maeno, T., Kanai, H., Kimura, Y., Kishi, S., and Kurabayashi, M. (2002). Induction of VEGF gene expression by retinoic acid through Sp1-binding sites in retinoblastoma Y79 cells. Invest. Ophthalmol. Vis. Sci. *43,* 1367-1374.

Aljada, A., O'Connor, L., Fu, Y.Y., and Mousa, S.A. (2008). PPAR gamma ligands, rosiglitazone and pioglitazone, inhibit bFGF- and VEGF-mediated angiogenesis. Angiogenesis *11,* 361-367.

Andre, E., Stoeger, T., Takenaka, S., Bahnweg, M., Ritter, B., Karg, E., Lentner, B., Reinhard, C., Schulz, H., and Wjst, M. (2006). Inhalation of ultrafine carbon particles triggers biphasic pro-inflammatory response in the mouse lung. Eur. Respir. J. *28,* 275-285.

Asano, A., Morimatsu, M., Nikami, H., Yoshida, T., and Saito, M. (1997). Adrenergic activation of vascular endothelial growth factor mRNA expression in rat brown adipose tissue: implication in cold-induced angiogenesis. Biochem. J. *328 (Pt 1),* 179-183.

Atit, R., Sgaier, S.K., Mohamed, O.A., Taketo, M.M., Dufort, D., Joyner, A.L., Niswander, L., and Conlon, R.A. (2006). Beta-catenin activation is necessary and sufficient to specify the dorsal dermal fate in the mouse. Dev. Biol. *296,* 164-176.

Auguet, T., Quintero, Y., Terra, X., Martinez, S., Lucas, A., Pellitero, S., Aguilar, C., Hernandez, M., del Castillo, D., and Richart, C. (2011). Upregulation of lipocalin 2 in adipose tissues of severely obese women: positive relationship with proinflammatory cytokines. Obesity (Silver Spring) *19,* 2295-2300.

Bachman, M.A., Miller, V.L., and Weiser, J.N. (2009). Mucosal lipocalin 2 has pro-inflammatory and iron-sequestering effects in response to bacterial enterobactin. PLoS Pathog. *5,* e1000622.

Barbatelli, G., Murano, I., Madsen, L., Hao, Q., Jimenez, M., Kristiansen, K., Giacobino, J.P., De Matteis, R., and Cinti, S. (2010). The emergence of cold-induced brown

adipocytes in mouse white fat depots is determined predominantly by white to brown adipocyte transdifferentiation. Am. J. Physiol. Endocrinol. Metab. *298*, E1244-53.

Barbera, M.J., Schluter, A., Pedraza, N., Iglesias, R., Villarroya, F., and Giralt, M. (2001). Peroxisome proliferator-activated receptor alpha activates transcription of the brown fat uncoupling protein-1 gene. A link between regulation of the thermogenic and lipid oxidation pathways in the brown fat cell. J. Biol. Chem. *276*, 1486-1493.

Bartelt, A., Bruns, O.T., Reimer, R., Hohenberg, H., Ittrich, H., Peldschus, K., Kaul, M.G., Tromsdorf, U.I., Weller, H., Waurisch, C., *et al.* (2011). Brown adipose tissue activity controls triglyceride clearance. Nat. Med. *17*, 200-205.

Behairy, B., Salama, E.I., Allam, A.A., Ali, M.A., and Elaziz, A.M. (2011). Lipocalin-2 as a marker of bacterial infections in chronic liver disease: a study in Egyptian children. Egypt. J. Immunol. *18*, 31-36.

Berger, T., Cheung, C.C., Elia, A.J., and Mak, T.W. (2010). Disruption of the Lcn2 gene in mice suppresses primary mammary tumor formation but does not decrease lung metastasis. Proc. Natl. Acad. Sci. U. S. A. *107*, 2995-3000.

Berger, T., Togawa, A., Duncan, G.S., Elia, A.J., You-Ten, A., Wakeham, A., Fong, H.E., Cheung, C.C., and Mak, T.W. (2006). Lipocalin 2-deficient mice exhibit increased sensitivity to Escherichia coli infection but not to ischemia-reperfusion injury. Proc. Natl. Acad. Sci. U. S. A. *103*, 1834-1839.

Bergman, R.N., Van Citters, G.W., Mittelman, S.D., Dea, M.K., Hamilton-Wessler, M., Kim, S.P., and Ellmerer, M. (2001). Central role of the adipocyte in the metabolic syndrome. J. Investig. Med. *49*, 119-126.

Bianco, A.C., and Silva, J.E. (1987). Intracellular conversion of thyroxine to triiodothyronine is required for the optimal thermogenic function of brown adipose tissue. J. Clin. Invest. *79*, 295-300.

Biddinger, S.B., Hernandez-Ono, A., Rask-Madsen, C., Haas, J.T., Aleman, J.O., Suzuki, R., Scapa, E.F., Agarwal, C., Carey, M.C., Stephanopoulos, G., *et al.* (2008). Hepatic insulin resistance is sufficient to produce dyslipidemia and susceptibility to atherosclerosis. Cell. Metab. *7*, 125-134.

BLIGH, E.G., and DYER, W.J. (1959). A rapid method of total lipid extraction and purification. Can. J. Biochem. Physiol. *37*, 911-917.

Boden, G. (2001). Free fatty acids-the link between obesity and insulin resistance. Endocr. Pract. *7*, 44-51.

Boden, G. (1997). Role of fatty acids in the pathogenesis of insulin resistance and NIDDM. Diabetes *46,* 3-10.

Bohnsack, B.L., Lai, L., Dolle, P., and Hirschi, K.K. (2004). Signaling hierarchy downstream of retinoic acid that independently regulates vascular remodeling and endothelial cell proliferation. Genes Dev. *18,* 1345-1358.

Bronnikov, G., Houstek, J., and Nedergaard, J. (1992). Beta-adrenergic, cAMP-mediated stimulation of proliferation of brown fat cells in primary culture. Mediation via beta 1 but not via beta 3 adrenoceptors. J. Biol. Chem. *267,* 2006-2013.

Bu, S.Y., Mashek, M.T., and Mashek, D.G. (2009). Suppression of long chain acyl-CoA synthetase 3 decreases hepatic de novo fatty acid synthesis through decreased transcriptional activity. J. Biol. Chem. *284,* 30474-30483.

Bukowiecki, L., Collet, A.J., Follea, N., Guay, G., and Jahjah, L. (1982). Brown adipose tissue hyperplasia: a fundamental mechanism of adaptation to cold and hyperphagia. Am. J. Physiol. *242,* E353-9.

Bukowiecki, L.J., Geloen, A., and Collet, A.J. (1986). Proliferation and differentiation of brown adipocytes from interstitial cells during cold acclimation. Am. J. Physiol. *250,* C880-7.

Burcelin, R., Uldry, M., Foretz, M., Perrin, C., Dacosta, A., Nenniger-Tosato, M., Seydoux, J., Cotecchia, S., and Thorens, B. (2004). Impaired glucose homeostasis in mice lacking the alpha1b-adrenergic receptor subtype. J. Biol. Chem. *279,* 1108-1115.

Butow, R.A., and Bahassi, E.M. (1999). Adaptive thermogenesis: orchestrating mitochondrial biogenesis. Curr. Biol. *9,* R767-9.

Cannon, B., and Nedergaard, J. (2010). Thyroid hormones: igniting brown fat via the brain. Nat. Med. *16,* 965-967.

Cannon, B., and Nedergaard, J. (2004). Brown adipose tissue: function and physiological significance. Physiol. Rev. *84,* 277-359.

Catalan, V., Gomez-Ambrosi, J., Rodriguez, A., Ramirez, B., Silva, C., Rotellar, F., Gil, M.J., Cienfuegos, J.A., Salvador, J., and Fruhbeck, G. (2009). Increased adipose tissue expression of lipocalin-2 in obesity is related to inflammation and matrix metalloproteinase-2 and metalloproteinase-9 activities in humans. J. Mol. Med. (Berl) *87,* 803-813.

Chen, X., Cushman, S.W., Pannell, L.K., and Hess, S. (2005). Quantitative proteomic analysis of the secretory proteins from rat adipose cells using a 2D liquid chromatography-MS/MS approach. J. Proteome Res. *4*, 570-577.

Chernogubova, E., Hutchinson, D.S., Nedergaard, J., and Bengtsson, T. (2005). Alpha1- and beta1-adrenoceptor signaling fully compensates for beta3-adrenoceptor deficiency in brown adipocyte norepinephrine-stimulated glucose uptake. Endocrinology *146*, 2271-2284.

Chintalgattu, V., Harris, G.S., Akula, S.M., and Katwa, L.C. (2007). PPAR-gamma agonists induce the expression of VEGF and its receptors in cultured cardiac myofibroblasts. Cardiovasc. Res. *74*, 140-150.

Choi, J.H., Banks, A.S., Estall, J.L., Kajimura, S., Bostrom, P., Laznik, D., Ruas, J.L., Chalmers, M.J., Kamenecka, T.M., Bluher, M., Griffin, P.R., and Spiegelman, B.M. (2010). Anti-diabetic drugs inhibit obesity-linked phosphorylation of PPARgamma by Cdk5. Nature *466*, 451-456.

Collins, S., Yehuda-Shnaidman, E., and Wang, H. (2010). Positive and negative control of Ucp1 gene transcription and the role of beta-adrenergic signaling networks. Int. J. Obes. (Lond) *34 Suppl 1*, S28-33.

Curtis, J.M., Grimsrud, P.A., Wright, W.S., Xu, X., Foncea, R.E., Graham, D.W., Brestoff, J.R., Wiczer, B.M., Ilkayeva, O., Cianflone, K., *et al.* (2010). Downregulation of adipose glutathione S-transferase A4 leads to increased protein carbonylation, oxidative stress, and mitochondrial dysfunction. Diabetes *59*, 1132-1142.

Cypess, A.M., Lehman, S., Williams, G., Tal, I., Rodman, D., Goldfine, A.B., Kuo, F.C., Palmer, E.L., Tseng, Y.H., Doria, A., Kolodny, G.M., and Kahn, C.R. (2009). Identification and importance of brown adipose tissue in adult humans. N. Engl. J. Med. *360*, 1509-1517.

DAVIS, T.R., JOHNSTON, D.R., BELL, F.C., and CREMER, B.J. (1960). Regulation of shivering and non-shivering heat production during acclimation of rats. Am. J. Physiol. *198*, 471-475.

DEPOCAS, F., HART, J.S., and HEROUX, O. (1956). Cold acclimation and the electromyogram of unanesthetized rats. J. Appl. Physiol. *9*, 404-408.

Deveaud, C., Beauvoit, B., Salin, B., Schaeffer, J., and Rigoulet, M. (2004). Regional differences in oxidative capacity of rat white adipose tissue are linked to the mitochondrial content of mature adipocytes. Mol. Cell. Biochem. *267*, 157-166.

Dhaliwal, S.S., and Welborn, T.A. (2009). Central obesity and multivariable cardiovascular risk as assessed by the Framingham prediction scores. Am. J. Cardiol. *103,* 1403-1407.

Dietschy, J.M., and Spady, D.K. (1984). Measurement of rates of cholesterol synthesis using tritiated water. J. Lipid Res. *25,* 1469-1476.

Digby, J.E., Montague, C.T., Sewter, C.P., Sanders, L., Wilkison, W.O., O'Rahilly, S., and Prins, J.B. (1998). Thiazolidinedione exposure increases the expression of uncoupling protein 1 in cultured human preadipocytes. Diabetes *47,* 138-141.

Du, X., Stocklauser-Farber, K., and Rosen, P. (1999). Generation of reactive oxygen intermediates, activation of NF-kappaB, and induction of apoptosis in human endothelial cells by glucose: role of nitric oxide synthase? Free Radic. Biol. Med. *27,* 752-763.

Ellinghaus, P., Wolfrum, C., Assmann, G., Spener, F., and Seedorf, U. (1999). Phytanic acid activates the peroxisome proliferator-activated receptor alpha (PPARalpha) in sterol carrier protein 2-/ sterol carrier protein x-deficient mice. J. Biol. Chem. *274,* 2766-2772.

Ellis, J.M., Li, L.O., Wu, P.C., Koves, T.R., Ilkayeva, O., Stevens, R.D., Watkins, S.M., Muoio, D.M., and Coleman, R.A. (2010). Adipose acyl-CoA synthetase-1 directs fatty acids toward beta-oxidation and is required for cold thermogenesis. Cell. Metab. *12,* 53-64.

Endo, T., and Kobayashi, T. (2008). Thyroid-stimulating hormone receptor in brown adipose tissue is involved in the regulation of thermogenesis. Am. J. Physiol. Endocrinol. Metab. *295,* E514-8.

Enerback, S., Jacobsson, A., Simpson, E.M., Guerra, C., Yamashita, H., Harper, M.E., and Kozak, L.P. (1997). Mice lacking mitochondrial uncoupling protein are cold-sensitive but not obese. Nature *387,* 90-94.

Fan, W., Boston, B.A., Kesterson, R.A., Hruby, V.J., and Cone, R.D. (1997). Role of melanocortinergic neurons in feeding and the agouti obesity syndrome. Nature *385,* 165-168.

Feldmann, H.M., Golozoubova, V., Cannon, B., and Nedergaard, J. (2009). UCP1 ablation induces obesity and abolishes diet-induced thermogenesis in mice exempt from thermal stress by living at thermoneutrality. Cell. Metab. *9,* 203-209.

Ferrara, N. (2004). Vascular endothelial growth factor: basic science and clinical progress. Endocr. Rev. *25,* 581-611.

Flier, J.S. (2004). Obesity wars: molecular progress confronts an expanding epidemic. Cell *116,* 337-350.

Flo, T.H., Smith, K.D., Sato, S., Rodriguez, D.J., Holmes, M.A., Strong, R.K., Akira, S., and Aderem, A. (2004). Lipocalin 2 mediates an innate immune response to bacterial infection by sequestrating iron. Nature *432,* 917-921.

Forner, F., Kumar, C., Luber, C.A., Fromme, T., Klingenspor, M., and Mann, M. (2009). Proteome differences between brown and white fat mitochondria reveal specialized metabolic functions. Cell. Metab. *10,* 324-335.

Foster, D.O., and Frydman, M.L. (1979). Tissue distribution of cold-induced thermogenesis in conscious warm- or cold-acclimated rats reevaluated from changes in tissue blood flow: the dominant role of brown adipose tissue in the replacement of shivering by nonshivering thermogenesis. Can. J. Physiol. Pharmacol. *57,* 257-270.

Foster, D.O., and Frydman, M.L. (1978). Nonshivering thermogenesis in the rat. II. Measurements of blood flow with microspheres point to brown adipose tissue as the dominant site of the calorigenesis induced by noradrenaline. Can. J. Physiol. Pharmacol. *56,* 110-122.

Fournier, B., Saudubray, J.M., Benichou, B., Lyonnet, S., Munnich, A., Clevers, H., and Poll-The, B.T. (1994). Large deletion of the peroxisomal acyl-CoA oxidase gene in pseudoneonatal adrenoleukodystrophy. J. Clin. Invest. *94,* 526-531.

Fredriksson, J.M., Lindquist, J.M., Bronnikov, G.E., and Nedergaard, J. (2000). Norepinephrine induces vascular endothelial growth factor gene expression in brown adipocytes through a beta -adrenoreceptor/cAMP/protein kinase A pathway involving Src but independently of Erk1/2. J. Biol. Chem. *275,* 13802-13811.

Fredriksson, J.M., Nikami, H., and Nedergaard, J. (2005). Cold-induced expression of the VEGF gene in brown adipose tissue is independent of thermogenic oxygen consumption. FEBS Lett. *579,* 5680-5684.

Fried, S.K., Bunkin, D.A., and Greenberg, A.S. (1998). Omental and subcutaneous adipose tissues of obese subjects release interleukin-6: depot difference and regulation by glucocorticoid. J. Clin. Endocrinol. Metab. *83,* 847-850.

G. Heldmaier, S. Klaus, H. Wiesinger, U. Friedrichs, and M. Wenzel. (1989). Cold acclimation and thermogenesis. In Living in the cold II, Ed A. Malan, B. Canguilbem ed. pp. 347-356.

Garay-Rojas, E., Harper, M., Hraba-Renevey, S., and Kress, M. (1996). An apparent autocrine mechanism amplifies the dexamethasone- and retinoic acid-induced expression of mouse lipocalin-encoding gene 24p3. Gene *170,* 173-180.

Gealekman, O., Burkart, A., Chouinard, M., Nicoloro, S.M., Straubhaar, J., and Corvera, S. (2008). Enhanced angiogenesis in obesity and in response to PPARgamma activators through adipocyte VEGF and ANGPTL4 production. Am. J. Physiol. Endocrinol. Metab. *295,* E1056-64.

Gee, M.F., Tsuchida, R., Eichler-Jonsson, C., Das, B., Baruchel, S., and Malkin, D. (2005). Vascular endothelial growth factor acts in an autocrine manner in rhabdomyosarcoma cell lines and can be inhibited with all-trans-retinoic acid. Oncogene *24,* 8025-8037.

Gesta, S., Tseng, Y.H., and Kahn, C.R. (2007). Developmental origin of fat: tracking obesity to its source. Cell *131,* 242-256.

Gloerich, J., van Vlies, N., Jansen, G.A., Denis, S., Ruiter, J.P., van Werkhoven, M.A., Duran, M., Vaz, F.M., Wanders, R.J., and Ferdinandusse, S. (2005). A phytol-enriched diet induces changes in fatty acid metabolism in mice both via PPARalpha-dependent and -independent pathways. J. Lipid Res. *46,* 716-726.

Goetz, D.H., Holmes, M.A., Borregaard, N., Bluhm, M.E., Raymond, K.N., and Strong, R.K. (2002). The neutrophil lipocalin NGAL is a bacteriostatic agent that interferes with siderophore-mediated iron acquisition. Mol. Cell *10,* 1033-1043.

Gray, S.L., Dalla Nora, E., Backlund, E.C., Manieri, M., Virtue, S., Noland, R.C., O'Rahilly, S., Cortright, R.N., Cinti, S., Cannon, B., and Vidal-Puig, A. (2006). Decreased brown adipocyte recruitment and thermogenic capacity in mice with impaired peroxisome proliferator-activated receptor (P465L PPARgamma) function. Endocrinology *147,* 5708-5714.

Gregoire, F.M., Zhang, F., Clarke, H.J., Gustafson, T.A., Sears, D.D., Favelyukis, S., Lenhard, J., Rentzeperis, D., Clemens, L.E., Mu, Y., and Lavan, B.E. (2009). MBX-102/JNJ39659100, a novel peroxisome proliferator-activated receptor-ligand with weak transactivation activity retains antidiabetic properties in the absence of weight gain and edema. Mol. Endocrinol. *23,* 975-988.

Guan, Y., Hao, C., Cha, D.R., Rao, R., Lu, W., Kohan, D.E., Magnuson, M.A., Redha, R., Zhang, Y., and Breyer, M.D. (2005). Thiazolidinediones expand body fluid volume through PPARgamma stimulation of ENaC-mediated renal salt absorption. Nat. Med. *11,* 861-866.

Guerra, C., Koza, R.A., Walsh, K., Kurtz, D.M., Wood, P.A., and Kozak, L.P. (1998a). Abnormal nonshivering thermogenesis in mice with inherited defects of fatty acid oxidation. J. Clin. Invest. *102,* 1724-1731.

Guerra, C., Koza, R.A., Yamashita, H., Walsh, K., and Kozak, L.P. (1998b). Emergence of brown adipocytes in white fat in mice is under genetic control. Effects on body weight and adiposity. J. Clin. Invest. *102,* 412-420.

Guo, H., Jin, D., Zhang, Y., Wright, W., Bazuine, M., Brockman, D.A., Bernlohr, D.A., and Chen, X. (2010). Lipocalin-2 deficiency impairs thermogenesis and potentiates diet-induced insulin resistance in mice. Diabetes *59,* 1376-1385.

Guo, H., Zhang, Y., Brockman, D.A., Hahn, W., Bernlohr, D.A., and Chen, X. (2012). Lipocalin 2 Deficiency Alters Estradiol Production and Estrogen Receptor Signaling in Female Mice. Endocrinology

Hajer, G.R., van Haeften, T.W., and Visseren, F.L. (2008). Adipose tissue dysfunction in obesity, diabetes, and vascular diseases. Eur. Heart J. *29,* 2959-2971.

Hall, J.A., Ribich, S., Christoffolete, M.A., Simovic, G., Correa-Medina, M., Patti, M.E., and Bianco, A.C. (2010). Absence of thyroid hormone activation during development underlies a permanent defect in adaptive thermogenesis. Endocrinology *151,* 4573-4582.

Hashimoto, T., Shimizu, N., Kimura, T., Takahashi, Y., and Ide, T. (2006). Polyunsaturated fats attenuate the dietary phytol-induced increase in hepatic fatty acid oxidation in mice. J. Nutr. *136,* 882-886.

Hattori, Y., Hattori, S., Sato, N., and Kasai, K. (2000). High-glucose-induced nuclear factor kappaB activation in vascular smooth muscle cells. Cardiovasc. Res. *46,* 188-197.

Hauner, H. (2005). Secretory factors from human adipose tissue and their functional role. Proc. Nutr. Soc. *64,* 163-169.

Hausman, G.J., and Richardson, R.L. (2004). Adipose tissue angiogenesis. J. Anim. Sci. *82,* 925-934.

Heilbronn, L., Smith, S.R., and Ravussin, E. (2004). Failure of fat cell proliferation, mitochondrial function and fat oxidation results in ectopic fat storage, insulin resistance and type II diabetes mellitus. Int. J. Obes. Relat. Metab. Disord. *28 Suppl 4,* S12-21.

Heim, M., Johnson, J., Boess, F., Bendik, I., Weber, P., Hunziker, W., and Fluhmann, B. (2002). Phytanic acid, a natural peroxisome proliferator-activated receptor (PPAR) agonist, regulates glucose metabolism in rat primary hepatocytes. FASEB J. *16,* 718-720.

Hoffmann, S., Rockenstein, A., Ramaswamy, A., Celik, I., Wunderlich, A., Lingelbach, S., Hofbauer, L.C., and Zielke, A. (2007). Retinoic acid inhibits angiogenesis and tumor growth of thyroid cancer cells. Mol. Cell. Endocrinol. *264*, 74-81.

Hoffstedt, J., Arner, P., Hellers, G., and Lonnqvist, F. (1997). Variation in adrenergic regulation of lipolysis between omental and subcutaneous adipocytes from obese and non-obese men. J. Lipid Res. *38*, 795-804.

Hu, H.T., Ma, Q.Y., Zhang, D., Shen, S.G., Han, L., Ma, Y.D., Li, R.F., and Xie, K.P. (2010). HIF-1alpha links beta-adrenoceptor agonists and pancreatic cancer cells under normoxic condition. Acta Pharmacol. Sin. *31*, 102-110.

Huang, H.L., Chu, S.T., and Chen, Y.H. (1999). Ovarian steroids regulate 24p3 expression in mouse uterus during the natural estrous cycle and the preimplantation period. J. Endocrinol. *162*, 11-19.

Huszar, D., Lynch, C.A., Fairchild-Huntress, V., Dunmore, J.H., Fang, Q., Berkemeier, L.R., Gu, W., Kesterson, R.A., Boston, B.A., Cone, R.D., *et al.* (1997). Targeted disruption of the melanocortin-4 receptor results in obesity in mice. Cell *88*, 131-141.

Iaccarino, G., Ciccarelli, M., Sorriento, D., Galasso, G., Campanile, A., Santulli, G., Cipolletta, E., Cerullo, V., Cimini, V., Altobelli, G.G., *et al.* (2005). Ischemic neoangiogenesis enhanced by beta2-adrenergic receptor overexpression: a novel role for the endothelial adrenergic system. Circ. Res. *97*, 1182-1189.

Iannetti, A., Pacifico, F., Acquaviva, R., Lavorgna, A., Crescenzi, E., Vascotto, C., Tell, G., Salzano, A.M., Scaloni, A., Vuttariello, E., *et al.* (2008). The neutrophil gelatinase-associated lipocalin (NGAL), a NF-kappaB-regulated gene, is a survival factor for thyroid neoplastic cells. Proc. Natl. Acad. Sci. U. S. A. *105*, 14058-14063.

Jang, Y., Lee, J.H., Wang, Y., and Sweeney, G. (2012). Emerging clinical and experimental evidence for the role of lipocalin-2 in metabolic syndrome. Clin. Exp. Pharmacol. Physiol. *39*, 194-199.

Jin, D., Guo, H., Bu, S.Y., Zhang, Y., Hannaford, J., Mashek, D.G., and Chen, X. (2011). Lipocalin 2 is a selective modulator of peroxisome proliferator-activated receptor-gamma activation and function in lipid homeostasis and energy expenditure. FASEB J. *25*, 754-764.

Jun, L.S., Siddall, C.P., and Rosen, E.D. (2011). A Minor Role for Lipocalin 2 in High Fat Diet-Induced Glucose Intolerance. Am. J. Physiol. Endocrinol. Metab.

Kajimura, S., Seale, P., Kubota, K., Lunsford, E., Frangioni, J.V., Gygi, S.P., and Spiegelman, B.M. (2009). Initiation of myoblast to brown fat switch by a PRDM16-C/EBP-beta transcriptional complex. Nature *460,* 1154-1158.

Kanaka-Gantenbein, C., Margeli, A., Pervanidou, P., Sakka, S., Mastorakos, G., Chrousos, G.P., and Papassotiriou, I. (2008). Retinol-binding protein 4 and lipocalin-2 in childhood and adolescent obesity: when children are not just "small adults". Clin. Chem. *54,* 1176-1182.

Kanata, S., Akagi, M., Nishimura, S., Hayakawa, S., Yoshida, K., Sawamura, T., Munakata, H., and Hamanishi, C. (2006). Oxidized LDL binding to LOX-1 upregulates VEGF expression in cultured bovine chondrocytes through activation of PPAR-gamma. Biochem. Biophys. Res. Commun. *348,* 1003-1010.

Karlsen, J.R., Borregaard, N., and Cowland, J.B. (2010). Induction of neutrophil gelatinase-associated lipocalin expression by co-stimulation with interleukin-17 and tumor necrosis factor-alpha is controlled by IkappaB-zeta but neither by C/EBP-beta nor C/EBP-delta. J. Biol. Chem. *285,* 14088-14100.

Kelley, D.E., Mokan, M., Simoneau, J.A., and Mandarino, L.J. (1993). Interaction between glucose and free fatty acid metabolism in human skeletal muscle. J. Clin. Invest. *92,* 91-98.

Kelly, L.J., Vicario, P.P., Thompson, G.M., Candelore, M.R., Doebber, T.W., Ventre, J., Wu, M.S., Meurer, R., Forrest, M.J., Conner, M.W., Cascieri, M.A., and Moller, D.E. (1998). Peroxisome proliferator-activated receptors gamma and alpha mediate in vivo regulation of uncoupling protein (UCP-1, UCP-2, UCP-3) gene expression. Endocrinology *139,* 4920-4927.

Kim, M.S., Kim, Y.K., Eun, H.C., Cho, K.H., and Chung, J.H. (2006). All-trans retinoic acid antagonizes UV-induced VEGF production and angiogenesis via the inhibition of ERK activation in human skin keratinocytes. J. Invest. Dermatol. *126,* 2697-2706.

Kini, A.R., Peterson, L.A., Tallman, M.S., and Lingen, M.W. (2001). Angiogenesis in acute promyelocytic leukemia: induction by vascular endothelial growth factor and inhibition by all-trans retinoic acid. Blood *97,* 3919-3924.

Kitareewan, S., Burka, L.T., Tomer, K.B., Parker, C.E., Deterding, L.J., Stevens, R.D., Forman, B.M., Mais, D.E., Heyman, R.A., McMorris, T., and Weinberger, C. (1996). Phytol metabolites are circulating dietary factors that activate the nuclear receptor RXR. Mol. Biol. Cell *7,* 1153-1166.

Kjeldsen, L., Bainton, D.F., Sengelov, H., and Borregaard, N. (1994). Identification of neutrophil gelatinase-associated lipocalin as a novel matrix protein of specific granules in human neutrophils. Blood *83,* 799-807.

Kjeldsen, L., Cowland, J.B., and Borregaard, N. (2000). Human neutrophil gelatinase-associated lipocalin and homologous proteins in rat and mouse. Biochim. Biophys. Acta *1482,* 272-283.

Kjeldsen, L., Johnsen, A.H., Sengelov, H., and Borregaard, N. (1993). Isolation and primary structure of NGAL, a novel protein associated with human neutrophil gelatinase. J. Biol. Chem. *268,* 10425-10432.

Kolata, G. (2007). Rethinking thin: The new science of weight loss – and the myths and realities of dieting.122.

Kontani, Y., Wang, Y., Kimura, K., Inokuma, K.I., Saito, M., Suzuki-Miura, T., Wang, Z., Sato, Y., Mori, N., and Yamashita, H. (2005). UCP1 deficiency increases susceptibility to diet-induced obesity with age. Aging Cell. *4,* 147-155.

Kramar, R. (1986). The contribution of peroxisomes to lipid metabolism. J. Clin. Chem. Clin. Biochem. *24,* 109-118.

Lachgar, S., Charveron, M., Gall, Y., and Bonafe, J.L. (1999). Inhibitory effects of retinoids on vascular endothelial growth factor production by cultured human skin keratinocytes. Dermatology *199 Suppl 1,* 25-27.

LaLonde, J.M., Bernlohr, D.A., and Banaszak, L.J. (1994). The up-and-down beta-barrel proteins. FASEB J. *8,* 1240-1247.

Lamy, S., Lachambre, M.P., Lord-Dufour, S., and Beliveau, R. (2010). Propranolol suppresses angiogenesis in vitro: inhibition of proliferation, migration, and differentiation of endothelial cells. Vascul Pharmacol. *53,* 200-208.

Larose, M., Cassard-Doulcier, A.M., Fleury, C., Serra, F., Champigny, O., Bouillaud, F., and Ricquier, D. (1996). Essential cis-acting elements in rat uncoupling protein gene are in an enhancer containing a complex retinoic acid response domain. J. Biol. Chem. *271,* 31533-31542.

Law, I.K., Xu, A., Lam, K.S., Berger, T., Mak, T.W., Vanhoutte, P.M., Liu, J.T., Sweeney, G., Zhou, M., Yang, B., and Wang, Y. (2010). Lipocalin-2 deficiency attenuates insulin resistance associated with aging and obesity. Diabetes *59,* 872-882.

Lee, S., Kim, J.H., Kim, J.H., Seo, J.W., Han, H.S., Lee, W.H., Mori, K., Nakao, K., Barasch, J., and Suk, K. (2011). Lipocalin-2 Is a chemokine inducer in the central

nervous system: role of chemokine ligand 10 (CXCL10) in lipocalin-2-induced cell migration. J. Biol. Chem. *286,* 43855-43870.

Lee, Y.H., Lee, S.H., Jung, E.S., Kim, J.S., Shim, C.Y., Ko, Y.G., Choi, D., Jang, Y., Chung, N., and Ha, J.W. (2010). Visceral adiposity and the severity of coronary artery disease in middle-aged subjects with normal waist circumference and its relation with lipocalin-2 and MCP-1. Atherosclerosis *213,* 592-597.

Lewin, T.M., Wang, S., Nagle, C.A., Van Horn, C.G., and Coleman, R.A. (2005). Mitochondrial glycerol-3-phosphate acyltransferase-1 directs the metabolic fate of exogenous fatty acids in hepatocytes. Am. J. Physiol. Endocrinol. Metab. *288,* E835-44.

Li, C., and Chan, Y.R. (2011). Lipocalin 2 regulation and its complex role in inflammation and cancer. Cytokine

Lipscombe, L.L., Gomes, T., Levesque, L.E., Hux, J.E., Juurlink, D.N., and Alter, D.A. (2007). Thiazolidinediones and cardiovascular outcomes in older patients with diabetes. JAMA *298,* 2634-2643.

Liu, X., Hamnvik, O.P., Petrou, M., Gong, H., Chamberland, J.P., Christophi, C.A., Kales, S.N., Christiani, D.C., and Mantzoros, C.S. (2011). Circulating lipocalin 2 is associated with body fat distribution at baseline but is not an independent predictor of insulin resistance: the prospective Cyprus Metabolism Study. Eur. J. Endocrinol. *165,* 805-812.

Lowell, B.B., and Spiegelman, B.M. (2000). Towards a molecular understanding of adaptive thermogenesis. Nature *404,* 652-660.

Lowell, B.B., S-Susulic, V., Hamann, A., Lawitts, J.A., Himms-Hagen, J., Boyer, B.B., Kozak, L.P., and Flier, J.S. (1993). Development of obesity in transgenic mice after genetic ablation of brown adipose tissue. Nature *366,* 740-742.

Macotela, Y., Boucher, J., Tran, T.T., and Kahn, C.R. (2009). Sex and depot differences in adipocyte insulin sensitivity and glucose metabolism. Diabetes *58,* 803-812.

Maeno, T., Tanaka, T., Sando, Y., Suga, T., Maeno, Y., Nakagawa, J., Hosono, T., Sato, M., Akiyama, H., Kishi, S., Nagai, R., and Kurabayashi, M. (2002). Stimulation of vascular endothelial growth factor gene transcription by all trans retinoic acid through Sp1 and Sp3 sites in human bronchioloalveolar carcinoma cells. Am. J. Respir. Cell Mol. Biol. *26,* 246-253.

Marette, A. (2003). Molecular mechanisms of inflammation in obesity-linked insulin resistance. Int. J. Obes. Relat. Metab. Disord. *27 Suppl 3,* S46-8.

Mattsson, C.L., Csikasz, R.I., Chernogubova, E., Yamamoto, D.L., Hogberg, H.T., Amri, E.Z., Hutchinson, D.S., and Bengtsson, T. (2011). beta(1)-Adrenergic receptors increase UCP1 in human MADS brown adipocytes and rescue cold-acclimated beta(3)-adrenergic receptor-knockout mice via nonshivering thermogenesis. Am. J. Physiol. Endocrinol. Metab. *301,* E1108-18.

McCarty, M.F., and Block, K.I. (2006). Preadministration of high-dose salicylates, suppressors of NF-kappaB activation, may increase the chemosensitivity of many cancers: an example of proapoptotic signal modulation therapy. Integr. Cancer. Ther. *5,* 252-268.

Meyer, C.W., Willershauser, M., Jastroch, M., Rourke, B.C., Fromme, T., Oelkrug, R., Heldmaier, G., and Klingenspor, M. (2010). Adaptive thermogenesis and thermal conductance in WT and UCP1-KO mice. Am. J. Physiol. Regul. Integr. Comp. Physiol. *299,* R1396-406.

Mogensen, M., Sahlin, K., Fernstrom, M., Glintborg, D., Vind, B.F., Beck-Nielsen, H., and Hojlund, K. (2007). Mitochondrial respiration is decreased in skeletal muscle of patients with type 2 diabetes. Diabetes *56,* 1592-1599.

Montague, C.T., and O'Rahilly, S. (2000). The perils of portliness: causes and consequences of visceral adiposity. Diabetes *49,* 883-888.

Moreno-Navarrete, J.M., Manco, M., Ibanez, J., Garcia-Fuentes, E., Ortega, F., Gorostiaga, E., Vendrell, J., Izquierdo, M., Martinez, C., Nolfe, G., *et al.* (2010). Metabolic endotoxemia and saturated fat contribute to circulating NGAL concentrations in subjects with insulin resistance. Int. J. Obes. (Lond) *34,* 240-249.

Mori, Y., Murakawa, Y., Okada, K., Horikoshi, H., Yokoyama, J., Tajima, N., and Ikeda, Y. (1999). Effect of troglitazone on body fat distribution in type 2 diabetic patients. Diabetes Care *22,* 908-912.

Morigi, M., Angioletti, S., Imberti, B., Donadelli, R., Micheletti, G., Figliuzzi, M., Remuzzi, A., Zoja, C., and Remuzzi, G. (1998). Leukocyte-endothelial interaction is augmented by high glucose concentrations and hyperglycemia in a NF-kB-dependent fashion. J. Clin. Invest. *101,* 1905-1915.

Murata, T., He, S., Hangai, M., Ishibashi, T., Xi, X.P., Kim, S., Hsueh, W.A., Ryan, S.J., Law, R.E., and Hinton, D.R. (2000). Peroxisome proliferator-activated receptor-gamma ligands inhibit choroidal neovascularization. Invest. Ophthalmol. Vis. Sci. *41,* 2309-2317.

Nedergaard, J., Alexson, S., and Cannon, B. (1980). Cold adaptation in the rat: increased brown fat peroxisomal beta-oxidation relative to maximal mitochondrial oxidative capacity. Am. J. Physiol. *239,* C208-16.

Nedergaard, J., Bengtsson, T., and Cannon, B. (2007). Unexpected evidence for active brown adipose tissue in adult humans. Am. J. Physiol. Endocrinol. Metab. *293,* E444-52.

Nedergaard, J., Petrovic, N., Lindgren, E.M., Jacobsson, A., and Cannon, B. (2005). PPARgamma in the control of brown adipocyte differentiation. Biochim. Biophys. Acta *1740,* 293-304.

Nikami, H., Nedergaard, J., and Fredriksson, J.M. (2005). Norepinephrine but not hypoxia stimulates HIF-1alpha gene expression in brown adipocytes. Biochem. Biophys. Res. Commun. *337,* 121-126.

Ocloo, A., Shabalina, I.G., Nedergaard, J., and Brand, M.D. (2007). Cold-induced alterations of phospholipid fatty acyl composition in brown adipose tissue mitochondria are independent of uncoupling protein-1. Am. J. Physiol. Regul. Integr. Comp. Physiol. *293,* R1086-93.

Ogden, C.L., Carroll, M.D., Kit, B.K., and Flegal, K.M. (2012). Prevalence of obesity in the United States, 2009-2010. NCHS Data Brief *(82),* 1-8.

Ollmann, M.M., Wilson, B.D., Yang, Y.K., Kerns, J.A., Chen, Y., Gantz, I., and Barsh, G.S. (1997). Antagonism of central melanocortin receptors in vitro and in vivo by agouti-related protein. Science *278,* 135-138.

Ouchi, N., Parker, J.L., Lugus, J.J., and Walsh, K. (2011). Adipokines in inflammation and metabolic disease. Nat. Rev. Immunol. *11,* 85-97.

Ouellet, V., Labbe, S.M., Blondin, D.P., Phoenix, S., Guerin, B., Haman, F., Turcotte, E.E., Richard, D., and Carpentier, A.C. (2012). Brown adipose tissue oxidative metabolism contributes to energy expenditure during acute cold exposure in humans. J. Clin. Invest. *122,* 545-552.

Ozes, O.N., Mayo, L.D., Gustin, J.A., Pfeffer, S.R., Pfeffer, L.M., and Donner, D.B. (1999). NF-kappaB activation by tumour necrosis factor requires the Akt serine-threonine kinase. Nature *401,* 82-85.

Panidis, D., Tziomalos, K., Koiou, E., Kandaraki, E.A., Tsourdi, E., Delkos, D., Kalaitzakis, E., and Katsikis, I. (2010). The effects of obesity and polycystic ovary syndrome on serum lipocalin-2 levels: a cross-sectional study. Reprod. Biol. Endocrinol. *8,* 151.

Pieper, G.M., and Riaz-ul-Haq. (1997). Activation of nuclear factor-kappaB in cultured endothelial cells by increased glucose concentration: prevention by calphostin C. J. Cardiovasc. Pharmacol. *30,* 528-532.

Porter, S.A., Massaro, J.M., Hoffmann, U., Vasan, R.S., O'Donnel, C.J., and Fox, C.S. (2009). Abdominal subcutaneous adipose tissue: a protective fat depot? Diabetes Care *32,* 1068-1075.

Puigserver, P., Wu, Z., Park, C.W., Graves, R., Wright, M., and Spiegelman, B.M. (1998). A cold-inducible coactivator of nuclear receptors linked to adaptive thermogenesis. Cell *92,* 829-839.

Rabelo, R., Reyes, C., Schifman, A., and Silva, J.E. (1996). A complex retinoic acid response element in the uncoupling protein gene defines a novel role for retinoids in thermogenesis. Endocrinology *137,* 3488-3496.

Rial, E., and Nicholls, D.G. (1984). The mitochondrial uncoupling protein from guinea-pig brown adipose tissue. Synchronous increase in structural and functional parameters during cold-adaptation. Biochem. J. *222,* 685-693.

Romashkova, J.A., and Makarov, S.S. (1999). NF-kappaB is a target of AKT in anti-apoptotic PDGF signalling. Nature *401,* 86-90.

Rosenfeld, M.G., Lunyak, V.V., and Glass, C.K. (2006). Sensors and signals: a coactivator/corepressor/epigenetic code for integrating signal-dependent programs of transcriptional response. Genes Dev. *20,* 1405-1428.

Roudkenar, M.H., Halabian, R., Roushandeh, A.M., Nourani, M.R., Masroori, N., Ebrahimi, M., Nikogoftar, M., Rouhbakhsh, M., Bahmani, P., Najafabadi, A.J., and Shokrgozar, M.A. (2009). Lipocalin 2 regulation by thermal stresses: protective role of Lcn2/NGAL against cold and heat stresses. Exp. Cell Res. *315,* 3140-3151.

Roudkenar, M.H., Kuwahara, Y., Baba, T., Roushandeh, A.M., Ebishima, S., Abe, S., Ohkubo, Y., and Fukumoto, M. (2007). Oxidative stress induced lipocalin 2 gene expression: addressing its expression under the harmful conditions. J. Radiat. Res. (Tokyo) *48,* 39-44.

Saito, A., Sugawara, A., Uruno, A., Kudo, M., Kagechika, H., Sato, Y., Owada, Y., Kondo, H., Sato, M., Kurabayashi, M., *et al.* (2007). All-trans retinoic acid induces in vitro angiogenesis via retinoic acid receptor: possible involvement of paracrine effects of endogenous vascular endothelial growth factor signaling. Endocrinology *148,* 1412-1423.

Saito, M., Okamatsu-Ogura, Y., Matsushita, M., Watanabe, K., Yoneshiro, T., Nio-Kobayashi, J., Iwanaga, T., Miyagawa, M., Kameya, T., Nakada, K., Kawai, Y., and Tsujisaki, M. (2009). High incidence of metabolically active brown adipose tissue in healthy adult humans: effects of cold exposure and adiposity. Diabetes *58,* 1526-1531.

Schluter, A., Barbera, M.J., Iglesias, R., Giralt, M., and Villarroya, F. (2002a). Phytanic acid, a novel activator of uncoupling protein-1 gene transcription and brown adipocyte differentiation. Biochem. J. *362,* 61-69.

Schluter, A., Giralt, M., Iglesias, R., and Villarroya, F. (2002b). Phytanic acid, but not pristanic acid, mediates the positive effects of phytol derivatives on brown adipocyte differentiation. FEBS Lett. *517,* 83-86.

Schroll, A., Eller, K., Feistritzer, C., Nairz, M., Sonnweber, T., Moser, P.A., Rosenkranz, A.R., Theurl, I., and Weiss, G. (2012). Lipocalin 2 ameliorates granulocyte functionality. Eur. J. Immunol.

Schweiger, M., Schoiswohl, G., Lass, A., Radner, F.P., Haemmerle, G., Malli, R., Graier, W., Cornaciu, I., Oberer, M., Salvayre, R., *et al.* (2008). The C-terminal region of human adipose triglyceride lipase affects enzyme activity and lipid droplet binding. J. Biol. Chem. *283,* 17211-17220.

Seale, P., Bjork, B., Yang, W., Kajimura, S., Chin, S., Kuang, S., Scime, A., Devarakonda, S., Conroe, H.M., Erdjument-Bromage, H., *et al.* (2008). PRDM16 controls a brown fat/skeletal muscle switch. Nature *454,* 961-967.

Seale, P., Kajimura, S., Yang, W., Chin, S., Rohas, L.M., Uldry, M., Tavernier, G., Langin, D., and Spiegelman, B.M. (2007). Transcriptional control of brown fat determination by PRDM16. Cell. Metab. *6,* 38-54.

Sears, I.B., MacGinnitie, M.A., Kovacs, L.G., and Graves, R.A. (1996). Differentiation-dependent expression of the brown adipocyte uncoupling protein gene: regulation by peroxisome proliferator-activated receptor gamma. Mol. Cell. Biol. *16,* 3410-3419.

Seth, P., Porter, D., Lahti-Domenici, J., Geng, Y., Richardson, A., and Polyak, K. (2002). Cellular and molecular targets of estrogen in normal human breast tissue. Cancer Res. *62,* 4540-4544.

Shen, F., Hu, Z., Goswami, J., and Gaffen, S.L. (2006). Identification of common transcriptional regulatory elements in interleukin-17 target genes. J. Biol. Chem. *281,* 24138-24148.

Silva, J.E. (2006). Thermogenic mechanisms and their hormonal regulation. Physiol. Rev. *86,* 435-464.

Silva, J.E., and Rabelo, R. (1997). Regulation of the uncoupling protein gene expression. Eur. J. Endocrinol. *136,* 251-264.

Smith, R.E., and Horwitz, B.A. (1969). Brown fat and thermogenesis. Physiol. Rev. *49,* 330-425.

Smith, S.R., De Jonge, L., Volaufova, J., Li, Y., Xie, H., and Bray, G.A. (2005). Effect of pioglitazone on body composition and energy expenditure: a randomized controlled trial. Metabolism *54,* 24-32.

Snyder, E.E., Walts, B., Perusse, L., Chagnon, Y.C., Weisnagel, S.J., Rankinen, T., and Bouchard, C. (2004). The human obesity gene map: the 2003 update. Obes. Res. *12,* 369-439.

Sommer, G., Weise, S., Kralisch, S., Lossner, U., Bluher, M., Stumvoll, M., and Fasshauer, M. (2009). Lipocalin-2 is induced by interleukin-1beta in murine adipocytes in vitro. J. Cell. Biochem. *106,* 103-108.

Susulic, V.S., Frederich, R.C., Lawitts, J., Tozzo, E., Kahn, B.B., Harper, M.E., Himms-Hagen, J., Flier, J.S., and Lowell, B.B. (1995). Targeted disruption of the beta 3-adrenergic receptor gene. J. Biol. Chem. *270,* 29483-29492.

Tan, B.K., Adya, R., Shan, X., Syed, F., Lewandowski, K.C., O'Hare, J.P., and Randeva, H.S. (2009). Ex vivo and in vivo regulation of lipocalin-2, a novel adipokine, by insulin. Diabetes Care *32,* 129-131.

Tartaglia, L.A., Dembski, M., Weng, X., Deng, N., Culpepper, J., Devos, R., Richards, G.J., Campfield, L.A., Clark, F.T., Deeds, J., *et al.* (1995). Identification and expression cloning of a leptin receptor, OB-R. Cell *83,* 1263-1271.

Timmons, J.A., Wennmalm, K., Larsson, O., Walden, T.B., Lassmann, T., Petrovic, N., Hamilton, D.L., Gimeno, R.E., Wahlestedt, C., Baar, K., Nedergaard, J., and Cannon, B. (2007). Myogenic gene expression signature establishes that brown and white adipocytes originate from distinct cell lineages. Proc. Natl. Acad. Sci. U. S. A. *104,* 4401-4406.

Trayhurn, P. (1981). Fatty acid synthesis in mouse brown adipose tissue. The influence of environmental temperature on the proportion of whole-body fatty acid synthesis in brown adipose tissue and the liver. Biochim. Biophys. Acta *664,* 549-560.

Tseng, Y.H., Kokkotou, E., Schulz, T.J., Huang, T.L., Winnay, J.N., Taniguchi, C.M., Tran, T.T., Suzuki, R., Espinoza, D.O., Yamamoto, Y., *et al.* (2008). New role of bone morphogenetic protein 7 in brown adipogenesis and energy expenditure. Nature *454,* 1000-1004.

Ueta, C.B., Fernandes, G.W., Capelo, L.P., Fonseca, T.L., Maculan, F.D., Gouveia, C.H., Brum, P.C., Christoffolete, M.A., Aoki, M.S., Lancellotti, C.L., *et al.* (2012). beta(1)

Adrenergic receptor is key to cold- and diet-induced thermogenesis in mice. J. Endocrinol. *214,* 359-365.

van Marken Lichtenbelt, W.D., Vanhommerig, J.W., Smulders, N.M., Drossaerts, J.M., Kemerink, G.J., Bouvy, N.D., Schrauwen, P., and Teule, G.J. (2009). Cold-activated brown adipose tissue in healthy men. N. Engl. J. Med. *360,* 1500-1508.

Vasudevan, A.R., and Balasubramanyam, A. (2004). Thiazolidinediones: a review of their mechanisms of insulin sensitization, therapeutic potential, clinical efficacy, and tolerability. Diabetes Technol. Ther. *6,* 850-863.

Vergnes, L., Chin, R., Young, S.G., and Reue, K. (2011). Heart-type fatty acid-binding protein is essential for efficient brown adipose tissue fatty acid oxidation and cold tolerance. J. Biol. Chem. *286,* 380-390.

Vijgen, G.H., Bouvy, N.D., Teule, G.J., Brans, B., Hoeks, J., Schrauwen, P., and van Marken Lichtenbelt, W.D. (2012). Increase in brown adipose tissue activity after weight loss in morbidly obese subjects. J. Clin. Endocrinol. Metab. *97,* E1229-33.

Vijgen, G.H., Bouvy, N.D., Teule, G.J., Brans, B., Schrauwen, P., and van Marken Lichtenbelt, W.D. (2011). Brown adipose tissue in morbidly obese subjects. PLoS One *6,* e17247.

Villena, J.A., Hock, M.B., Chang, W.Y., Barcas, J.E., Giguere, V., and Kralli, A. (2007). Orphan nuclear receptor estrogen-related receptor alpha is essential for adaptive thermogenesis. Proc. Natl. Acad. Sci. U. S. A. *104,* 1418-1423.

Virtanen, K.A., Lidell, M.E., Orava, J., Heglind, M., Westergren, R., Niemi, T., Taittonen, M., Laine, J., Savisto, N.J., Enerback, S., and Nuutila, P. (2009). Functional brown adipose tissue in healthy adults. N. Engl. J. Med. *360,* 1518-1525.

Virtanen, K.A., Lonnroth, P., Parkkola, R., Peltoniemi, P., Asola, M., Viljanen, T., Tolvanen, T., Knuuti, J., Ronnemaa, T., Huupponen, R., and Nuutila, P. (2002). Glucose uptake and perfusion in subcutaneous and visceral adipose tissue during insulin stimulation in nonobese and obese humans. J. Clin. Endocrinol. Metab. *87,* 3902-3910.

Virtanen, K.A., and Nuutila, P. (2011). Brown adipose tissue in humans. Curr. Opin. Lipidol. *22,* 49-54.

Wajchenberg, B.L. (2000). Subcutaneous and visceral adipose tissue: their relation to the metabolic syndrome. Endocr. Rev. *21,* 697-738.

Waki, H., and Tontonoz, P. (2007). Endocrine functions of adipose tissue. Annu. Rev. Pathol. *2,* 31-56.

Walden, T.B., Timmons, J.A., Keller, P., Nedergaard, J., and Cannon, B. (2009). Distinct expression of muscle-specific microRNAs (myomirs) in brown adipocytes. J. Cell. Physiol. *218*, 444-449.

Wang, Y., Lam, K.S., Kraegen, E.W., Sweeney, G., Zhang, J., Tso, A.W., Chow, W.S., Wat, N.M., Xu, J.Y., Hoo, R.L., and Xu, A. (2007). Lipocalin-2 is an inflammatory marker closely associated with obesity, insulin resistance, and hyperglycemia in humans. Clin. Chem. *53*, 34-41.

Watanabe, M., Yamamoto, T., Mori, C., Okada, N., Yamazaki, N., Kajimoto, K., Kataoka, M., and Shinohara, Y. (2008). Cold-induced changes in gene expression in brown adipose tissue: implications for the activation of thermogenesis. Biol. Pharm. Bull. *31*, 775-784.

Weisberg, S.P., McCann, D., Desai, M., Rosenbaum, M., Leibel, R.L., and Ferrante, A.W.,Jr. (2003). Obesity is associated with macrophage accumulation in adipose tissue. J. Clin. Invest. *112*, 1796-1808.

Weyer, C., Foley, J.E., Bogardus, C., Tataranni, P.A., and Pratley, R.E. (2000). Enlarged subcutaneous abdominal adipocyte size, but not obesity itself, predicts type II diabetes independent of insulin resistance. Diabetologia *43*, 1498-1506.

Wijers, S.L., Saris, W.H., and van Marken Lichtenbelt, W.D. (2009). Recent advances in adaptive thermogenesis: potential implications for the treatment of obesity. Obes. Rev. *10*, 218-226.

Wu, H., Santoni-Rugiu, E., Ralfkiaer, E., Porse, B.T., Moser, C., Hoiby, N., Borregaard, N., and Cowland, J.B. (2010). Lipocalin 2 is protective against E. coli pneumonia. Respir. Res. *11*, 96.

Wu, J., Bostrom, P., Sparks, L.M., Ye, L., Choi, J.H., Giang, A.H., Khandekar, M., Virtanen, K.A., Nuutila, P., Schaart, G., *et al.* (2012). Beige adipocytes are a distinct type of thermogenic fat cell in mouse and human. Cell *150*, 366-376.

Wu, Z., Puigserver, P., Andersson, U., Zhang, C., Adelmant, G., Mootha, V., Troy, A., Cinti, S., Lowell, B., Scarpulla, R.C., and Spiegelman, B.M. (1999). Mechanisms controlling mitochondrial biogenesis and respiration through the thermogenic coactivator PGC-1. Cell *98*, 115-124.

Xiang, C.C., Wu, Y.J., Ma, L., Ding, L., Lisinski, I., Brownstein, M.J., Cushman, S.W., and Chen, X. (2007). Characterisation of insulin-resistant phenotype of cultured rat primary adipose cells. Diabetologia *50*, 1070-1079.

Xu, H., Barnes, G.T., Yang, Q., Tan, G., Yang, D., Chou, C.J., Sole, J., Nichols, A., Ross, J.S., Tartaglia, L.A., and Chen, H. (2003). Chronic inflammation in fat plays a crucial role in the development of obesity-related insulin resistance. J. Clin. Invest. *112*, 1821-1830.

Xue, Y., Petrovic, N., Cao, R., Larsson, O., Lim, S., Chen, S., Feldmann, H.M., Liang, Z., Zhu, Z., Nedergaard, J., Cannon, B., and Cao, Y. (2009). Hypoxia-independent angiogenesis in adipose tissues during cold acclimation. Cell. Metab. *9*, 99-109.

Yamakawa, K., Hosoi, M., Koyama, H., Tanaka, S., Fukumoto, S., Morii, H., and Nishizawa, Y. (2000). Peroxisome proliferator-activated receptor-gamma agonists increase vascular endothelial growth factor expression in human vascular smooth muscle cells. Biochem. Biophys. Res. Commun. *271*, 571-574.

Yan, Q.W., Yang, Q., Mody, N., Graham, T.E., Hsu, C.H., Xu, Z., Houstis, N.E., Kahn, B.B., and Rosen, E.D. (2007). The adipokine lipocalin 2 is regulated by obesity and promotes insulin resistance. Diabetes *56*, 2533-2540.

Yang, J., Bielenberg, D.R., Rodig, S.J., Doiron, R., Clifton, M.C., Kung, A.L., Strong, R.K., Zurakowski, D., and Moses, M.A. (2009). Lipocalin 2 promotes breast cancer progression. Proc. Natl. Acad. Sci. U. S. A. *106*, 3913-3918.

Yang, J., and Moses, M.A. (2009). Lipocalin 2: a multifaceted modulator of human cancer. Cell. Cycle *8*, 2347-2352.

Yasuda, E., Tokuda, H., Ishisaki, A., Hirade, K., Kanno, Y., Hanai, Y., Nakamura, N., Noda, T., Katagiri, Y., and Kozawa, O. (2005). PPAR-gamma ligands upregulate basic fibroblast growth factor-induced VEGF release through amplifying SAPK/JNK activation in osteoblasts. Biochem. Biophys. Res. Commun. *328*, 137-143.

Yerneni, K.K., Bai, W., Khan, B.V., Medford, R.M., and Natarajan, R. (1999). Hyperglycemia-induced activation of nuclear transcription factor kappaB in vascular smooth muscle cells. Diabetes *48*, 855-864.

Yki-Jarvinen, H. (2005). Fat in the liver and insulin resistance. Ann. Med. *37*, 347-356.

Zhang, J., Wu, Y., Zhang, Y., Leroith, D., Bernlohr, D.A., and Chen, X. (2008). The role of lipocalin 2 in the regulation of inflammation in adipocytes and macrophages. Mol. Endocrinol. *22*, 1416-1426.

Zhang, Q.X., Magovern, C.J., Mack, C.A., Budenbender, K.T., Ko, W., and Rosengart, T.K. (1997). Vascular endothelial growth factor is the major angiogenic factor in omentum: mechanism of the omentum-mediated angiogenesis. J. Surg. Res. *67*, 147-154.

Zhang, Y., Proenca, R., Maffei, M., Barone, M., Leopold, L., and Friedman, J.M. (1994). Positional cloning of the mouse obese gene and its human homologue. Nature *372*, 425-432.

Zingaretti, M.C., Crosta, F., Vitali, A., Guerrieri, M., Frontini, A., Cannon, B., Nedergaard, J., and Cinti, S. (2009). The presence of UCP1 demonstrates that metabolically active adipose tissue in the neck of adult humans truly represents brown adipose tissue. FASEB J. *23,* 3113-3120.